Jay N. Damask
Baruch College
City University of New York

Signal Processing Applied To Finance

Lecture Notes for 2014

February 9, 2014

build: 175

Contents

Chapter 1
Introduction

A time series is simply a mathematical function whose principal parameter is time. Time has the particular property of order; the collection of time-series values absent their order is not a time series at all, it is a set or a range. A time series contains information, both in when the series occurs and what its values are. A time series can be transformed into a histogram, for instance, but not the other way around because ordinal information has been lost. Two or more time series that share a temporal overlap can be analyzed for correlation and causation because they share a common time axis. Whether the evolution of one series can forecast the direction of another is a statistical problem yet one where time intervals play a central role.

Time-series analysis in finance, strictly speaking, is the study of forecasts based on past series observations. One's goal is always to construct a process that models the time series; the observations are then represented as the underlying process coupled with noise. Such a representation introduces model risk, where the risk of divergence between observations and model beyond the expected error is possible (and happens all the time). For a given model, a forecast is the process extrapolated to a future time conditioned on all the information up to the current time, along with an error bound.

The reader should be cognizant that forecasts based on time series analysis is not the only choice available. For instance, fundamental analysis of corporations and sector competition yields indications for many traders of whether to buy or sell equity or debt instruments; their entry and exit points may not have much to do with the details of a stock chart. I might even argue that the largest, if infrequent, returns come from strong fundamental views that turn out to be correct; for instance, those who shorted mortgage-backed securities in 2007 and 2008 did quite well.

This course takes a signal-processing approach to time series analysis. In the vocabulary of signal-processing, a "filter" is applied to a time series to make a new time series with, presumably, appealing properties. Much of this course deals with the design of filters.

Fig. 1.1 The models developed in these lectures do not simultaneously consume time points and time values. Time points are replaced by index points that are equally spaced. This loss of information needs to be managed in some manner.

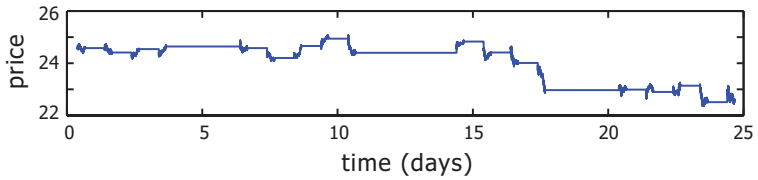

Fig. 1.2 Time series of Nasdaq-traded prices for CSCO on one-second-minimum intervals, over Jan 2010. The abscissa is actual, or "wall-clock", time, the ordinate is price.

1.1 Time

Since a time series is a function of time I ought to begin with time itself. Time is ordered, is infinitely divisible, and has measure: the distance between two time points is simply duration. I label continuous time by t, and particular time points by $t_1, t_2, \ldots$. The interval between time points t_p and t_q is $\tau_{p,q} = t_q - t_p$, being positive or negative. There are many financial processes the occur, at least theoretically, in continuous time, for example bond accrual or options value decay. These processes, however, are deterministic in the absence of new information.

Information is added to the market through events. Events are ordered, but their times are not infinitely divisible. Interarrival time is one measure adjacent event ordinal distinct, and another is simply the running count of events. A running count is just that: $1, 2, 3, \ldots$ where the interval is always fixed.

There are two basic processes that govern events: the interarrival time and the outcome of the event. The term "wall clock" time means that event timepoints are marked by a time piece. The term "event clock" means that events are measured only by their outcome and order but the interarrival time is dropped. I label "event time" by the index $n \in \mathbb{Z}$ and particular event indices by $n_1, n_2, \ldots$.

The time-series methods developed in these lectures focus on event outcomes, not interarrival times. That is, these methods do not simultaneously consume interarrival wall-clock times and event outcomes. The time points

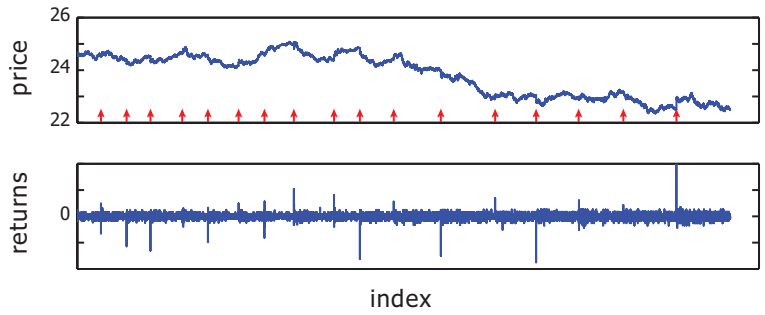

Fig. 1.3 (a) Same series plotted by index. The red arrows indicate day breaks. (b) Log-return series. The spikes are due to large price changes from close to open.

are intended to be equally spaced along some index axis, as illustrated in Fig. 1.1. Such an approach represents a loss of information, but affords a simplification so that we can focus on learning how to deal with the time series of event outcomes.

1.1.1 Example: Classification by Scale

Figure 1.2 illustrates the time-series of traded prices for CSCO during the month of Jan. 2010. The data is event-driven in that only wall-clock times where the price changed is reported, and the minimum interval is one second due to the resolution of the reporting clock. The long flat-lines are the overnight and weekend intervals; the tightly packed fluctuations are the intraday trades. Clearly the way this series is presented makes little sense.

There are two processes embedded here: the overnight process, where the price changes from close to open; and the intraday process during normal trading hours. "Overnight" in fact included weekdays, weekends and, for this data, one holiday.

We could chose to ignore wall-clock time and simply tabulate the price series one after the other to form an index series. Figure 1.3(a) illustrates the same data where the abscissa is index. The vertical lines indicate the day breaks. However this is no solution because, as shown in Fig. 1.3(b), the returns series shows large jumps. These jumps are only explained by the obvious fact that over-nights and weekends are included.

Classification by scale is an attempt to separate multiple time-series processes by their relative time intervals. I cannot say that one can make a clean boundary, but as an analysis tool classification simplifies. The overnight process has few data points, so a longer series is required for statistical analysis.

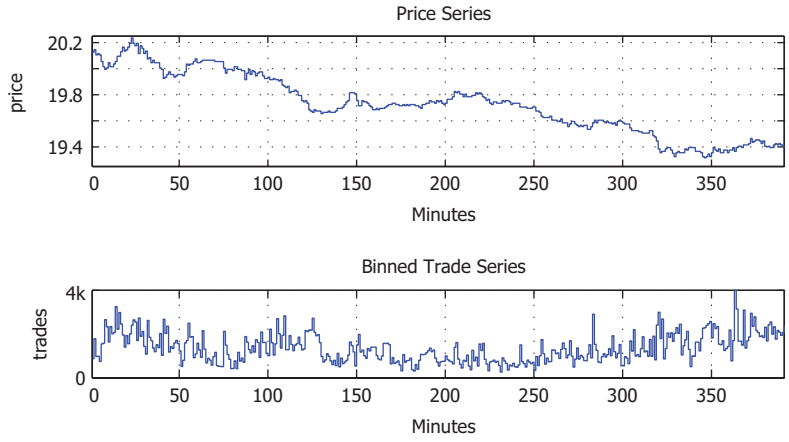

Fig. 1.4 Example time series of a stock price (top) and trade events binned by one-minute intervals (bottom).

Likewise the intraday process can be modeled after the overnight process is removed.

1.2 Filter Design Overview

In this section event outcomes are values such as price or trade volume, see Fig 1.4. The series in the figure are discontinuous and have random innovations. Yet the eye easily picks up the general downward trend of the stock price and the U-shape of the binned trade events. The eye is good at averaging, and in particular *local* averaging.

In statistics there is the well-known concept of regularization. Regularization is a local-average process where the value at each point is replaced by an average of values located in the point's neighborhood. The regularized version of a function $y(x)$ might be written

$$\tilde{y}(x) \equiv \text{Avg}\left(y_i \,|x_i \in \mathcal{N}_\chi(x)\right) \tag{1.1}$$

where Avg is the average function and $\mathcal{N}_\chi$ represents an isotropic neighborhood around x that is χ wide.

I want to adopt the concept of regularization for time-series analysis but the neighborhood cannot include time in the future. What remains are times in the present and recent past. A time-series regularization is conceptually adjusted to read

$$\tilde{y}(t) \equiv \text{Avg}\left(y_i \,\middle|\, t_i \in \mathcal{N}_\tau^-(t)\right) \tag{1.2}$$

where $\mathcal{N}_\tau^-$ represents a neighborhood of t that is τ wide but only including the present and past, indicated by the $-$ sign.

Regularization using only past and present neighborhoods makes the analysis "causal", which is to say only the past causes the present. These lecture notes will deal exclusively with filters of the causal type.

1.2.1 Filters for Local Averaging

Many simple signal processing filters provide causal time series regularization. Figure 1.5 illustrates a box and exponential-moving average (ema) window. A window is a function characterized by its amplitude profile and its temporal extent, and a causal window is zero in amplitude for all times greater than zero. The box window is the most literal. It has a constant amplitude over its domain and has finite support.

As illustrated in Fig. 1.6 the box local average is used as follows. At event m the right edge of the window is aligned to m. Each value of the time series, here representing price, that falls within the non-zero part of the window is included in the average. Each price is multiplied by the associated window amplitude, being constant for a box, and the sum is recorded in the output value at location m. The window is moved to the next event and the process is repeated. The result is a new time series that has been smoothed out.

The ema window illustrated in Figure 1.5 is applied to a time series in the same way but its amplitude profile and support are different. Given its decaying profile, values in the recent past have higher weight than those further away. Even though the ema-window support is semi-infinite (see Fig. 1.6), the average is effectively local. The effective localization length is on the order of the first moment of the ema, which I denote as N_{eff} in discrete time. The effective length N_{eff} is the number of events covered by an e-fold decay in amplitude.

Figure 1.7 shows the result of applying the box and ema windows illustrated above to the price series of Fig. 1.4. There are several features on which to remark. First, both windows smooth out the price series. The degrees of smoothness of the box and ema windows are roughly the same because the effective localization lengths are $\mathcal{L}_1$ matched[1]: $N_{\text{box}} = N_{\text{eff}} / \left(1 - e^{-1}\right)$. A longer window generates more smoothness, a shorter window less. Second, the smoothed series are delayed with respect to the price series. Delay is intrinsic to a regularized time series. A longer window generates more delay, a shorter window less. Lastly, the box and ema smoothed series are not the same. The price difference is plotted in the lowest panel of Fig. 1.7 and deviation of as much as five cents is apparent. The question, "which window is right" is not a valid question. One may only have a preference. Any criteria

[1] A better way to match two filters is spectral matching via Parceval's Theorem.

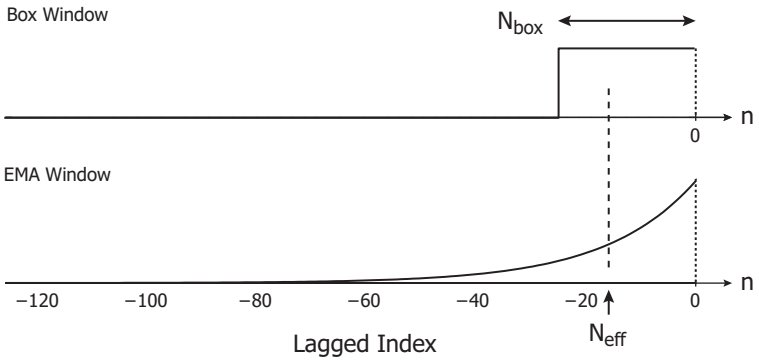

Fig. 1.5 Two examples of local-average windows. The box window has constant amplitude over a fixed interval, here event interval $[0, N_{\rm box}]$. The exponential-moving average (ema) window has an exponential-decay amplitude profile, which gives higher weight to more recent data, and extends to $-\infty$. The effective length of the ema window is $N_{\rm eff}$, which coincides with its first moment.

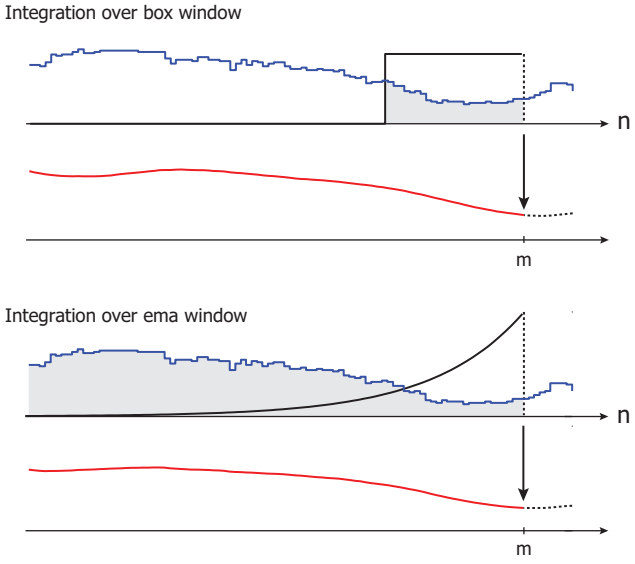

Fig. 1.6 Illustrations of box and ema local-average windows as applied to a time series. At event m the right edge of the box or ema window is aligned to m and data that falls within the window is used in the average. The ema decay is theoretically infinite so all the historical data is used in the average. Yet data within the first low multiple of $N_{\rm eff}$ backwards from m dominates the ema value.

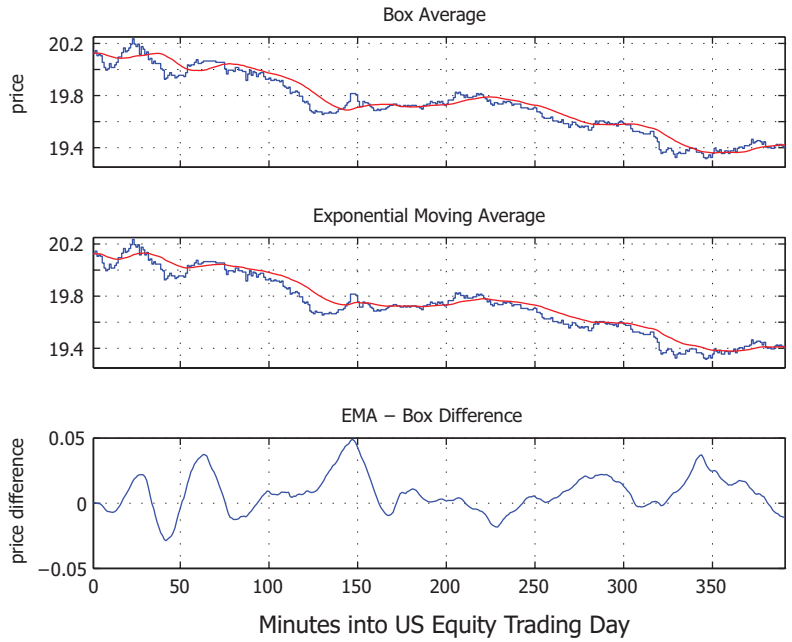

Fig. 1.7 Illustrations of box and ema averages over a discrete price series. The ema has effective length $N_{\text{eff}} = 16$ and the box average is an L_1 equivalent, with the result that these two averages are comparable. Top, Middle: Price series with local-average overlay. The local averages are smooth versions of the price series, and both exhibit delay. Bottom: The price difference between the two local averages. One cannot say that one averaging scheme is right and the other is wrong. However the ema generally has better characteristics.

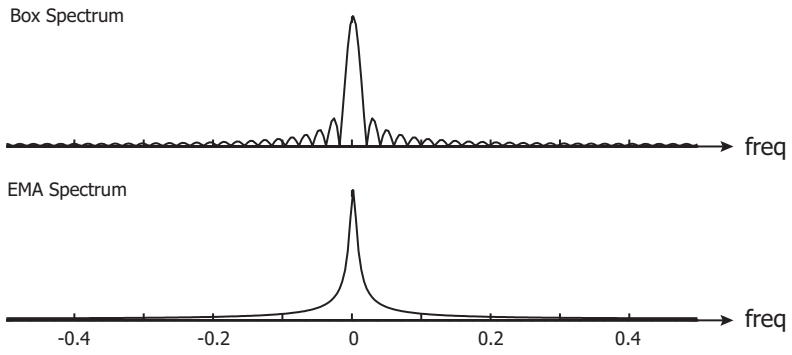

Fig. 1.8 Amplitude spectra of box and ema windows. The box spectrum is functionally $\sin(x)/x$ and clearly has periodic amplitude nulls. The ema spectrum is smooth with no nulls, but does peak at $\omega = 0$ without a vanishing first derivative.

can be used to find a preference. Common criteria are: tolerance to outliers, spectra qualities, ease of implementation, and update speed.

Figure 1.8 illustrates the amplitude spectra of the box and ema windows. Both spectra represent low-pass filters because higher frequencies are attenuated in comparison with the lower frequencies. Such differential attenuation is evident in the smoothed series of Fig 1.7 because the rough parts are largely removed.

Let's now compare the two amplitude spectra to one another. The box spectrum follows the $\sin(x)/x$ profile one expects. Accordingly, there are periodic zeros across the entire spectrum. One would expect distortion in an output series due to the non-monotone, periodic-null amplitude spectrum. The ema spectrum has a monotone decay absent of zeros, so one can expect a smoother output series compared with the box.

1.2.2 Filters for Regularized Differences

Making smooth versions of a rough time series is one important application of a filter. Another important application is making smooth versions of differences. A common difference that arises finance is the log return:

$$r\left(t_{a+h}, t_a\right) = \log\left(p\left(t_{a+h}\right)\right) - \log\left(p\left(t_a\right)\right) \tag{1.3}$$

The right-hand side expresses the difference between two price values p taken at adjacent yet non-overlapping times t_{a+h} and t_a. Such a difference possesses the variance of the process that changes the (log) price from one event to the next. What does a filter look like that can squeeze this variance?

A simple illustration of the window function implicit in the above returns expression will help. Figure 1.9(top) implements a first-order difference with two box windows. One window is positive and has a width of one, the other is negative, has a width of one and is offset one event to the left. Since application of a window function to a time series is completely linear we can consider the upper and lower box windows separately.

Recall from the preceding section that a narrow box window imparts little regularization, with the consequence that an output series is not much smoothed with respect to the input. We are on safe ground to infer that the first-order box differencer in Fig. 1.9(top) will not offer any regularization at all since both boxes have a width of one.

Let's extrapolate and consider a box differencer where each box has significant width, as in Fig. 1.9(middle). Here the upper and lower box windows have the same width as in Fig. 1.5, and the lower box is delayed by a full box width. In this way the two boxes do not overlap nor is there a gap between them. I propose to write an equation that represents this dual-box window as such:

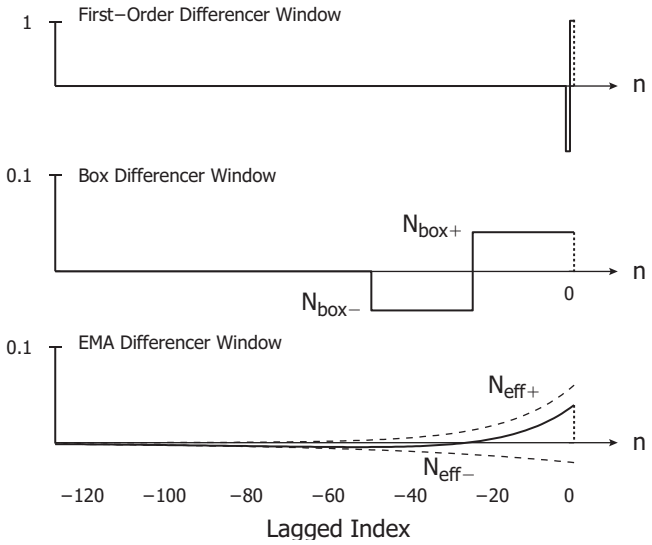

Fig. 1.9 Window functions of three differencers. Top: a first-order differencer composed of two box windows, one positive and one negative, both of unit width and the negative box delayed by one. Middle: a box differencer similar to the one above but where each box has width N_{box}. The negative box is delayed by N_{box}. Bottom: an ema differencer composed of two ema windows of opposite sign, both starting at zero. Here the negative ema has a longer N_{eff} than the positive one, yielding a non-zero composite, illustrated by the solid line.

$$\tilde{r}\left(\mathcal{N}_{\text{box}}(t-\tau), \mathcal{N}_{\text{box}}(t-3\tau)\right) = \log\left(\tilde{p}\left(\mathcal{N}_{\text{box}}(t-\tau)\right)\right) - \log\left(\tilde{p}\left(\mathcal{N}_{\text{box}}(t-3\tau)\right)\right) \tag{1.4}$$

where $\tilde{r}$ and $\tilde{p}$ represent regularized return and price, $\mathcal{N}$ represents the (symmetric) neighborhood centered at times $t-\tau$ and $t-3\tau$, and τ represents half of the box width. This equation is similar to Eq. (1.3) and so I will call this a regularized return, which is itself based on a regularized difference.

The top three panels of Fig. 1.10 show the application of the first-order and box differencers to the same price series shown in Fig. 1.4. The top panel is the original price series. The next panel is the result of applying the first-order differencer window to the prices. Note that the unconditional average is nearly zero and the rate of change in the series is rapid. In fact the advancement of two time steps is all that is required to decorrelate returns. In contrast, the third panel, the result of applying the box differencer, looks nothing like the panel above. The series fluctuation is slow, the amplitude swings are more pronounced, and there is much more autocorrelation. One characteristic is preserved: the unconditional mean is zero (or is so asymptotically).

Still, this study is not complete. The preceding section is written with my bias towards the ema over the box window. How can the ema be applied to a regularized differencer?

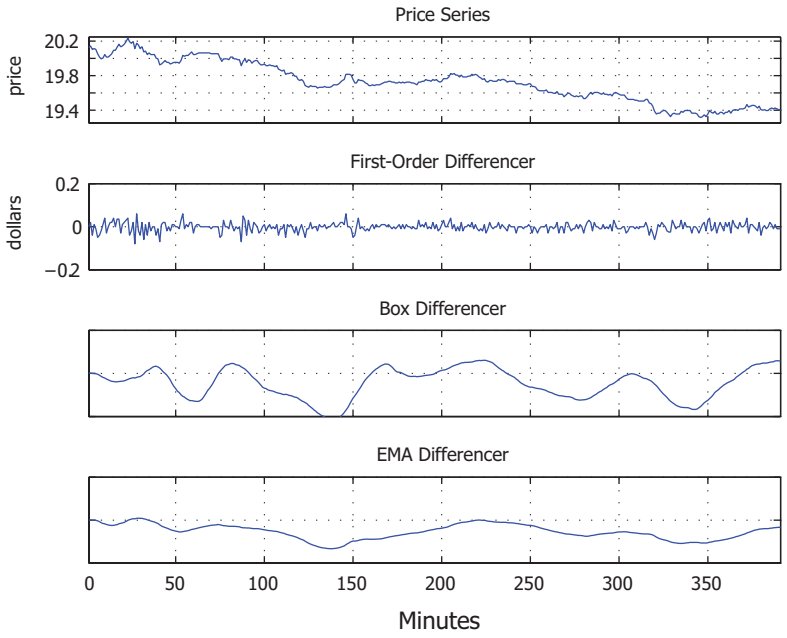

Fig. 1.10 Application of the three differencers of Fig. 1.9 to a price series. Properly constructed differencers yield a zero-centered signal. Top: A price series. Second: The first-order differencer generates high-frequency components and no low-frequency components. Third: The box differencer, which is the same as the first-order but with a wider box, generates a lower-frequency signal. Bottom: The signal from the ema differencer is somewhat lower frequency than above even though the positive arm was L_1 matched to the box differencer.

Principally, we have to violate the no-overlap feature of the box differencers. As long as the two ema's have different characteristic lengths then a solution is feasible. The result is an industry standard called "moving-average convergence-divergence" (macd), which connotates a trading-specific signal but really is just the difference between two ema's.

Figure 1.9(bottom) illustrates the macd window. First, there are two arms each made with an ema. One is positive, the other negative, and the lengths differ. The area under each arm is the same, albeit with opposite sign, so that the area of the sum is zero. The ema-based differencer window is the sum of these two arms. The solid line of the figure shows the difference. This causal curve has one section with positive area and a second section with negative area separated by the zero-crossing of the curve. While the shape of the positive and negative sections are not the same they do both generate local averaging.

Figure 1.10(bottom) shows the application of the ema-based differencer window to the price series. This time series is also highly regularized and fluctuates more slowly than the box differencer, even though the ema's were

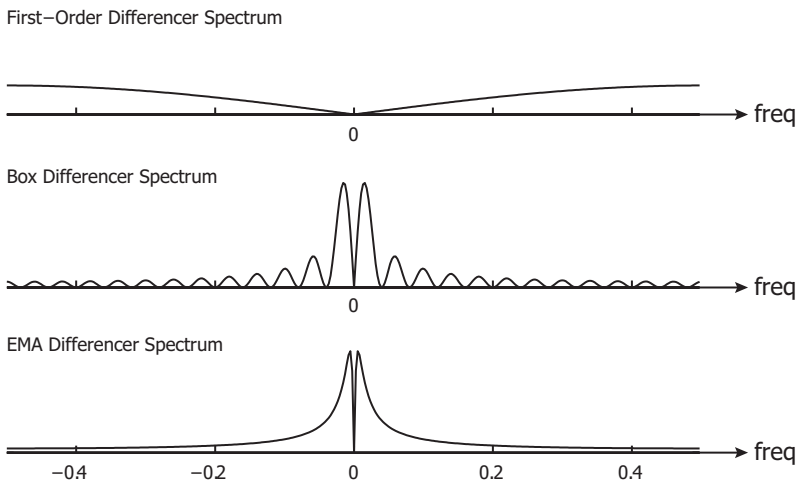

Fig. 1.11 Amplitude spectra of the first-order, box and ema differencers. All spectra have vanishing amplitude at zero frequency, which mean that the DC component of any incoming signal is removed in steady state. Top: The first-order differencer has the widest bandwidth, thus capturing high-frequency components. Middle: The box differencer has a narrower version of the above spectrum. The the box local average, this spectrum has periodic amplitude nulls. Bottom: The ema differencer has a smooth amplitude profile other than $\omega = 0$.

roughly $\mathcal{L}_1$ matched to the box-window counterpart. A better match can be made via spectral analysis but I am illustrating here that a naïve match is not suitable.

A complement of the differencer windows is their spectrum. The amplitude spectrum of the three differencers thus far considered is illustrated in Fig. 1.11. A common feature is that the DC amplitude[2] is zero in all cases. The zero amplitude at DC annihilates any unconditional average present in the input series. Figure 1.10 illustrates as much.

The first-order differencer is narrow in time and therefore wide in frequency. Its amplitude spectrum, for the frequency range I used, does not reach its first non-DC null; that is, the first-order differencer has a broad spectrum. This, too, is evident in the corresponding fast-moving output signal in Fig. 1.10. The box differencer has the same functional form as the first-order differencer but due to its comparatively long temporal duration the spectrum is more compact. Here the periodic nulls that were present for the box-type local-average window appear again. Due to the tighter spectrum fewer high-frequency components are admitted with the result of a low-frequency output (except DC).

[2] In electrical engineering DC refers to direct current and carries the connotation of zero frequency, i.e. $\omega = 0$.

The ema differencer is smooth, like its local-average counterpart, except for the null at DC. It is apparent that this spectrum is more compressed than the box differencer, which is the real reason behind the slower moving output. Matching the spectral widths, while inexact, would allow for a more direct comparison of these two filters.

1.2.3 Higher-Order Local-Averaging Filters

Regularized averages and differences of a price series have dominated the preceding sections. One typical feature of a price series is that innovations are somewhat Gaussian, excluding event-based jumps. Another type of financial series is one driven by innovations that are somewhat Poisson. A series drawn from a one-sided distribution can be less smooth than, say, a price series. A higher degree of regularization might be sought, so are there better methods than simply widening the filter window?

The answer is yes and this brings us to higher-order filters. I have not yet presented what the order of a filter means, although *order* is in the sense of polynomial order, not rank order. Suffice it to say that an ema is first-order and a box filter is very high order. Second-, third- and higher-order filters offer more degrees of freedom to design the shape of the regularization window and can, in many cases, add smoothness without increasing the length of the window.

Figure 1.12(top) illustrates a trade series. The series represents the number of trades that occur in a consecutive series of one-minute intervals. The question at hand is how to smooth out this data.

The box and ema filters are two candidates. The next two panels show the result of applying a box and ema filter with equivalent lengths. Both filters smooth the trade-bin data, however neither output is particularly smooth.

To increase smoothness without increasing the window length two filters can be applied in succession. In the case of trades, it makes physical sense to first accumulate the trades rather than working with binned trades because accumulation, or integration in continuous time, reduces noise. The accumulated trades are then differenced but not with a first-order differencer, which would recover the original series, but with a regularizing macd differencer.

The two steps of accumulation and differencing can be combined into a single step in this way: Rather than applying the first filter to the input and the second filter to the result, one filter can be applied to the other before either is applied to the input. Figure 1.13 illustrates this. The top panel shows the accumulating window, which is semi-infinite. The accumulating window does not yield a local average, it remembers the complete history of the input. The middle panel illustrates an macd window. It happens that this macd window is special because the N_{eff} of the positive and negative arms is the same. A later chapter will cover what this means. The bottom panel

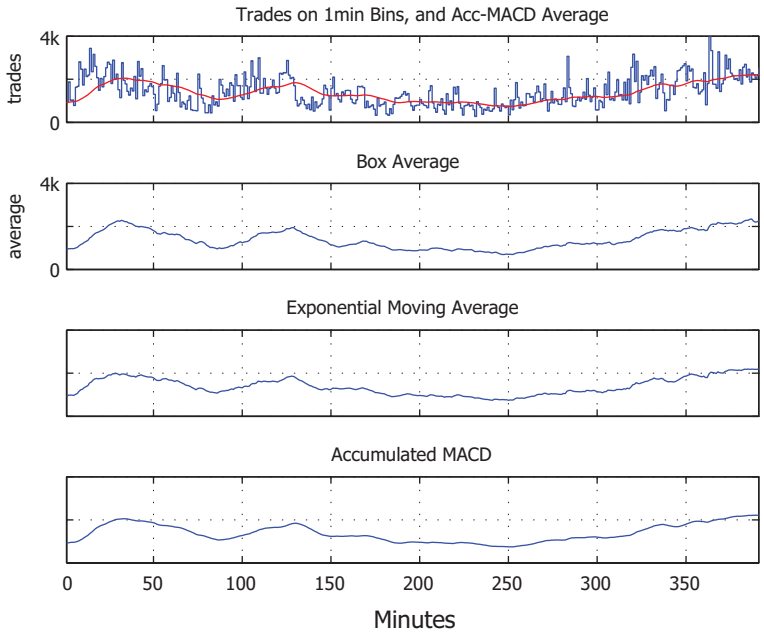

Fig. 1.12 Local averages over a trades process. A second-order window yields first-order smoothness. Top: A trades process that counts the number of trades in fixed wall-clock bins (1 min). A local average model, indicated in red, indicates average trade intensity. Second: The trades process averaged by a box window. The signal is continuous but has discontinuities in its first derivative. Third: Application of an ema window of equivalent length. Bottom: Application of higher-order filter yields a smoother series with little sacrifice of bandwidth. The filter used here is what I call an accumulating macd filter.

shows the result of applying the accumulator to the macd; I call the resulting window an accumulating macd. This shape is a higher-order filter.

Figure 1.12(bottom) shows the result of applying the accumulating-macd window to the binned trade series. The bandwidth is nearly the same as the box and ema filters (and can be further tuned to have identical bandwidths) but the series is quite a bit smoother.

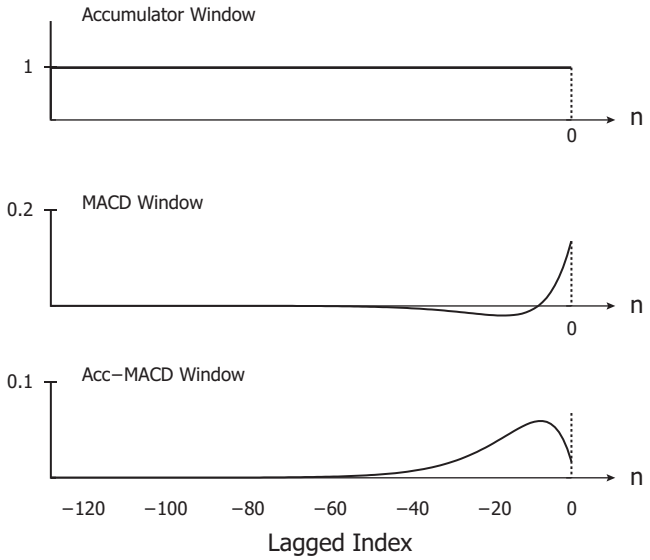

Fig. 1.13 The accumulating macd filter, as I call it, is derived in two steps. An accumulator window (top) is applied to make a cumulative sum of the trade quantities. This window is semi-infinite and has infinite area. Next, an macd window (middle) is applied to take a regularized difference. These two steps may be combined by applying the macd to the accumulator before either is applied to the trades series. The result is the accumulating macd filter (bottom).

1.3 Common Mistakes

In preparing the examples for this chapter I have avoided the common mistakes that are easily made. At a pedagogical level it seems important to highlight some of the ways to get a wrong result.

Two of the easiest attributes to get wrong are *level* and *gain*. Regarding level let's decompose a finite-sample price series $p_n : n \in [0, N]$ as follows:

$$p_n = p_0 + \sum_{k=1}^{n} dp_k \tag{1.5}$$

where $dp_k = p_k - p_{k-1}$. The initial price p_0 is constant over the whole series. Now let's apply an ema to the price series. Later chapters will present the mathematics but here I just write $f(p_n; \text{ema})$ where $f(\cdot)$ is a linear function. Thus

$$f(p_n; \text{ema}) = f(p_0; \text{ema}) + f\left(\sum_{k=1}^{n} dp_k; \text{ema}\right)$$

The result is the sum of two ema's, the first over the constant p_0 and the second over the price series less the initial value, see Fig. 1.14(top). The ema over p_0 is equivalent to taking an ema of an accumulator scaled by p_0, which results in a large start-up transient. The start-up transient in fact looks just like an integrated ema, or approximately $1 - \exp(-t/\tau)$. So, as calculated and plotted, the applied ema has a bad initialization.

Gain error has its own characteristic. Consider an arbitrary scale factor g applied to an ema window. Application of that window to a price-difference series gives

$$f(p_n - p_0; g \text{ ema}) = gf(p_n - p_0; \text{ema})$$

again due to the linearity of the filter. The amplitude of the ema output follows the scale-factor g. Unless there is a compelling reason, the scale factor, or what is properly called gain, of a local-averaging filter should always be unity. Figure 1.14(bottom) illustrates an ema with a gain of 1/10.

A good question is what is the right gain for a regularized differencer. A differencer of any regularization degree ought to difference, annihilating the DC value. Well, indeed the gain of a differencer is always zero. This leaves an arbitrary common scale to the positive and negative arms that make up the differencer. In the context of differencers, the choice of common gain of the arms is what is called the *gauge*. A typical gauge is unity.

Another common problem is the incorrect use of clock. Recall from Fig. 1.1 that a discrete-time series uses an index n as a proxy for time. The index n needs to represent informative events. I do not believe that one can say there is a correct clock because a clock must only be consistent with a model. But an incorrect clock is pretty easy to achieve.

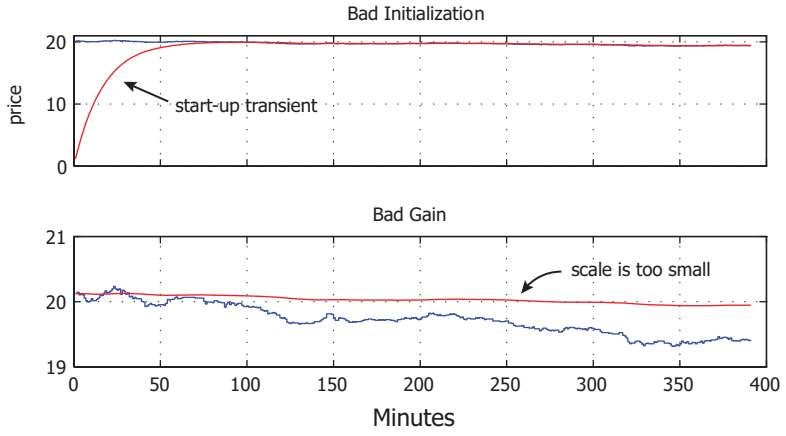

Fig. 1.14 Error types when a window is misapplied to a signal. Top: Bad initialization leads to a significant start-up transient feature. Bottom: Bad gain means that there is a scale difference between the input and the resulting signal. As illustrated the gain is too small.

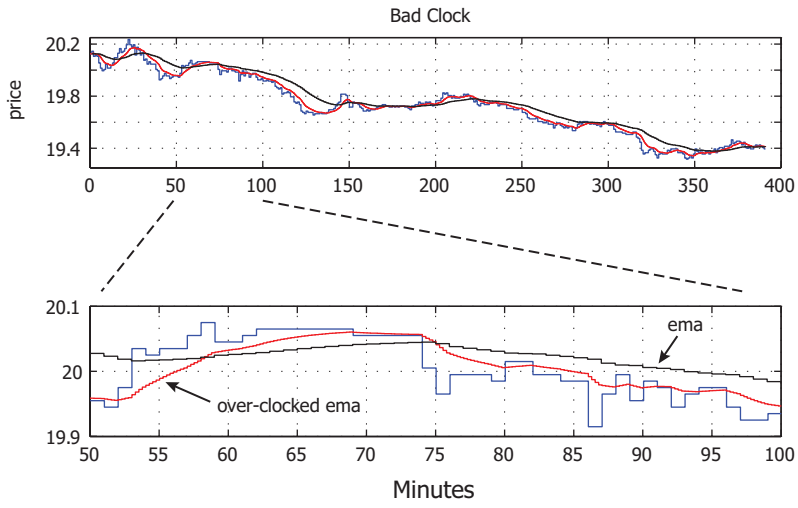

Fig. 1.15 Illustration of an input price series and two ema windows, one with the "correct" clock and the other that is overclocked. A clock event should reflect an information event. Overclocking refers to uninformative clock events. Top: Overlay of price series with two local averages. The overclocked average closely hugs the input, effectively shortening its window length. Bottom: Inset of price changes on 1-minute intervals, the ema signal and its overclocked counterpart.

As in Fig. 1.15 two ema's are applied to a price series. In the first case, the ema is updated at each one-minute interval, which is consistent with the arrival of the data in this example. The characteristic length of the ema is the same as in earlier figures. In the second case, another ema is updated multiple times within and at each one-minute interval. The result is an effective decrease of the window length, which in turn permits the ema output to hug the price series more closely. What is wrong with this? Well, nothing perhaps, but the ema of the second type does not correspond to the level of smoothness originally intended by the model. Moreover, at least in this case, the updates between one-minute boundaries are uninformative, so the ema output is fictitious. In a more realistic example the number of updates per one-minute interval is stochastic so there is a random, variable length of the filter window.

The best recommendation regarding clock is to ensure that updates represent the arrival of new information.

Chapter 2
Convolution

Convolution is the mathematical framework used to apply a regularizing window to an ordered series such as a time series. Convolution is a succinct, rigorous approach but as with all frameworks there are caveats. Principally, the window function must be fixed in shape: the window cannot change as a function of position. Secondly, boundary conditions have to be considered. The two flavors of boundary conditions are *open* and *circular*. Financial applications need to apply open convolutions and you the reader need to know which of the two flavors is being used by a software package. The remaining considerations are technical.

Convolution plays a significant role in the theory of signal processing because it is the dual of multiplication in transform space. A good way to consider the duality in a financial context is that convolution is the method to apply a window to an input series, transform methods provide the way to create windows having desired properties.

This chapter starts to change the vocabulary from the colloquial terms that I used in the introduction to their more rigorous counterparts. The most important change is this: a **window shape** is replaced by an **impulse response**, and to boot, impulse responses are mirror-images, or left-right flips, of window shapes. The left-right flip is not arbitrary but follows from the derivation; it is my pedagogical window shape that is in fact the flip of the impulse response. Figure 2.1 illustrates the difference.

Finally, it is customary to denote an impulse response with the letter h. In continuous and discrete time this is written as $h(t)$ and $h[n]$. The impulse response $h(\cdot)$ encodes the flip of a fixed-shape regularization window that can be applied to any input series.

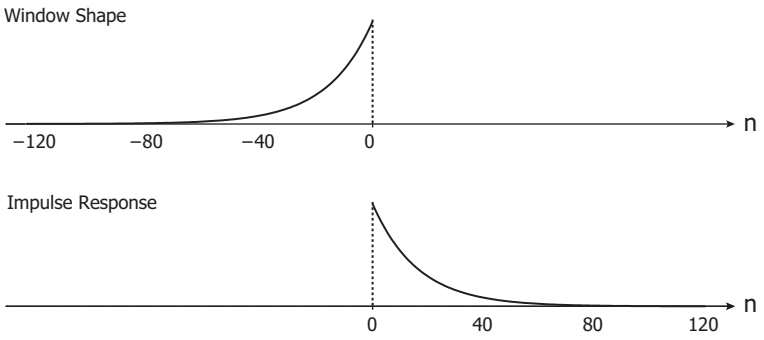

Fig. 2.1 Illustration of an ema window shape and its corresponding impulse response. A causal window tails off to the left, while a causal impulse response has support on non-negative index values.

2.1 Superposition Construction of Series $x[n]$

The mechanics of convolution are best learned in discrete time, the generalization to continuous time early follows. In discrete time I use the index n to indicate position. This contrasts with many texts that use the symbol t even in a discrete context; I prefer to be very clear with the representation of time.

Denote an arbitrary discrete-time series by $x[n]$. The series $x[n]$ can be realized as a pair of vectors that forms a matrix:

$$\begin{aligned} x[n] \ &\sim (\mathbf{n} \quad \mathbf{x_n}) \\ &= \begin{pmatrix} \cdots & \cdots \\ -2 & x_{-2} \\ -1 & x_{-1} \\ 0 & x_0 \\ 1 & x_1 \\ \cdots & \cdots \end{pmatrix} \end{aligned} \tag{2.1}$$

The first column stores the positions n in the series, the second the amplitudes x_n. Amplitudes x_n are just a collection of numbers, they don't have a position. The matrix above can be rewritten as a map between n and x_n or a function. In any event the point is that a series $x[n]$ has two parts: position and amplitude. A computer will represent a time series in this way. In fact the position n is often implied and the programmer must explicitly track the index range.

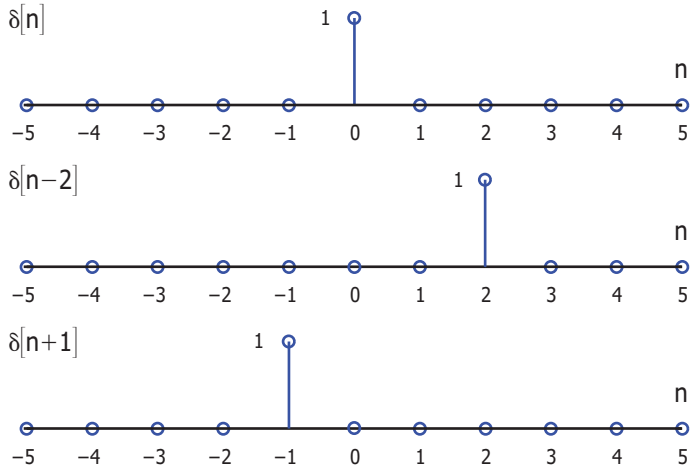

Fig. 2.2 The delta function at three positions. $\delta[n]$ is unity at $n = 0$ and zero elsewhere. $\delta[n-2]$ is unity at $n = 2$, which is to the right of the origin. The -2 parameter means delay so the impulse is right-shifted by two slots. $\delta[n+1]$ is unity at $n = -1$, to the left of the origin.

An alternative representation is to use the superposition construction. Using a discrete-time impulse function will allow us to account for both position and amplitude as orthogonal components.

The basic unit of a discrete-time series is the impulse function, denoted $\delta[n]$, and defined by

$$\delta[n] = \begin{cases} 1, & n = 0 \\ 0, & \text{otherwise} \end{cases} \tag{2.2}$$

Figure 2.2 illustrates the impulse function. An impulse is zero everywhere and unity when its argument is zero. The impulse is shifted to a higher index n when written $\delta[n-k]$ for positive k and shifted to a lower index for $\delta[n+k]$. The impulse function is also known as a Kronecker delta function, and in continuous time it is the Dirac delta function.

The property of the impulse function is that it picks out one element of a series $x[n]$. For instance, using the impulse $\delta[n]$, which is unity only for $n = 0$, the product $\delta[n]x[n] = x[0]$ for $n = 0$ and is zero otherwise. The impulse $\delta[n-1]$ when multiplying $x[n]$ yields $x[1]$ at $n = 1$ and zero otherwise. The general expression is

$$x[n] = \sum_{k=-\infty}^{\infty} \delta[n-k]x[k] \tag{2.3}$$

Equation (2.3) is the *superposition* construction of $x[n]$. Each coefficient $x[k]$ is simply an amplitude; the position of this amplitude in a time series is determined by the index n of the impulse function. The full series $x[n]$ is the sum of all properly weighted impulse functions across n. In reference to the preceding, $\delta[n-k]$ plays the role of $\mathbf{n}$ to give position, and $x[k]$ plays the role of $\mathbf{x_n}$ to specify amplitude.

Note that while this equation appears straightforward, the indexing of the impulse within the sum runs backward as a function of k. As the summation index k sweeps the integer axis with positive increments the impulse argument $n-k$ sweeps in the opposite direction. The index to the impulse has a left-right reversal about the offset n. The left-right flip that I highlighted earlier already makes an appearance in the superposition construction of $x[n]$.

2.2 Transformation of Series $x[n]$ by Operator $T[\cdot]$

Consider now two time series, $x[n]$ and $y[n]$. An input series, say $x[n]$, is transformed into an output series, say $y[n]$ via a transformation function $T[\cdot]$:

$$y[n] = T\left[x[n]\right] \tag{2.4}$$

This equation expresses a transformation of one series into another, however $T\left[.\right]$ is not the univariate function one thinks of when one writes $y = f(x)$. The input here is a series $x[n]$, not a scalar. A good way to think about the action of $T[\cdot]$ is to use the matrix notation from above. Equation 2.4 may be written as

$$\begin{pmatrix} | & | \\ n & y_n \\ | & | \end{pmatrix} = T \begin{pmatrix} | & | \\ n & x_n \\ | & | \end{pmatrix} \tag{2.5}$$

In general $T\left[.\right]$ is a function of both $\mathbf{n}$ and $\mathbf{x_n}$ and maps the result onto the same positions $\mathbf{n}$ with new amplitudes $\mathbf{y_n}$. To emphasize the point, the amplitudes $\mathbf{y_n}$ can be a function of all $\mathbf{n}$ from the input.

This is all very general. To progress let us limit the possibilities for the transformation T.

Given a series $x[n]$, the transform $T\left[x[n]\right] \rightarrow y[n]$ is *linear* if and only if

$$T\left[x_1[n] + x_2[n]\right] = T\left[x_1[n]\right] + T\left[x_2[n]\right] = y_1[n] + y_2[n] \tag{2.6}$$

and

$$T\left[ax[n]\right] = ay[n] \tag{2.7}$$

where a is a constant. The first equation expresses *linearity*, the second *homogeneity. Superposition* is a consequence of linearity and homogeneity; for constant coefficients $a_{1,2}$, superposition is defined by

$$T\left[a_1x_1[n] + a_2x_2[n]\right] = a_1T\left[x_1[n]\right] + a_2T\left[x_2[n]\right] = a_1y_1[n] + a_2y_2[n] \quad (2.8)$$

Linearity and homogeneity, or in short, superposition, are properties of $T[\cdot]$ alone; they hold for arbitrary inputs $x[n]$.

Consider another transform $T'\left[x[n]\right] \rightarrow y[n]$. This function is *time invariant* if for all N

$$T'\left[x[n-N]\right] = y[n-N] \quad (2.9)$$

Like linearity, time invariance is a property of $T'\left[\cdot\right]$ in that the transform itself is independent of $n-N$. To explain time invariance refer to the matrix transform relation written in (2.5). For positive N the series $x[n-N]$ is delayed, which means that the amplitudes x_n are shifted downwards in the second column by N rows; the first column of the matrix is unchanged. Time invariance is to say that the output $y[n]$ has its amplitudes y_n shifted down by N rows but is otherwise unaltered. For example, with $N = 1$:

$$\begin{pmatrix} \cdots & \cdots \\ -2 & y_{-3} \\ -1 & y_{-2} \\ 0 & y_{-1} \\ 1 & y_0 \\ \cdots & \cdots \end{pmatrix} = T' \begin{pmatrix} \cdots & \cdots \\ -2 & x_{-3} \\ -1 & x_{-2} \\ 0 & x_{-1} \\ 1 & x_0 \\ \cdots & \cdots \end{pmatrix}$$

In contrast, when a transform is not time invariant then one can only write

$$T^{\text{non}-\text{invariant}}\left[x[n-N]\right] = y[n;N]$$

That is, $y[n;N]$ is a function of (n,N) rather than simply $n-N$.

2.3 The Impulse Response: A Linear Time-Invariant Transformation

Let us combine the series transformation (2.4), the superposition construction of $x[n]$ (2.3) and linear and time-invariant properties to $T\left[\cdot\right]$ (2.8-2.9). Using the superposition form of $x[n]$ and investing $T\left[\cdot\right]$ with linearity gives

$$\begin{aligned} y[n] &= T\left[\sum_{k=-\infty}^{\infty} \delta[n-k]x[k]\right] \\ &= \sum_{k=-\infty}^{\infty} T\left[\delta[n-k]x[k]\right] \end{aligned}$$

Now, $T[\cdot]$ operates on positions $\mathbf{n}$ and associated amplitudes. The amplitudes of $\delta[n-k]x[k]$ are zero except for $n=k$, where the amplitude is $x[k]$. We can just as well replace all amplitudes x_n with a single value x_k knowing that the impulse will select x_k in the right position and vanish elsewhere. Next, give $T[\cdot]$ the property of homogeneity and we have

$$T\left[\delta[n-k]x[k]\right] = T\left[\delta[n-k]\right]x[k]$$

which then gives

$$\begin{aligned} y[n] &= \sum_{k=-\infty}^{\infty} T\left[\delta[n-k]\right]x[k] \\ &= \sum_{k=-\infty}^{\infty} h[n;k]x[k] \end{aligned}$$

Lastly, adding time-invariance to the attributes of $T[\cdot]$ yields

$$\begin{aligned} T\left[\delta[n-k]\right] &= h[n;k] \\ &\rightarrow h[n-k] \end{aligned}$$

Putting these pieces together we have

$$\begin{aligned} x[n] &= \sum_{k=-\infty}^{\infty} \delta[n-k]x[k] \\ y[n] &= \sum_{k=-\infty}^{\infty} h[n-k]x[k] \end{aligned} \tag{2.10}$$

The first equation forms $x[n]$ via the superposition of amplitudes x_k and impulse functions, the second equation forms $y[n]$ via the superposition of the same amplitudes x_k and an *impulse-response* function $h[n]$. The impulse response function is determined solely by the transformation $T[\cdot]$ is defined as

$$h[n] \equiv T\left[\delta[n]\right] \tag{2.11}$$

The series $h[n]$ is generated the linear, time-invariant (LTI) transformation of a single impulse function that is unity only at position $n=0$. This is why $h[\cdot]$ is called an *impulse response*.

The LTI transformation $T[\cdot]$ is the generator of the impulse response $h[n]$. $T[\cdot]$ and $h[\cdot]$ are characteristics of the system (or, alternatively, the filter), which has nothing to do with a particular input to the system.

Equation 2.10 expresses the output $y[n]$ as the *convolution* of the impulse response $h[\cdot]$ with an input $x[n]$. Let's write the discrete- and continuous-time versions here in one place. The discrete-time, open convolution is

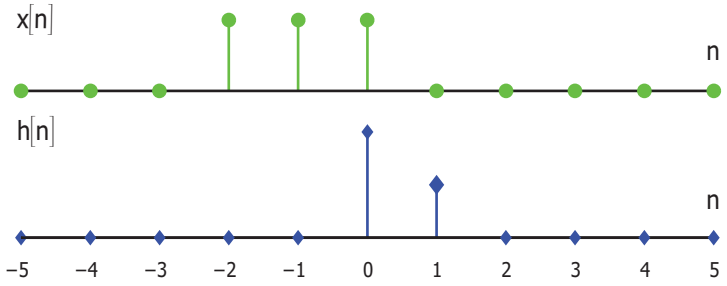

Fig. 2.3 An input $x[n]$ will be convolved step-by-step with a finite-length system response $h[n]$. Note that $h[0] > h[1]$.

$$y[n] = \sum_{k=-\infty}^{\infty} h[n-k]x[k] \tag{2.12}$$

and the continuous-time (open) expression is

$$y(t) = \int_{-\infty}^{\infty} h(t-\tau)x(\tau)d\tau \tag{2.13}$$

It is customary to write convolution with the shorthand operator $*$, as in

$$y[n] = h[n] * x[n] \tag{2.14}$$

In fact, the superposition representation of a series, e.g. Eq (2.3), is a convolution, one with a delta function: $x[n] = \delta[n] * x[n]$.

2.3.1 Procedure

The procedure to evaluate convolution is best learned in discrete time. Figure 1.6 on page 12 of the Introduction has already illustrated the concept. Now we must work through the details of Eq. 2.12.

I start with a very simple example. Figure 2.3 plots the time series for input $x[n]$ and impulse response $h[n]$. $x[n]$ is a box that is finite at positions $(-2, -1, 0)$. The impulse response is finite in length and non-zero at positions $(0, 1)$. Note that $h[0] > h[1]$ in this example. The convolution $y[n]$ will be evaluated step by step in n.

First, take n such the two signals don't overlap: say $n = -3$, Fig. 2.4(a). The convolution is

$$y[-3] = \sum_{k=-\infty}^{-3} h[-3-k]x[k] \tag{2.15}$$

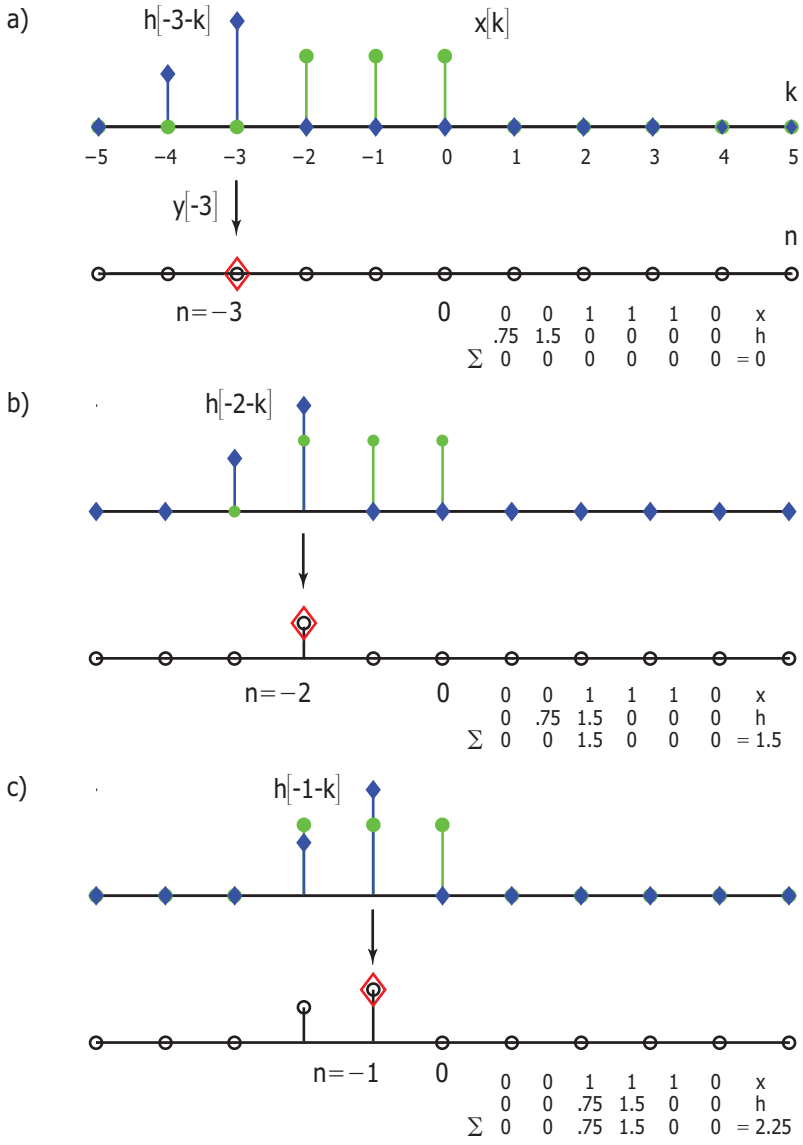

Fig. 2.4 Step by step convolution. a) $n = -3$, the input $x[k]$ remains fixed (in this construction) on the k axis. That is, there is the replacement $n \to k$. The impulse response $h[n]$ is flipped and shifted when indexed as $h[-3-k]$. The $h \times x$ product is taken for all k and summed: the result is recorded at $y[-3]$. b) $n = -2$, there is overlap between $x[k]$ and $h[-2-k]$. A finite value is recorded at $y[-2]$. c) $n = -1$.

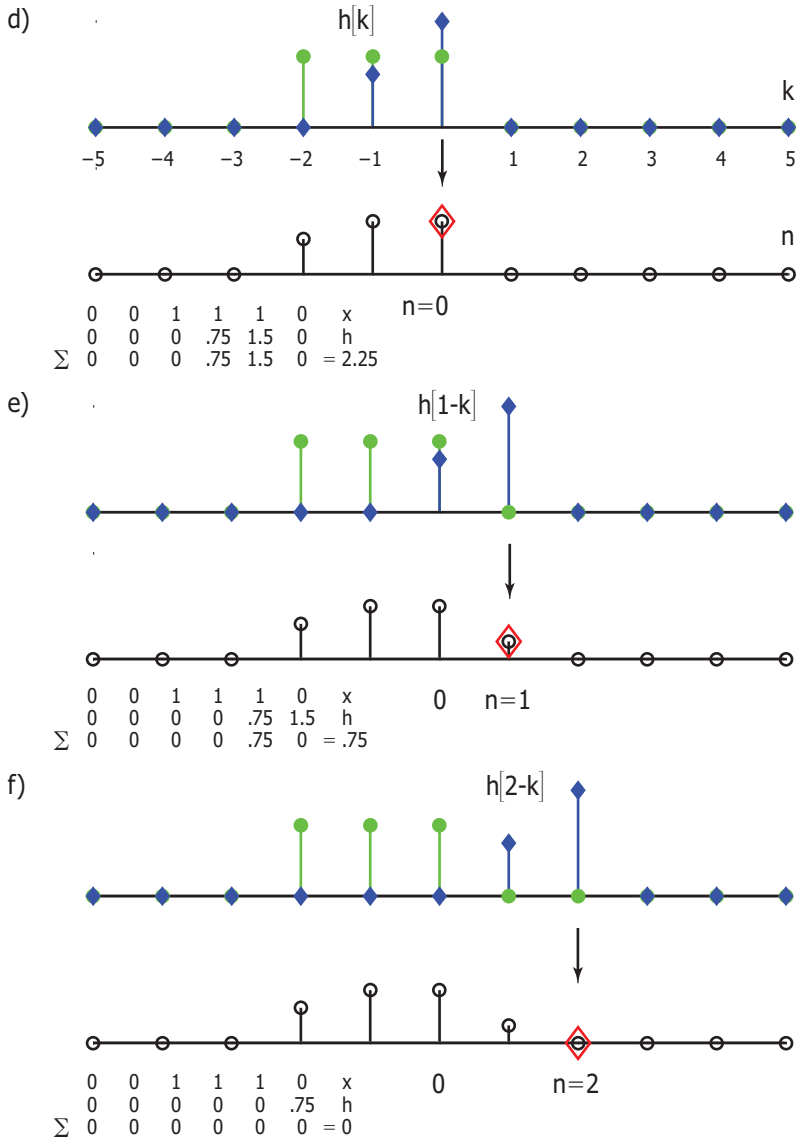

Fig. 2.5 Step by step convolution continued. a) $n = 0$. b) $n = 1$. c) $n = 2$, there is no longer overlap between the input and impulse responses. For $n \geq 2$ the output $y[n] = 0$. The result of the two-point impulse response with the three-point input is a four-point output the remains causal but has its energy spread along the position axis.

In the figure, $x[k]$ is in the same place as in Fig. 2.3 as $x[n]$. In fact the input $x[k]$ will not move as each position n is evaluated. In contrast, $h[-3-k]$ has done two things.

First and foremost the time series $h[n]$ as in Fig. 2.3 is *flipped* left to right. This is due to the $-k$ term in $h[n-k]$. In fact $h[-n]$ is the window shape, shifted to position n, that corresponds to impulse function $h[n]$. While we will deal with impulse responses in this and the following chapters, the procedure of convolution in fact deals with window shapes.

Second, the position of $h[n=0]$ impulse is shifted to $n=-3$. So, there is a flip then a shift.

Accordingly, $h[-3-k] \times x[k]$ is calculated for each k and summed. At position $n=-3$ the sum is zero; this value is recorded in $y[-3]$ as illustrated.

The next position is $n=-2$, see Fig. 2.4(b). The step up is the same: $x[k]$ is fixed in position; $h[-2-k]$ is a flipped compared with $h[n]$ and shifted to $n=-2$; the product $x \times h$ is point-wise computed and then summed. The result, $y[-2]$, is recorded at this position. Since there is overlap between $x[k]$ and $h[-2-k]$, $y[-2]$ is finite.

This procedure is repeated for all values of n, see the remaining figures 2.4(c-f). The next notable position is $n=2$: from this point on $x[k]$ and $h[n-k]$ no longer overlap, so $y[n]$ will be zero for the remaining n.

Let us compare the output $y[n]$ with the input $x[n]$. The associated figures are Fig. 2.3 (top) for $x[n]$ and Fig. 2.5(f) (bottom) for $y[n]$. The output is wider than the input: the impulse response has spread the energy in $x[n]$ along the axis. While the output is wider, its starting point remains at $n=-2$: this particular impulse response has not position-shifted the output. Finally, the features of the output are less sharp than the input. This is not fundamental, but happens to be true for this example.

2.4 Properties of Convolution

Convolution is the consequence of linear, time-invariant transforms of a time series. Additional properties may include causality, stability, gain and k-order moments.

2.4.1 Causality

A system is said to be *causal* if its output at time t does not depend on the future of its input. In the current context $y[n]$ cannot depend on $x[n+N]$ for $N>0$. In terms of convolution, Eq. (2.10) is restricted to

$$y[n] = \sum_{k=-\infty}^{n} h[n-k]x[k] \tag{2.16}$$

This restriction may be imposed simply by saying that $h[n]$ must be zero for $n < 0$; that is, $h[n]$ is finite on the right-hand side of zero (inclusive). Thus:

$$h[n] = \sum_{k=0}^{\infty} \delta[n-k]h[k] \tag{2.17}$$

Causality makes sense from a forecasting perspective, but one should know that in other contexts this constraint can be relaxed. For instance, there are several algorithms to insert estimates for missing data points. Some of these algorithms are completely linear, such as the Kalman smoother, but require an entire series to find the best estimates. Convolution is used, or implied, but causality is not a constraint in such a context.

2.4.2 Stability

The stability one considers for LTI systems is called bounded input bounded output, or BIBO. BIBO stability says than for any bounded input series the output is also bounded. BIBO stability is a property of the system, not any one input. It also may not exist so its absence needs to be identified.

For a finite value B_x the series $x[n]$ is bounded when $|x[n]| < B_x$ for all n. A transformed series $y[n]$ is bounded when

$$\begin{aligned} |y[n]| &= \left| \sum_{k=-\infty}^{\infty} h[n-k]x[k] \right| \\ &\leq \sum_{k=-\infty}^{\infty} |h[n-k]|\,|x[n]| \\ &\leq B_x \sum_{k=-\infty}^{\infty} |h[n-k]| \end{aligned}$$

Clearly the output is bounded only when the system response is itself bounded:

$$B_h = \sum_{n=-\infty}^{\infty} |h[n]| < \infty \tag{2.18}$$

The inequality $B_h < \infty$ is the necessary and sufficient condition for BIBO stability of an LTI system.

2.4.3 Gain

Gain is the change in overall scale between input and output due to the system response $h[n]$. For a stable system gain g is the sum of the impulse response over all time:

$$g \equiv \sum_{n=-\infty}^{\infty} h[n] \tag{2.19}$$

Generally it is good form to set $g = 1$ when feasible. A geometrically decaying series is a feasible example. Examples where this is not possible are a differencer, where $h[n] = ((0,1),(1,-1))$ giving a gain of zero; or an accumulator, where the gain is infinite.

2.4.4 k-Order Moments

The first-, second-, and higher-order moments of an impulse response are often of interest. Gain is really the zeroth-order moment. The k^{th}-order moment $M^{(k)}$ is defined in discrete time as

$$M^{(k)} \equiv \sum_{n=-\infty}^{\infty} n^k h[n] \tag{2.20}$$

As with gain, not all impulse responses have finite moments.

2.5 Examples

Several key examples are now detailed.

2.5.1 Ideal Delay

To ideally delay a signal is to shift the input series to a higher index without altering its shape[1]. Figure 2.6 illustrates the impulse response that delays an input by one position: $h[n] = \delta[1]$. The output is a replica of the input shifted to the right.

An ideal delay $\delta[n]$ is causal as long as $n \geq 0$. Otherwise the output would predict the input. An ideal delay is also BIBO stable since clearly $B_h < \infty$. Finally, an ideal delay is the simplest of FIR impulse responses.

[1] Refer to convolution/illustrate_convolution_pure_delay.m

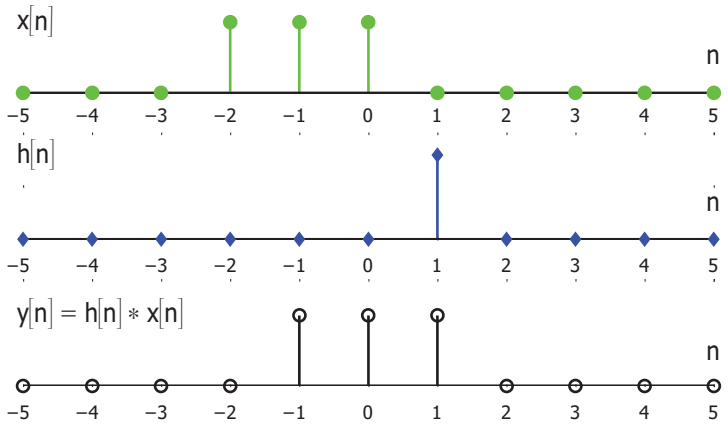

Fig. 2.6 An ideal delay convolved with an input box. The system response is causal, stable and has zero gain. The output shape exactly matches the input but delayed by one position.

2.5.2 Unit Step

The unit step $u[n]$ impulse response is defined by

$$h[n] = u[n] \equiv \sum_{k=0}^{\infty} \delta[n-k] \tag{2.21}$$

Here $u[n]$ is causal but not BIBO stable. The unit-step impulse response accumulates the input stream; in continuous time it is an integrator. An obvious application is to transform a compound returns series into a price – this requires accumulation.

2.5.3 Infinite Comb and Replication

Consider a comb impulse response, defined as

$$h[n] = \sum_{k=-\infty}^{\infty} \delta[n-kN] \tag{2.22}$$

where N is the step size between adjacent impulses, Fig. 2.7. The comb impulse response *replicates* an input series $x[n]$ in time with a replication spacing of N. That is,

Fig. 2.7 In either domain of a Fourier dual, a shape convolved with an impulse comb generates replications of the shape at each impulse location.

$$\begin{aligned} y[n] &= \sum_{i=-\infty}^{\infty} \sum_{k=-\infty}^{\infty} \delta[n - kN - i]\, x[i] \\ &= \sum_{k=-\infty}^{\infty} x[n - kN] \end{aligned} \tag{2.23}$$

Figure 2.7 illustrates the resultant $y[n]$. At every index $n = kN$ the signal $x[n]$ is repeated as if the index were reset to zero. If the temporal extent of $xx[n]$ is $< N$ then there is no overlap between adjacent replicas, otherwise overlaps exists. Overlap due to replication is called *aliasing*: The signal $x[n]$ is aliased by the impulse response.

2.5.4 FIR Response

Finite-impulse response (FIR) is characterized by a finite-length output given a finite-length input. Figure 2.8 illustrates a box impulse response convolved with a different box at the input. A box impulse response is an example of an FIR system response: the response is zero everywhere but for a finite number of samples. An finite FIR response is always BIBO stable.

The output $y[n]$ in this example has five parts. The first and last parts are zero: there is no intersection of the input with the system response. In particular, the output is zero until the input becomes finite at $n = 0$. The second part is an upward ramp; for each position n to the right of zero there is a larger intersection of the input with the system response, culminating in complete overlap between the two. The third part is the region of full overlap: the output remains at its maximum level (value 11). And finally the fourth part has an output that is a downward ramp, which is where the input and system response walk off one another.

In discrete time, the length of the output is the sum of the input and system response minus one: $\text{Len}\,(y[n]) = \text{Len}\,(x[h]) + \text{Len}\,(h[n]) - 1$.

In this example there is also gain. The sum of the impulse response is 11, not one. The total output energy is eleven times the input.

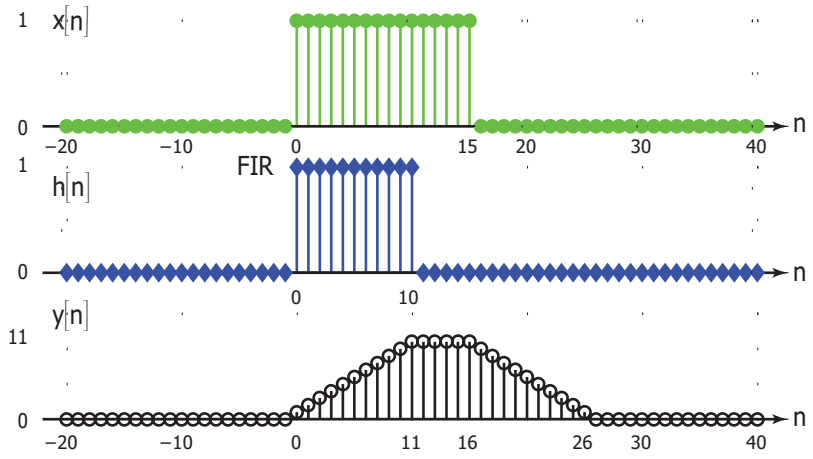

Fig. 2.8 Finite-impulse response (FIR) of a moving average with an input box. The system response is causal and not delayed, but imparts a gain of 11. The output shape is different from the input but remains finite in length. Note that the vertical axis scale varies across graphs.

2.5.5 IIR Response

Infinite-impulse response (IIR) is characterized by a infinite-length output given a finite-length input. Figure 2.9 illustrates one such example where the system response is an exponential moving average and the input, as before, is a box. A study of the ema will be deferred until the section on z-transforms, so here the ema impulse response is stated without derivation:

$$h[n] = (1-d)\sum_{k=0}^{\infty} d^k \delta[n-k] \tag{2.24}$$

where the decay factor d is bound to $(-1, 1)$ for stability. This ema is causal since it is zero for $n < 0$. It is also BIBO stable with unit gain since $\sum h[n] = 1$. The ema is clearly IIR because its (asymptotically) exponential tail never vanishes.

Figure 2.9 illustrates an ema convolved with a box. The output first exponentially rises towards one. Once the box has fully entered the system the output changes and begins an exponential decay. The tail of the decaying signal never reaches zero; there is a permanent impact due to the system.

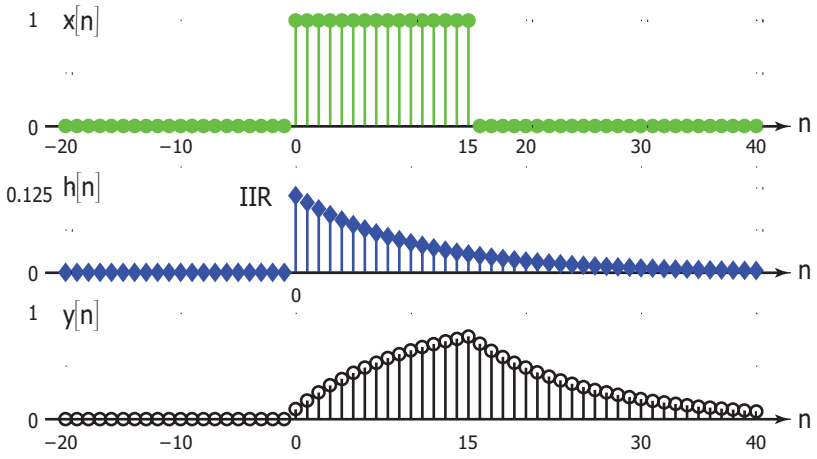

Fig. 2.9 Infinite-impulse response (IIR) of an exponential moving average with an input ox. The system response is causal and not delayed, and there is unit gain. The output shape is not only different from the input but never again reaches zero. Note that the vertical axis scale varies across graphs.

2.5.6 Compound example

Consider now a cascade of two LTI systems, Fig. 2.10. The first impulse response is a truncated ema (and thus FIR), illustrated in Fig. 2.11. The second impulse response is a first-order differencer, defined by

$$h[n] = \delta[0] - \delta[1] \tag{2.25}$$

This response is FIR and generates a differential of the input signal. Note the implicit $\Delta n = 1$ scale since the two impulses are one step away from one another.

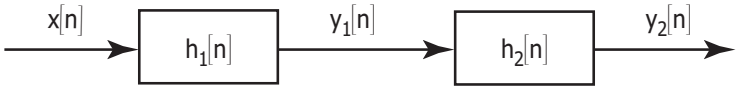

Fig. 2.10 A cascade of two LTI systems with impulse responses $h_1[n]$ and $h_2[n]$.

The unit-step input $x[n]$ is first convolved with the truncated ema. A rising exponential is the result ($y_1[n]$). Next, the output is fed into the differencing system $h_2[n]$. The output $y_2[n]$ is the truncated ema $h_1[n]$.

To explain this, recall that LTI systems commute given their linearity. We can reorder the cascade so that the unit step $x[n]$ feeds through the differencer $h_2[n]$ first; the result is a unit impulse $\delta[n]$. Once this unit impulse is fed through the truncated ema the output is simply the truncated ema system response $h_1[n]$.

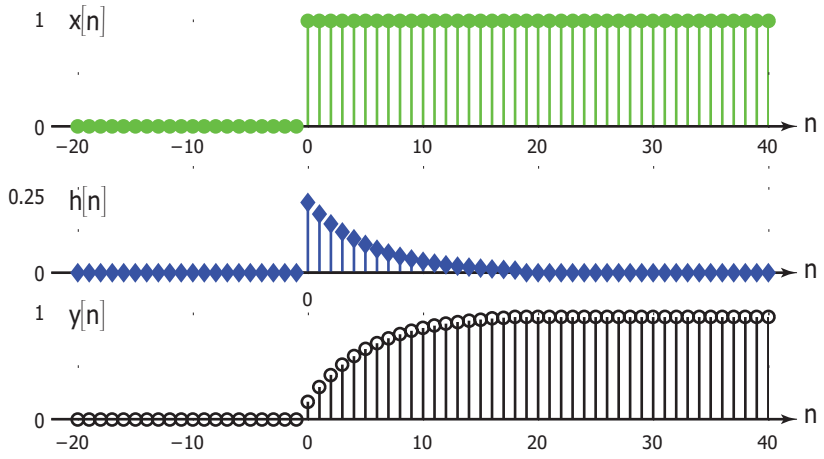

Fig. 2.11 An ema convolved with a unit step. The output is a saturating exponential. Note that the vertical axis scale varies across graphs.

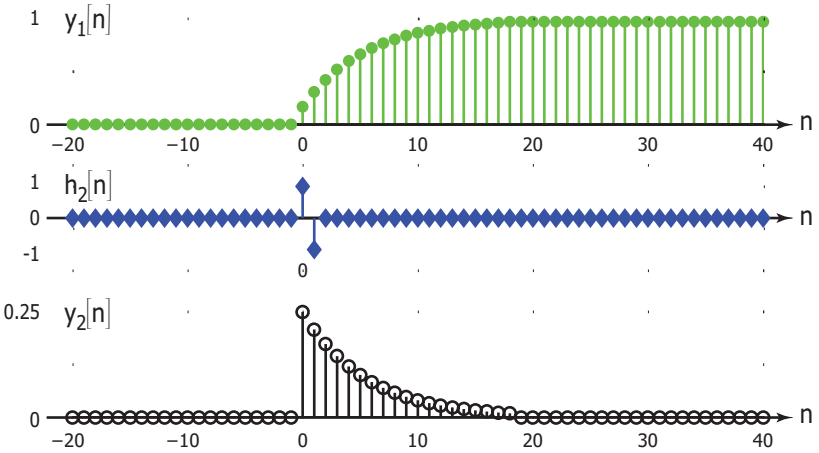

Fig. 2.12 A differential FIR convolved with the output of the preceding system. The result

Chapter 3
The Fourier Transform

Window shapes and impulse responses have been, thus far in these lecture notes, pulled out of the air in order to focus on the application of such impulse responses to a time series, and to focus on differentiating the behavior of different types of responses.

This and the next several chapters deal with impulse-response creation. A response is constructed by writing a linear difference equation and then solving this equation for all time. In continuous time we would write differential equations and then integrate them to find the solution (to within the constants of integration).

The tool to write and solve linear difference equations is the z-transform. The z-transform is a generalization of the Fourier transform, and thus I begin here.

3.1 Definitions

The Fourier method is one of projection and reconstruction via linear superposition. The basis on which a signal is projected is the complete, orthonormal set of complex exponentials. Each complex exponential, or simply a sine and cosine wave pair, in the Fourier basis is infinite in temporal extent: it starts at $-\infty$ and continues to $+\infty$. The complex exponential is, in contrast, perfectly localized in frequency.

The projection of a time series onto the Fourier basis determines the amplitude and phase of each complex exponential. Reconstruction combines the scaled and offset exponentials to approximate, and in the limit, reproduce, the original signal.

The most general Fourier transform pair is

$$X(\omega) = \int_{\mathbb{R}} x(t) e^{-j\omega t} dt \tag{3.1}$$

$$x(t) = \frac{1}{2\pi} \int_{\mathbb{R}} X(\omega) e^{j\omega t} d\omega \tag{3.2}$$

where the signal $x(t)$ is continuous in time (CT) with infinite extent and $X(\omega)$ is its Fourier transform which is a function of radial frequency ω [1]. The integrals are over the entire real axis $\mathbb{R}$. The 2π factor is attributed to the inverse transform in this text, although where the 2π is accounted for is arbitrary. The equations are equivalently called transform and inverse transform, *analysis* and *synthesis*, or transform and reconstruction.

Note for future reference that the notation $X(\omega)$ is shorthand for $X\left(e^{j\omega}\right)$; the argument is clearly complex. The parameterization of the z- and Laplace-transforms will be evident in the argument of $X(\cdot)$.

In operator notation, the Fourier transform and its inverse are denoted $\mathcal{F}$ and $\mathcal{F}^{-1}$. Thus

$$\begin{aligned} X(\omega) &= \mathcal{F}\{x(t)\} \\ x(t) &= \mathcal{F}^{-1}\{X(\omega)\} \\ x(t) &= \mathcal{F}^{-1}\{\mathcal{F}\{x(t)\}\} \end{aligned} \tag{3.3}$$

In order for a Fourier transform and its inverse to exist, the integrals must converge.

3.2 Lossless Reconstruction

The Fourier transform is a lossless representation of the original signal. This is most generally shown using the CT transform pair. Placing the Fourier transform into the synthesis equation gives

$$\begin{aligned} x(t) &= \frac{1}{2\pi} \int_{\mathbb{R}} \left[\int_{\mathbb{R}} x(u) e^{-j\omega u} du \right] e^{j\omega t} d\omega \\ &= \frac{1}{2\pi} \int_{\mathbb{R}} d\omega \, e^{j\omega(t-u)} \int_{\mathbb{R}} x(u) du \\ &= \frac{1}{2\pi} \int_{\mathbb{R}} 2\pi \delta(t-u) x(u) du \\ &= x(t) \end{aligned} \tag{3.4}$$

[1] Engineering texts use $\exp(-j\omega t)$ in the transform equation. Physicists and mathematicians use $\exp(i\omega t)$. Consistency is all that is mathematically necessary. The differing choices have to do with physical interpretation.

where the definition

$$\frac{1}{2\pi}\int_{\mathbb{R}} e^{j\omega t}d\omega \equiv \delta(t) \tag{3.5}$$

is used. That (3.5) holds can be seen as follows. Using Euler's formula for the complex exponential, define

$$I_s + I_a = \int_{\mathbb{R}} \cos(\omega t)d\omega + j\int_{\mathbb{R}} \sin(\omega t)d\omega \tag{3.6}$$

The asymmetric integral $I_a = 0$ since the integrand is an asymmetric function (sin) about $\omega = 0$. The symmetric integral I_s does not vanish due to symmetry, so consider I_s as a limit of a definite integral:

$$\begin{aligned} I_s &= \lim_{w\to\infty}\int_{-\omega}^{\omega} \cos utdu \\ &= \lim_{w\to\infty} 2\,\frac{\sin\omega t}{t} \end{aligned}$$

This limit is not behaved for all t except for $t = 0$, in which case $I_s \to \infty$. For $t \neq 0$, I_s fluctuates infinitely rapidly and its contribution to any integral is zero. Following this argument (it is not a proof), one can define (3.5) with some confidence[2]. The appearance of the 2π coefficient is necessary for consistency between the analysis and synthesis formulas.

3.3 The Inverse Transform as Superposition

Superposition is a linear operation on a basis that only works when the basis is orthogonal. Consider two arbitrary basis components of the CTFT at radial frequencies $\omega_{1,2}$: $b_{1,2} = (2\pi)^{-1/2}e^{-j\omega_{1,2}t}$. The projection of b_2 onto b_1, $\langle b_1 b_2^*\rangle$, is

$$\frac{1}{2\pi}\int_{\mathbb{R}} e^{-j\omega_1 t}e^{+j\omega_2 t}dt = \delta(\omega_1 - \omega_2) \tag{3.8}$$

Only when $\omega_1 = \omega_2$ is the projection finite, else the bases are perpendicular.

[2] In the 25 years since I first learned (3.5) I only recently found a mathematical proof [1]. The proof requires several interesting contour integrals, but I won't cover them here. At a heuristic level I can recognize that the Fourier transform is the projection of a signal onto the complex exponential basis. Thus is makes sense to ensure that for each ω an integral number of periods is covered by the integration limits: $\omega t = 2m\pi, m = 1, 2, \ldots$. The symmetric integral then reads

$$I_s = \lim_{m\to\infty}\int_{-m\pi/t}^{m\pi/t} \cos utdt = 2\,\frac{\sin m\pi}{t} \tag{3.7}$$

which is zero for $t \neq 0$ and infinite at $t = 0$, thus $I_s = \delta(t)$ to within a coefficient.

The reconstruction of $x(t)$ from $X(\omega)$ is a superposition of infinitesimally narrow complex exponentials of the form

$$X(\omega)e^{j\omega t}d\omega \tag{3.9}$$

For each radial frequency ω there is a complex coefficient $X(\omega)$, the latter begin a continuous function of ω. This coefficient scales the complex exponential having the same radial frequency ω.

A complex number is equivalently expressed in cartesian or polar form. Time-series analysis almost exclusively uses the polar notation because of the physical connection. Consider the complex coefficient $X(\omega)$ in polar form:

$$X(\omega) = |X(\omega)| \ \exp\left(j\angle X(\omega)\right) \tag{3.10}$$

The angle $\angle X(\omega)$ is more simply written as a phase $\phi_X(\omega)$. One superposition component then reads

$$|X(\omega)| \exp\left(j\left(\omega t + \phi_X(\omega)\right)\right) d\omega \tag{3.11}$$

Amplitude $|X(\omega)|$ encodes the weight of each superposition component and phase $\phi_X(\omega)$ encodes 'location'. Since the basis is periodic, absolute location has no meaning but phase shift with respect to a reference is meaningful.

3.4 Fourier Theorems

3.4.1 Convolution Representation

Time and frequency domains are duals of one another, and convolution and Fourier transforms are dual operations. The convolution of a input with an impulse response is the dual of *multiplication* of the Fourier transforms of the input and impulse responses, that is:

$$y(t) = h(t) * x(t) \xleftrightarrow{\mathcal{F}} Y(\omega) = H(\omega)X(\omega) \tag{3.12}$$

Equivalence is shown by direct substitution. As setup, we have

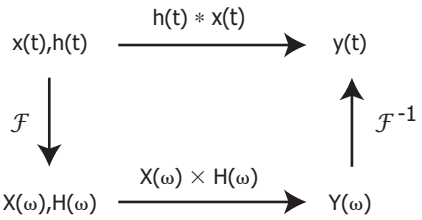

Fig. 3.1 Convolution and multiplication duality. The convolution of two time series is equivalent to multiplication of their respective Fourier transforms. To arrive at $y(t)$ one may directly compute the convolution, or switch to the Fourier domain, multiply, and invert the transform. Both approaches have their important applications.

$$
\begin{aligned}
y(t) &= \int_{\mathbb{R}} x(\tau)h(t-\tau)d\tau \\
Y(\omega) &= \int_{\mathbb{R}} y(t)e^{-j\omega t}dt \\
x(\tau) &= \frac{1}{2\pi}\int_{\mathbb{R}} X(\omega)e^{j\omega\tau}d\omega \\
h(t-\tau) &= \frac{1}{2\pi}\int_{\mathbb{R}} H(\omega)e^{j\omega(t-\tau)}d\omega
\end{aligned}
$$

The Fourier transform of $Y(\omega)$ is then

$$
\begin{aligned}
Y(\omega) &= \frac{1}{(2\pi)^2}\int_{\mathbb{R}} dt\; e^{-j\omega t}\int_{\mathbb{R}} d\tau \int_{\mathbb{R}} d\omega\; X(\omega)e^{j\omega\tau}\int_{\mathbb{R}} d\omega'\; H(\omega')e^{j\omega'(t-\tau)} \\
&= \frac{1}{(2\pi)^2}\int_{\mathbb{R}} dt\; e^{-j(\omega-\omega')t}\int_{\mathbb{R}} d\tau\; e^{j(\omega-\omega')\tau}\int_{\mathbb{R}} d\omega\; X(\omega)\int_{\mathbb{R}} d\omega'\; H(\omega') \\
&= \iint_{\mathbb{R}^2} d\omega d\omega'\; \delta(w'-w)\delta(w-w')X(\omega)H(\omega') \\
&= \int_{\mathbb{R}} d\omega'\; \delta(w'-w)X(\omega')H(\omega') \\
&= X(\omega)H(\omega)
\end{aligned}
$$

Figure 3.1 illustrates this duality between the time and frequency domains. To evaluate the convolution of two signals, one may directly convolve; alternatively, the Fourier transforms of the signals can be found, their spectra multiplied, and the result inverse-transformed. That answer will be the same, as long as boundary conditions are carefully considered.

There is a parallel theorem, stated here without proof, that convolution in frequency is the product in time. That is, for CT signals,

$$
y(t) = x(t)h(t) \xleftrightarrow{\mathcal{F}} Y(\omega) = X(\omega) * H(\omega) \tag{3.13}
$$

The convolution / multiplication equivalence holds for any CT generalization of the CT Fourier transform, such as the Laplace transform, as well as for their discrete-time counterparts.

3.4.2 Energy Conservation

Parseval's Theorem shows that the total energy in the dual domains is equal. The energy densities at frequency ω and time t are simply $X^*(\omega)X(\omega)$, and $x^*(t)x(t)$. Parseval's theorem states

$$\int_{\mathbb{R}} x^*(t)x(t)dt = \frac{1}{2\pi}\int_{\mathbb{R}} X^*(\omega)X(\omega)d\omega \tag{3.14}$$

One can show equality via direct substitution:

$$\begin{aligned}
\int_{\mathbb{R}} X^*(\omega)X(\omega)d\omega &= \int_{\mathbb{R}} d\omega \int_{\mathbb{R}} x^*(u)e^{j\omega u}du \int_{\mathbb{R}} x(v)e^{-j\omega v}dv \\
&= \iint_{\mathbb{R}^2} x^*(u)x(v)dudv \int_{\mathbb{R}} e^{j\omega(u-v)}d\omega \\
&= 2\pi \iint_{\mathbb{R}^2} \delta(u-v)\, x^*(u)x(v)dudv \\
&= 2\pi \int_{\mathbb{R}} x^*(t)x(t)dt
\end{aligned}$$

This theorem can only apply for finite-energy signals. That is, one requires $\int_{\mathbb{R}} x^*(t)x(t)dt < \infty$.

3.4.3 Time and Frequency Shifts

Consider a signal $x(t)$ whose Fourier transform is $X(\omega)$. The FT of $x(t-t_o)$ is

$$\begin{aligned}
X_{t-t_o}(\omega) &= \int_{\mathbb{R}} x(t-t_o)e^{-j\omega t}dt \\
&= \int_{\mathbb{R}} x(t')e^{-j\omega(t'+t_o)}dt' \\
&= e^{-j\omega t_o}X(\omega)
\end{aligned}$$

Thus

$$x(t-t_o) \xleftrightarrow{\mathcal{F}} e^{-j\omega t_o}X(\omega) \tag{3.15}$$

Time shift imparts a phase ramp in frequency. Direct substitution likewise shows that a frequency shift imparts a phase shift in time:

$$e^{j\omega_w t}x(t) \xleftrightarrow{\mathcal{F}} X(\omega - \omega_o) \tag{3.16}$$

3.4.4 Differentiation in Time and Frequency

Consider the Fourier pair: $x(t) \overset{\mathcal{F}}{\longleftrightarrow} X(\omega)$. A derivative in time yields:

$$\frac{d}{dt}x(t) = \frac{1}{2\pi}\frac{d}{dt}\int_{\mathbb{R}} X(\omega)e^{j\omega t}d\omega \xleftrightarrow{\mathcal{F}} j\omega X(\omega)$$

A temporal derivative adds a $j\omega$ coefficient to its Fourier transform. Similarly, a derivative in frequency yields:

$$\frac{d}{d\omega}X(\omega) = \frac{d}{d\omega}\int_{\mathbb{R}} x(t)e^{-j\omega t}dt \xleftrightarrow{\mathcal{F}} -jtx(t) \tag{3.17}$$

3.4.5 Gain

The Fourier transform of the system response $H(\omega)$ imparts a frequency-dependent coefficient to input $X(\omega)$ and also imparts overall gain. As a shape, gain is flat; it is just a constant multiplier. Indeed, the system gain is calculated at the special point $w = 0$:

$$g = H(\omega = 0) \tag{3.18}$$

The zero-frequency, or DC, component of the system spectrum gives the gain directly. The dual of $H(\omega)$ is $h(t)$ and they are related as

$$\begin{aligned} H(\omega) &= \int_{\mathbb{R}} h(t)e^{-j\omega t}dt \\ H(0) &= \int_{\mathbb{R}} h(t)dt \end{aligned} \tag{3.19}$$

Of course when the system is causal $\mathbb{R} \to \mathbb{R}^+$ (c.f. (2.19)). In most cases it is much simpler to compute the gain in the transform domain rather than the temporal domain.

3.4.6 k-Order Moments

The k-order moment of $h(t)$ is

$$M^{(k)} \equiv \int_{\mathbb{R}} t^k h(t) dt \tag{3.20}$$

Applying the differentiation-in-frequency property we arrive at a simple way to compute the k^{th} moment:

$$M^{(k)} = (j)^k \frac{d^{(k)}}{dw^{(k)}} H(w)\Big|_{\omega=0} \tag{3.21}$$

3.5 Examples

3.5.1 Pure Tones

Since the Fourier basis is sines and cosines (or equivalently complex exponentials) let's look at the simplest example possible: $x(t) = \cos(\omega_o t + \phi)$. Using Euler's formula, the FT is

$$\begin{aligned} X(\omega) &= \int_{\mathbb{R}} \frac{1}{2} \left[e^{j(\omega_o t + \phi)} + e^{-j(\omega_o t + \phi)} \right] e^{-j\omega t} dt \\ &= \frac{1}{2} \left[\delta(f - f_o) e^{j\phi} + \delta(f + f_o) e^{-j\phi} \right] \end{aligned} \tag{3.22}$$

where radial frequency ω has been replaced with cycle frequency f: $2\pi f = \omega$.

Figure 3.2 illustrates $\mathcal{F}\{x(t)\}$ in time and frequency for several periods, all with zero phase ϕ. The interpretation is the following. A cosine of zero frequency is just everywhere unity; its transform is a delta function at $f = 0$. Cosines of increasing frequency have shorter temporal periods and their transform is composed of an impulse pair at $\pm f_o$. Note that a single impulse pair $e^{\pm\phi}\delta(f \pm f_o)$ represents the entire temporal waveform. Also, it is clear that localization in frequency, most simply the $\delta(t)$ function, represents complete non-locality in time.

Figure 3.3 illustrates the cosine FT for a fixed frequency but shifting phase. Since the frequency here remains the same, the impulse locations are fixed. However, they acquire a phase shift that reflects the location of the cosine within the frame.

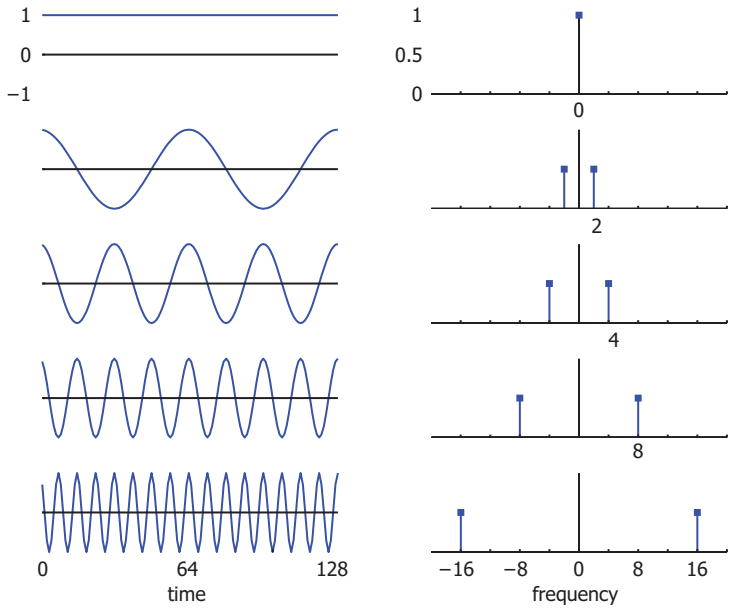

Fig. 3.2 Dual representation of time and frequency domains. A constant level in time has frequency energy at $f = 0$. Cosine waves of $2, 4, 8$ and 16 periods in the frame have Fourier energies at frequencies $\pm 2, \pm 4, \pm 8$ and ± 16.

3.5.2 Impulse Comb

An example essential to relate the Fourier transform to the Discrete-time Fourier transform, and then on to the z-transform, is that of the impulse comb. Define a continuous-time signal $x(t)$ as

$$x(t) = \sum_{n=-\infty}^{\infty} \delta\left(t - nT\right) \tag{3.23}$$

where n is an integer and T is measured in time. Only at those times when $t = nT$ does $x(t)$ have non-zero value. The interval between adjacent impulses is period T. Figure 3.4(left) illustrates this.

The first steps in the direct Fourier transform calculation are

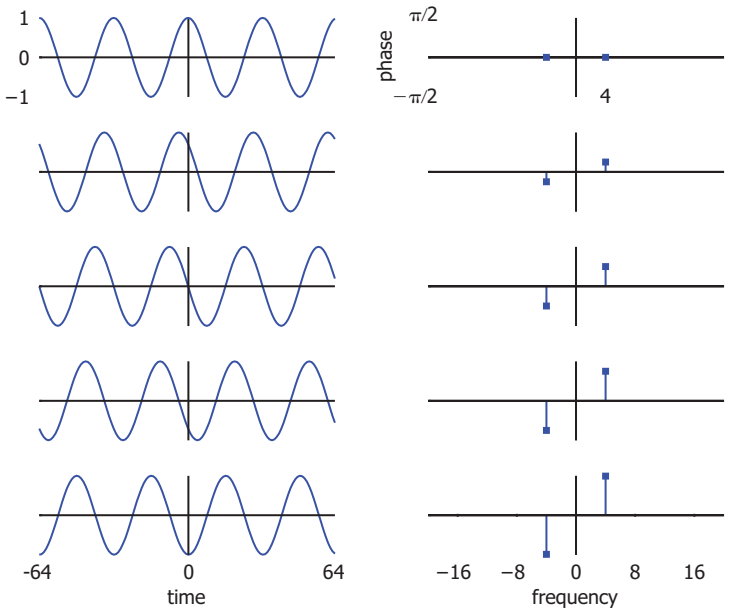

Fig. 3.3 Fourier phase representation of position. As the cosine wave is translated to the left its position within the frame shifts. Position of a periodic signal is represented as phase-shift with respect to a reference, which in this case is the edge of the frame. The Fourier phase indicates this shift.

$$\begin{aligned} X(\omega) &= \sum_{n=-\infty}^{\infty} \int_{\mathbb{R}} \delta\left(t - nT\right) e^{-j\omega t} dt \\ &= \sum_{n=-\infty}^{\infty} e^{-jn\omega T} \\ &= \sum_{n=-\infty}^{\infty} \left(\cos\left(\omega nT\right) - j \sin\left(\omega nT\right)\right) \\ &= S_s + S_a \end{aligned} \tag{3.24}$$

where, echoing (3.6), Euler's formula is used. As before, the asymmetric part vanishes leaving only the symmetric piece. Rather than compute S_s directly let us write the limit of a finite sum, which produces

$$\begin{aligned} S_s &= \lim_{N\to\infty} \sum_{n=-N}^{N} \cos\left(\omega T\right) \\ &= \lim_{N\to\infty} \frac{\sin\left(\left(1+2N\right)\omega T/2\right)}{\sin\left(\omega T/2\right)} \end{aligned} \tag{3.25}$$

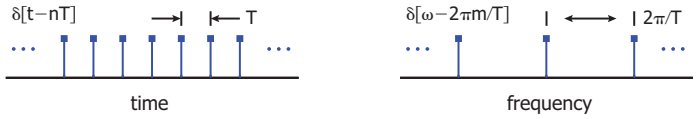

Fig. 3.4 An impulse comb in time and its Fourier transform. Left: comb of impulses spaced in time by T. Right: The Fourier transform of an impulse comb in time is an impulse comb in frequency with spacing $2\pi/T$.

This function is periodic with the principal period defined by the denominator: $\omega T/2 = \pi m$ for integral m. For the moment, replace $\omega T/2$ with ϕ and consider the limit

$$\lim_{\substack{N\to\infty \\ N\phi\to 0}} \frac{\sin\left((1+2N)\,\phi\right)}{\sin\left(\phi\right)}$$

The latter limit can be achieved parametrically by defining $\phi_w \equiv N^{-(1+\alpha)}$ for $\alpha > 0$: $\lim_{N\to\infty} N\phi_w = \lim_{N\to\infty} N^{-\alpha} = 0$. With this limit and parameterization L'Hôpital's Rule can be used for the limit:

$$\lim_{N\to\infty} \frac{\sin\left((1+2N)\,\phi_w\right)}{\sin\left(\phi_w\right)}\Big|_{\phi_w = N^{-(1+\alpha)}} = \lim_{N\to\infty} 1 + 2N \to \infty$$

Therefore, when $\omega T = 2\pi m$ the sum $S_s \to \infty$ and the width of the region $\phi_w = N^{-(1+\alpha)} \to 0$. For phase values $\phi > \phi_w$ no limit exists. It is not the case that $S_s \to 0$ for $\omega T \neq 2\pi m$, rather the function oscillates infinitely quickly but it bounded and symmetric about zero. Integrating the product of this oscillation with a well-behaved function yields zero. In this spirit the limit in (3.25) is written as

$$S_s \equiv C \sum_{m=-\infty}^{\infty} \delta\left(\omega - \frac{2\pi m}{T}\right)$$

where the coefficient C is found as follows.

Parseval's theorem cannot be applied because the input series, being periodic, has infinite energy. We can, however, take advantage of the periodicity and look to equate the area over one period. That area is

$$A_t = \int_{-T/2}^{T/2} \delta(t)dt = 1$$

Equivalently, the area over a frequency period is

$$\begin{aligned} A_\omega &= \int_{-\pi/T}^{\pi/T} \sum_{n=-\infty}^{\infty} \cos(n\omega T)\, d\omega \\ &= \sum_{n=-\infty}^{\infty} \int_{-\pi/T}^{\pi/T} \cos(n\omega T)\, d\omega \\ &= \begin{cases} 2\pi/T, & n = 0 \\ 0, & \text{otherwise} \end{cases} \end{aligned}$$

Therefore $C = 2\pi/T$ to equate areas. In summary, the transform of a temporal impulse comb is a spectral impulse comb:

$$\sum_{n=-\infty}^{\infty} \delta(t - nT) \xleftrightarrow{\mathcal{F}} \frac{2\pi}{T} \sum_{m=-\infty}^{\infty} \delta\left(\omega - \frac{2\pi m}{T}\right) \tag{3.26}$$

Figure 3.4(right) illustrates the frequency-based impulse comb. The most significant aspect is the Fourier transform of a temporal comb with period T is a frequency comb with period $\sim 1/T$. Periodicity in time is matched with periodicity in frequency, albeit with an adjusted period.

3.5.3 One-Sided Exponential

The one-sided exponential waveform plays a prominent role in z-transforms, so let's consider its spectrum. The waveform is

$$x(t) = \int_{\mathbb{R}^+} \tau^{-1} e^{-t/\tau} dt \tag{3.27}$$

where $\mathbb{R}^+$ is non-negative part of the real number line. Its Fourier transform is $X(\omega) = \frac{1}{1+j\omega\tau}$ and is known as a Lorentz filter. As this is a complex number and a function of ω consider the log magnitude squared and angle:

$$\begin{aligned} \log |X(\omega)|^2 &= \log\left(\frac{1}{1+\omega^2\tau^2}\right) \\ \angle X(\omega) &= -\tan^{-1}\omega\tau \end{aligned}$$

There are two regimes here: $\omega \ll \tau$ and $\omega \gg \tau$. Asymptotically the magnitude (not squared) tends to

$$\log |X(\omega)| = \begin{cases} \log\tau & \omega \ll \tau \\ -\log\omega & \omega \gg \tau \end{cases} \tag{3.28}$$

and the angle tends to

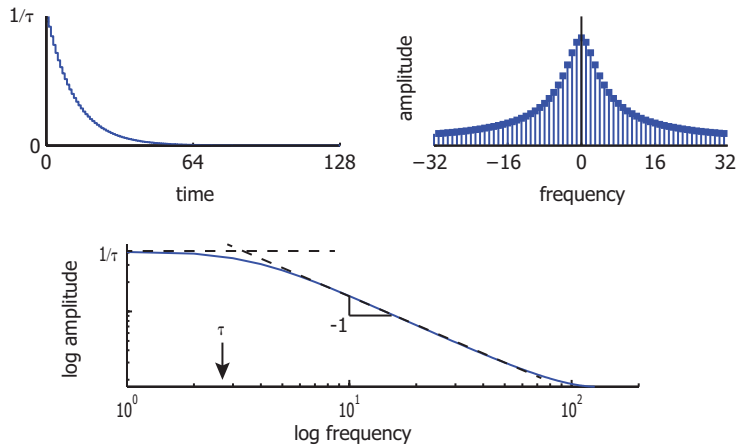

Fig. 3.5 One-sided exponential waveform and its magnitude spectrum. This spectrum is known as a Lorentz filter. The Bode plot of the magnitude spectrum is illustrated below. This is a log-log plot. Asymptotically the magnitude is flat or falls with a slope of -1; the break-point is $\omega = \tau$.

$$\angle X(\omega) = \begin{cases} 0 & \omega \ll \tau \\ -\pi/2 & \omega \gg \tau \end{cases} \tag{3.29}$$

This simple form of the log magnitude leads to the Bode plot. On a log-log scale, log magnitude and log frequency, the two asymptotes are a flat line and a line with slope $= -1$. System response spectra are generally plotted in this method for continuous-time signals.

3.5.4 Gaussian Pulse

Consider a pulse with a Gaussian shape:

$$x(t) = \frac{1}{\sqrt{2\pi\sigma^2}}\, e^{-(t-t_o)^2/2\sigma^2} \tag{3.30}$$

for $t \in \mathbb{R}$. Define $u = t - t_o$, with differential $du = dt$, then $\mathcal{F}\{x(t)\}$ is

$$X(\omega) = \frac{e^{-j\omega t_o}}{\sqrt{2\pi\sigma^2}} \int_{\mathbb{R}} e^{-u^2/2\sigma^2} e^{-j\omega u} du$$

Completing the square in the exponential argument of the integrand is next. Clearly

$$-\frac{u^2}{2\sigma^2} - j\omega u = -\frac{(u + j\sigma^2\omega)^2}{2\sigma^2} - \frac{\sigma^4\omega^2}{2}$$

Thus

$$X(\omega) = e^{-j\omega t_o} e^{-\sigma^2\omega^2/2} \frac{1}{\sqrt{2\pi\sigma^2}} \int_{\mathbb{R}} e^{-(u+j\sigma^2\omega)^2/2\sigma^2} du$$

The integral is translation invariant on the imaginary axis and is therefore equal to $\sqrt{2\pi\sigma^2}$. Therefore, a Gaussian pulse has a Gaussian spectrum:

$$\frac{1}{\sqrt{2\pi\sigma^2}} e^{-(t-t_o)^2/2\sigma^2} \quad \overset{\mathcal{F}}{\longleftrightarrow} \quad e^{-j\omega t_o} e^{-\sigma^2\omega^2/2} \tag{3.31}$$

This shows that the Gaussian shape is an eigenfunction of the Fourier transform. This is not the only eigenfunction: the hyperbolic secant is a well-known eigenfunction is physics.

In terms of scale, when the dispersion parameter σ is large the pulse is temporally distributed. Consequently is spectrum is tight around $\omega = 0$. Conversely, a small dispersion parameter yields a broad spectral distribution. Once again the Fourier transform localizes in one domain and delocalizes in the other.

Notice as well that temporal shift t_o shows up as a phase in the transform. Since the transform is a function of ω this phase induces a linear phase ramp across the width of the spectrum.

3.5.5 Wavelet at Different Scales

What is commonly known as the Mexican hat wavelet is, to within a constant c, the second derivative of a gaussian. Without loss of generality, set $t_o = 0$ in (3.30) and take its second derivative with respect to time to get:

$$mh(t) = \frac{d^2}{dt^2} x(t) = \frac{c}{\sqrt{\sigma}} \left(1 - \frac{t^2}{\sigma^2}\right) e^{-t^2/2\sigma^2} \tag{3.32}$$

This waveform is known as a continuous-time wavelet because it is localized both in time and frequency. The scale parameter of this wavelet is the width σ.

The Fourier transform is best computed using the derivative rule for these transforms. Consider

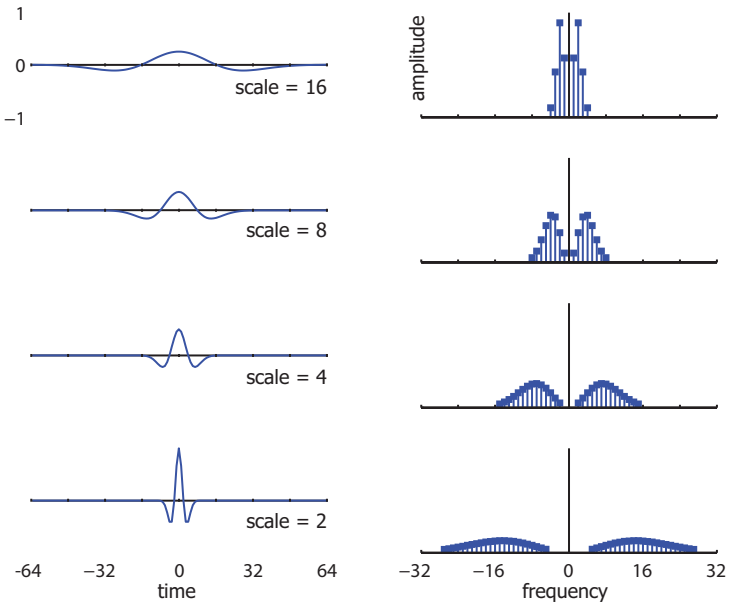

Fig. 3.6 Duals of Mexican hat wavelet: time and frequency amplitude. When the wavelet is delocalized in time it is localized in frequency. As the scale parameter is decreased, tightening the wavelet in time, its spectrum expands.

$$\begin{aligned}\frac{d}{dt}X(\omega) &= 0 \\ &= \frac{d}{dt}\int_{\mathbb{R}} x(t)e^{-j\omega t}dt \\ &= \int_{\mathbb{R}} \left(\dot{x(t)} - j\omega x(t)\right) e^{-j\omega t}dt \\ &= \int_{\mathbb{R}} \dot{x(t)}e^{-j\omega t}dt - j\omega X(\omega)\end{aligned}$$

thus

$$\frac{d}{dt}x(t) \stackrel{\mathcal{F}}{\longleftrightarrow} j\omega X(\omega) \tag{3.33}$$

The Fourier transform of the Mexican hat wavelet now can be found by inspection:

$$\mathcal{F}\{mh(t)\} = -c\,\omega^2 e^{-\sigma^2\omega^2/2} \tag{3.34}$$

Figure 3.6 illustrates this wavelet with several scale parameters. While the support for this wavelet is infinite in both time and frequency, the Gaussian envelope limits its significant energy in time and frequency.

3.5.6 Temporal Derivative and Shift Expansion

Given an FT pair $x(t) \overset{\mathcal{F}}{\leftrightarrow} X(\omega)$, consider the time derivative of $x(t)$ and its (lagged) first-order differential approximation:

$$\frac{d}{dt}x(t) \simeq \frac{x(t) - x(t - \Delta t)}{\Delta t} \tag{3.35}$$

The derivative theorem shows that the Fourier transform of the left-hand side is $j\omega X(\omega)$. Linearity and the time-shift theorem leads the FT of the right-hand side to be:

$$\begin{aligned} \frac{x(t) - x(t - \Delta t)}{\Delta t} &\overset{\mathcal{F}}{\longleftrightarrow} \frac{1 - e^{-j\omega\Delta t}}{\Delta t} X(\omega) \\ &\simeq j\omega X(\omega) \end{aligned}$$

3.6 Modes of Convergence

The Fourier transform and its inverse are, in the continuous-time case, integrals that must converge for a transform pair to exist. In discrete contexts, the respective sums must converge. The manner of convergence is related to the nature of the signal.

3.6.1 Pointwise Convergence

Signals that are everywhere differentiable exhibit pointwise convergence. One way to illustrate such convergence is to refer to the reconstruction equation and replace the limits with the cutoff value ω_c:

$$x_{\omega_c}(t) = \int_{-\omega_c}^{\omega_c} X(\omega) e^{j\omega t} d\omega$$

As ω_c is increased more Fourier components are added to the reconstruction. Pointwise convergence exists when the limit

$$x(t) = \lim_{\omega_c \to \infty} x_{\omega_c}(t)$$

holds. Figure 3.7 illustrates pointwise convergence of the Mexican hat wavelet, as approximated in the discrete-time, discrete-frequency domains.

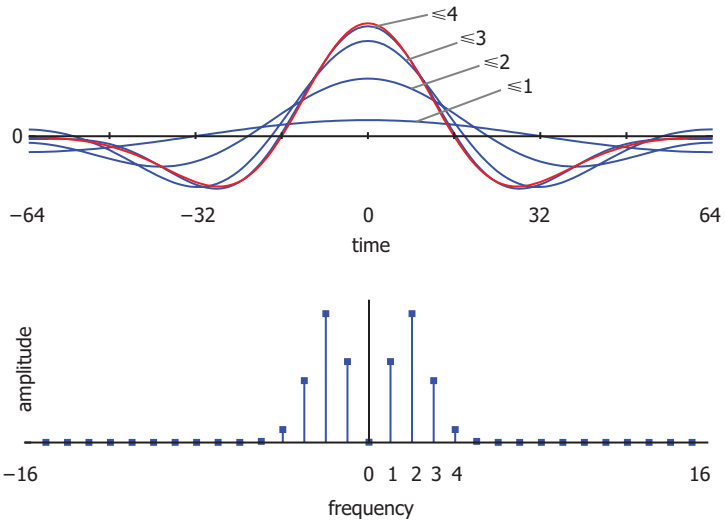

Fig. 3.7 Pointwise convergence of the absolutely summable continuous-time Mexican hat waveform. Top) Original waveform (red) and increasingly accurate approximations made by the inclusion of more Fourier components in the reconstruction. Bottom) The Fourier amplitude spectrum.

3.6.2 Mean Square Convergence

Signals that have discontinuities do not converge pointwise. An alternative convergence is in mean-square, where

$$\lim_{\omega_c \to \infty} |x(t) - x_{\omega_c}(t)|^2 = 0$$

Figures 3.8-3.9 illustrate mean-square convergence for a one-sided exponential signal. Clearly the reconstruction does not converge smoothly to the exponential shape, but it is guaranteed to in mean-square in the limit.

3.6.3 Generalized Convergence

A constant signal $x(t) = 1$ or constant spectrum $X(\omega) = 1$ does not lead to a convergent transform counterpart in the classic sense. Clearly $\int_{\mathbb{R}} |x(t)|\, dt \not< \infty$, nor does $x(t)$ converge in mean-square. In fact it has infinite energy. As touched on in section 3.3, convergence exists in the context of generalized functions. Two transforms that rely on generalized convergence are stated here without further proof.

The transform of a constant is

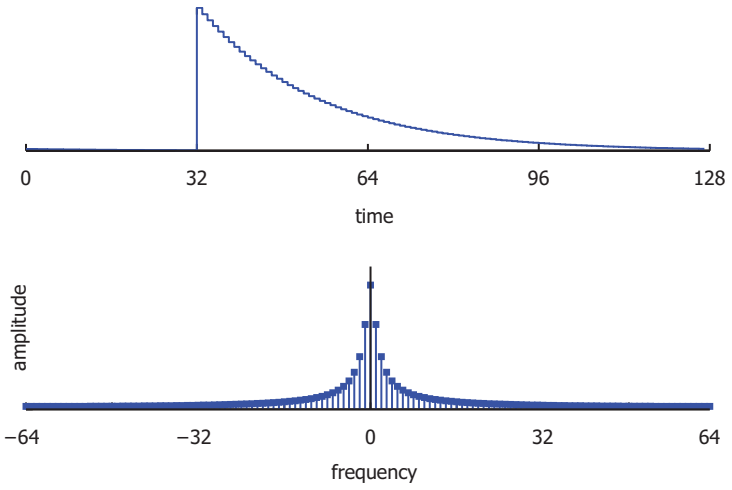

Fig. 3.8 A one-sided exponential decaying signal and its amplitude spectrum.

$$1 \xleftrightarrow{\mathcal{F}} 2\pi\delta(\omega)$$

The unit-step function $u(t)$, also known as the Heavyside function, has the transform

$$u(t) \xleftrightarrow{\mathcal{F}} \pi\delta(\omega) + \frac{1}{j\omega} \tag{3.36}$$

Figure 3.10 illustrates reconstruction of a delta-function in time. Like mean-square convergence the reconstruction 'rings' as it approximates the target, but the exact nature of this behavior is not know to this author.

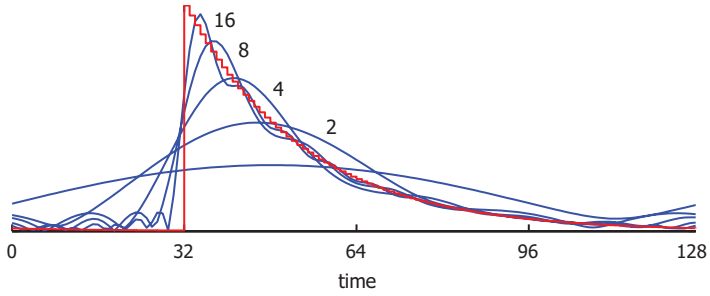

Fig. 3.9 The discontinuity in the signal breaks pointwise convergence, but this signal still converges in mean-square. Increasingly accurate approximations of $x(t)$ are illustrated as the cutoff frequency increases. Note, however, the persistent ringing around the leading edge. This ringing is known as the Gibb's phenomenon and for finite-length discrete signals never disappears.

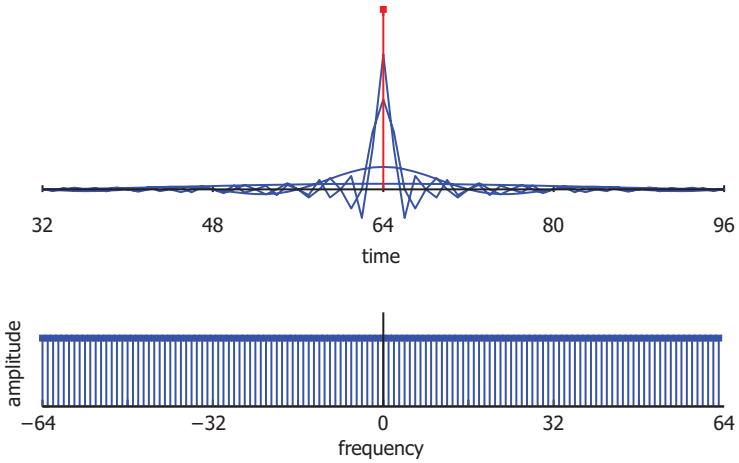

Fig. 3.10 Reconstruction approximations of a delta function in time. Note that the spectrum is constant in frequency.

3.7 Sampling and Replication

From this point forward I depart from continuous-time analysis and work towards the discrete domain. This process brings us to the discrete-time Fourier transform (DTFT) and, in the next chapter, the z-transform. It all starts with sampling.

A discrete time series does not have compact support with respect to wall-clock time but is simply an ordered series of values. "Time" is an index such as $n \in \mathbb{Z}$, the distance between two indices (n, m) is $|n - m|$, and the distance between adjacent discrete-time points is just unity.

We can construct a discrete-time series by *sampling* an underlying continuous-time series. Say we sample a series $x(t)$ on a fixed time period T. With the vocabulary previously developed I can express the sampling instances by an infinite comb,

$$h_{\text{comb}}(t) = \sum_{n=-\infty}^{\infty} \delta\left(t - nT\right) \tag{3.37}$$

Sampling of $x(t)$ at these instances requires the *multiplication* of the two series

$$x_{\text{sampled}}(t) = h_{\text{comb}}(t) \times x(t) \tag{3.38}$$

The discrete-time series $x[n]$ is then associated by the definition

$$x[n] \equiv x_{\text{sampled}}(t)$$

(Note that impulse response $h_{\text{comb}}(t)$ is neither causal nor BIBO stable. The comb is a device to help explain the consequence of sampling a signal.)

Let's now take the Fourier transform of the sampled signal. Each series is replaced with its Fourier transform and multiplication is replaced with convolution:

$$h_{\text{comb}}(t) \times x(t) \xleftrightarrow{\mathcal{F}} H_{\text{comb}}(\omega) * X(\omega)$$

Recall from Eq. 3.26 on page 54 that the Fourier transform of an impulse comb is itself an impulse comb in frequency:

$$H_{\text{comb}}(\omega) = \frac{2\pi}{T} \sum_{n=-\infty}^{\infty} \delta\left(w - \frac{2\pi n}{T}\right) \tag{3.39}$$

Also recall from Sec. 2.5.3 on page 37 that convolution with a comb *replicates* the input series, see Fig. 2.7. In this case the comb, input series and replication all happen in the *frequency* domain rather than the time domain. That is,

$$H_{\text{comb}}(\omega) * X(\omega) = \frac{2\pi}{T} \sum_{n=-\infty}^{\infty} X\left(w - \frac{2\pi n}{T}\right) \tag{3.40}$$

Sampling and *replication* are Fourier duals of one another:

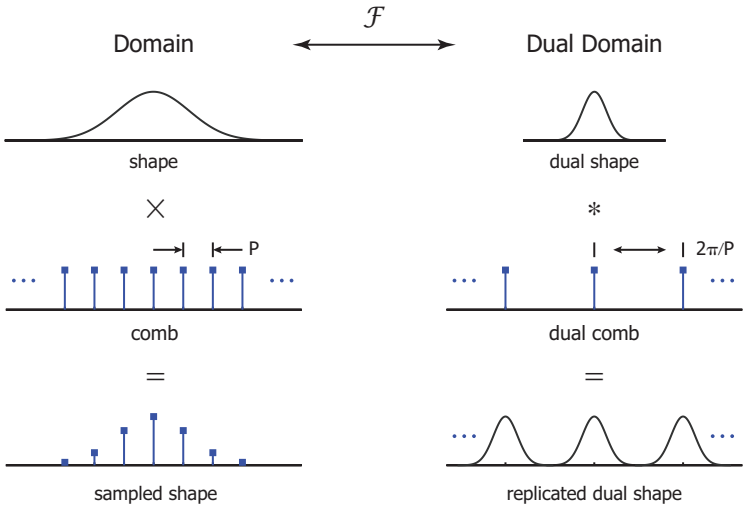

Fig. 3.11 Duality between sampling and replicating. Regardless of the specific domains, the right and left columns are Fourier duals. From top to bottom: a shape and its dual, their extents are inversely proportional; multiplication and convolution are dual operators; two combs are Fourier duals given that their periods are inversely related. The result of multiplying a signal with a comb (left column) is a sampled version of the signal. The result of convolving a signal with a comb (right column) is replication. Replication and sampling are Fourier dual operations.

$$\text{sampling} \overset{\mathcal{F}}{\longleftrightarrow} \text{replication} \tag{3.41}$$

It does not matter if the sampled domain is time, frequency or another domain altogether, as long as there exists a Fourier analogue to the domain of interest, sampling in one domain will lead to replication in the other. Figure 3.11 illustrates these operations after abstracting the detail of which domain is sampled.

3.8 The Discrete-Time Fourier Transform

The discrete-time Fourier transform (DTFT) replaces the continuous-time series with a sampled series, but the frequency domain remains continuous. Let us replace $x(t)$ in Eq. (3.1) on page 44 with its sampled version

$$x(t) = \sum_{n=-\infty}^{\infty} x[n]\delta\left(t - nT\right) \tag{3.42}$$

where T is the sampling interval. Substitution into the Fourier transform pair Eqs. (3.1-3.2)

$$X(\omega) = \sum_{n=-\infty}^{\infty} x[n] e^{-j\omega nT} \tag{3.43}$$

$$x[n] = \frac{1}{2\pi} \int_{-\pi/T}^{\pi/T} X(\omega) e^{j\omega nT} d\omega \tag{3.44}$$

Together these define the DTFT pair.

The inverse transform equation requires some discussion. Clearly the integrals of the Fourier transform and its inverse must converge in order to exist. However the energy in a spectrum that is infinitely replicated from a finite-energy spectrum is clearly infinite. The fix is very simple in this case because replication means that the integral over one period is the same as for any other period. Moreover the integral over one period is finite, again given the original spectrum is bound. Thus, the domain of integration for the inverse DTFT is $[-\pi/T, \pi/T)$ in place of $\mathbb{R}$.

All of the properties of the CTFT are conveyed to the DTFT: lossless reconstruction, convolution duality, energy conservation, time and frequency shifts, and differentiation in either time or frequency.

3.8.1 Example: An ARMA(2,1) Model

Consider a generic autoregressive moving-average (ARMA)$(2, 1)$ recurrence relation

$$y[n] = \phi_1 y[n-1] + \phi_2 y[n-2] + \epsilon[n] + \theta_1 \epsilon[n-1] \tag{3.45}$$

This recurrence can be solved by Fourier methods.

Using linearity and the time-shift theorems, the DTFT of this model is

$$\left(1 - \phi_1 e^{-j\omega} - \phi_2 e^{-2j\omega}\right) Y(\omega) = \left(1 + \theta_1 e^{-j\omega}\right) \epsilon(\omega)$$

This expression is a product of functions and can be solved with algebraic methods. As long as the left-hand side coefficient to $Y(\omega)$ is not zero then one can solve for $Y(\omega)$. Denoting $p_{1,2}$ as the roots to the polynomial coefficient to $Y(\omega)$ and $c_{1,2}$ the partial-fraction coefficients we have

$$\begin{aligned} Y(\omega) &= \frac{1 + \theta_1 e^{-j\omega}}{1 - \phi_1 e^{-j\omega} - \phi_2 e^{-2j\omega}} \, \epsilon(\omega) \\ &= \left(\frac{c_1}{1 - p_1 e^{-j\omega}} + \frac{c_2}{1 - p_2 e^{-2j\omega}} \right) \epsilon(\omega) \end{aligned}$$

To proceed we need to know the DTFT pair that have Fourier functions in the form $1/\left(1 - pe^{-j\omega}\right)$.

To do so, define the discrete-time series $h[n] = a^n u[n]$, where $u[n]$ is the discrete unit-step function and $|a| < 1$. This is a discrete geometric decay analogous to one-sided exponential decay. The DTFT is

$$\begin{aligned} X(\omega) &= \sum_{n=0}^{\infty} \left(ae^{-j\omega T}\right)^n \\ &= \frac{1}{1 - ae^{-j\omega T}} \end{aligned}$$

where the sample interval is T. The ARMA expression used unit offsets, so set $T = 1$.

Now we can associate the transform terms with time-series terms. As long as the series converge (an essential matter but the overall framework is the focus here), the inverse transform of $Y(\omega)$ can be read directly using linearity and the convolution theorem:

$$y[n] = (c_1 h_1[n] + c_2 h_2[n]) * \epsilon[n]$$

This is an important result. The action of an ARMA$(2, 1)$ filter, as long as it is stable, is to convolve the innovation term $\epsilon[n]$ with two geometrically decaying series.

This analysis can be generalized to an ARMA$(p.q)$ equations. The Fourier transform of the equation is

$$\begin{aligned} Y(\omega) &= \frac{P(\omega)}{Q(\omega)}\, \epsilon(\omega) \\ &= H(\omega)\epsilon(\omega) \end{aligned}$$

where $P(\omega)/Q(\omega)$ is a rational polynomial fraction[3]. Replacing that fraction with $H(\omega)$ we see that the ARMA filter specifies a system function that filters incoming innovations. The general solution is

$$y[n] = h[n] * \epsilon[n]$$

where $h[n]$ is determined by the specification of the linear difference equations.

[3] Note that p, q as arguments do not correspond to $P(\omega)$ and $Q(\omega)$; the lack of consistency is due to terminology that is common with the respective literature but inconsistent across fields.

Chapter 4
The z-transform

4.1 Z-transform Definitions and Relation to the Fourier Transform

The z-transform is a generalization of the discrete-time Fourier transform (DTFT) and is applicable for discrete-time signals [6, 4]. The continuous-time analogue is the Laplace transform, but Laplace will not be the focus of study here. Since the z-transform is a DTFT generalization it inherits the properties of the DTFT and adds its own features.

The z-transform and its inverse are defined as

$$X(z) = \sum_{n=-\infty}^{\infty} x[n] z^{-n} \tag{4.1}$$

$$x[n] = \frac{1}{2\pi j} \oint_C X(z) z^{n-1} dz \tag{4.2}$$

where z is a complex variable and C is a counter-clockwise circular contour in the complex plane centered at the origin and having radius r, where r will be addressed below. The function $X(z)$ replaces the time series $x[n]$ and can be treated with analytic methods. The reconstruction of $x[n]$ from $X(z)$ is not unique until additional attributes are specified, such as causality.

The Fourier transform was conceived by projecting a time-series onto a complete orthonormal basis of complex exponentials $e^{j\omega t}$. Equations (4.1-4.2) appear quite removed from the physical intuition. Yet the association goes as follows. Recall the DTFT pair Eqs (3.43-3.44):

$$X(\omega) = \sum_{n=-\infty}^{\infty} x[n] e^{-j\omega nT}$$

$$x[n] = \frac{T}{2\pi} \int_{-\pi/T}^{\pi/T} X(\omega) e^{j\omega nT} d\omega$$

In discrete time it was found that the spectrum is periodic with the condition $\omega nT = 2\pi$; so while the support of ω remains $(-\infty, \infty)$ on the real number line, the informative content is restricted to $[-\pi, \pi)$ (modulo 2π).

Consider, then, u defined as $u = e^{j\omega T}$. The number u is a complex number restricted to the unit circle in the complex plane. As ω increases u traces a circle in the counter-clockwise direction (obeying common convention) and returns to the original position every $\omega_n = 2\pi n/T$. In this sense the unit circle better represents the spectral periodicity of the DTFT than the real-number line does[1]. One can replace the complex exponential in the DTFT pair with u, but its just a tautology.

The generalization that the z-transform brings to the Fourier transform is to add an arbitrary radius to u; that is,

$$z \equiv ru, \quad r \in [0, \infty) \tag{4.3}$$

This generalization changes the convergence properties of the Fourier transform and will allow us to identify in detail the factors that determine the spectrum of a system response. In fact we will be able to reverse the problem so that we can design filters to our choosing. In "exchange" for this generalization we pay the price of always having to ensure the stability of a system response, and having to ensure uniqueness of the inverse transform by specifying additional attributes of the filter.

Now let's work out the consequences of this generalization. Given $z = re^{j\omega T}$, the transform equation is

$$\begin{aligned} X(z) &= \sum_{n=-\infty}^{\infty} x[n] z^{-n} \\ &= \sum_{n=-\infty}^{\infty} x[n] \left(re^{j\omega T}\right)^{-n} \\ &= \sum_{n=-\infty}^{\infty} \left(x[n] r^{-n}\right) e^{-j\omega nT} \\ &= \mathcal{F}\left\{x[n] r^{-n}\right\} \end{aligned}$$

where the Fourier transform $\mathcal{F}$ is the DTFT. As long as $x[n]r^{-n}$ converges then the inverse transform can be taken:

$$\begin{aligned} x[n] r^{-n} &= \mathcal{F}^{-1}\left\{X(z)\right\} \\ x[n] &= \frac{T}{2\pi} \int_{-\pi/T}^{\pi/T} X(z) r^n e^{j\omega nT} d\omega \end{aligned}$$

[1] Moreover, the relation $U = e^{jH}$ is a significant relation in matrix theory because it associates a Hermitian matrix H with a unitary matrix U. Hermitian-matrix eigenvalues are real while those of the unitary-matrix are complex and lie on the unit circle.

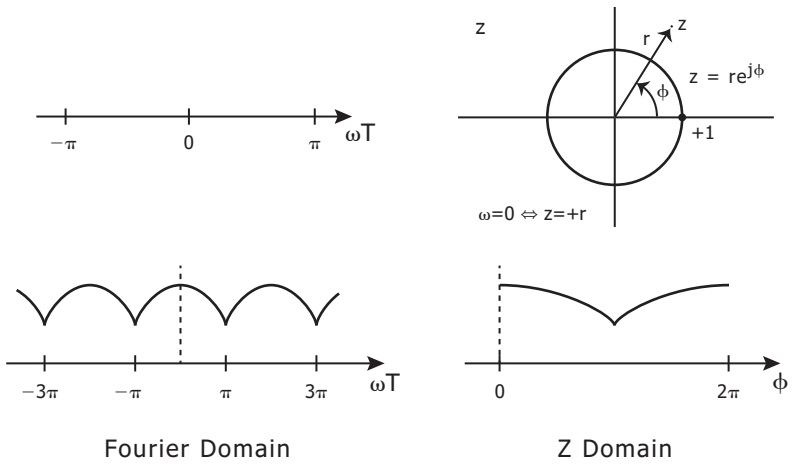

Fig. 4.1 Fourier and z domains. Upper part: the real line corresponds to a circle centered at the origin in the complex plane. Lower part: the periodic spectrum of the DTFT corresponds to a bound range of $[0, 2\pi)$ in angle ϕ.

At this point we want to change parameterization of the integral to z from ω. This requires the measure to change to dz from $d\omega$ and the line of the integral to change. Clearly $dz = jrTe^{j\omega T}d\omega$, thus

$$d\omega = \frac{1}{jT}z^{-1}dz \tag{4.4}$$

The line integral is more interesting. The original, Riemann integral is over $\omega \in [-\pi, \pi)$ on the real-number line. Parameterized as z, the line traces a counter-clockwise circle of radius r in the complex plane. The Riemann integral is replaced with a contour integral in the complex plane. Thus

$$\begin{aligned} x[n] &= \frac{T}{2\pi}\int_{-\pi/T}^{\pi/T} X(z)r^n e^{j\omega nT}d\omega \\ &= \frac{1}{2\pi}\oint_C X(z)z^n\frac{1}{j}z^{-1}dz \\ &= \frac{1}{2\pi j}\oint_C X(z)z^{n-1}dz \end{aligned}$$

We have thus arrived at the transform pair that corresponds to the DTFT pair along with the generalization $z = ru$.

The upper part of Fig. 4.1 illustrates the Fourier domain, ω, and the z-domain. The Fourier domain is the real line while the z-domain is the entire complex plane. For a given radius r a circle centered at the origin is traced out in the complex plane as ω sweeps from 0 to 2π. In particular, when $r = 1$

the DTFT is recovered from the z transform. At zero frequency $\omega = 0$ and unit radius the corresponding point in the z-domain is $z = +1$. Therefore the DC spectral component of the z-transform is at $z = +1$; this coordinate plays an essential role in several time-series analyses. The highest-frequency component in the DTFT is $\omega = \pi$, a point, which corresponds to the line $z \leq 0$ in the complex plane; at $r = 1$ the highest-frequency component is at $z = -1$.

4.1.1 Gain

Recall from §3.4.5 in Fourier analysis that the integral over all time of a signal $x(t)$ is found in the Fourier spectrum at $\omega = 0$. That is, $X(\omega = 0) = \int_{-\infty}^{\infty} x(t)dt$. The equivalent point for the z-transform is $X(z = 1)$. Referring to (4.1), the gain of a signal, or equivalently, a transform, is

$$g \equiv X(z = 1) = \sum_{n=-\infty}^{\infty} x[n] \tag{4.5}$$

assuming that the series converges. That $z = 1$ ties the Fourier- and Z-gain definitions together is not surprising because at this point $r = 1$.

4.1.2 Reconstruction and the Cauchy Integral Theorem

Unlike the inverse Fourier transform, the inverse z-transform requires a contour integral. While this course will not particularly use direct contour-integration, and in fact will rely on partial-fraction expansion which is a series of rules made possible by only ever having to invert rational quotients of polynomials, integration over poles and zeros and proof of signal reconstruction will be the exceptions.

Recall Cauchy's Integral Theorem [5]:

$$\oint_C f(z)dz = 0 \tag{4.6}$$

where $f(z)$ has no singularities inside the contour C. A minor specialization is to introduce a polynomial coefficient to $f(z)$ that has $m - 1$ roots at z_o. The Cauchy integral is unaltered:

$$\oint_C (z - z_o)^{m-1} f(z)dz = 0, \qquad m = 1, 2, \ldots \tag{4.7}$$

However, for $m \leq 0$ the integrand becomes an $1 - m$ singularity at z_o. There is a profound result in complex analysis which reads, using $n = -m$ as an

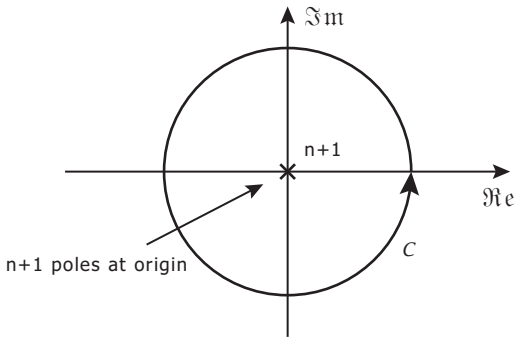

Fig. 4.2 A Cauchy integral for $z_o = 0$ having $n+1$ denominator roots. For $f(z) = z$ the contour integral evaluates to $\delta[n]$.

index:

$$f^{(n)}(z_o) = \frac{n!}{2\pi j} \oint_C \frac{f(z)}{(z - z_o)^{n+1}}\, dz, \qquad n = 0, 1, 2, \ldots \tag{4.8}$$

A smooth function f of z integrated about a point z_o that is a $(n+1)$-order singularity yields the n^{th} derivative of f at z_o. These two formulae are summarized as

$$\frac{1}{2\pi j} \oint_C \frac{f(z)}{(z - z_o)^{n+1}}\, dz = \begin{cases} 0 & n = \ldots, -2, -1 \\ \frac{1}{n!} f^{(n)}(z_o) & n = 0, 1, 2, \ldots \end{cases} \tag{4.9}$$

For the present purpose, set $z_o = 0$ and $f(z) = z$. Clearly $f^{(n)} = 0$ for $n > 0$. Cauchy's theorem reduces to

$$\frac{1}{2\pi j} \oint_C \frac{1}{z^{n+1}}\, dz = \begin{cases} 1 & n = 0 \\ 0 & \text{otherwise} \end{cases} \tag{4.10}$$

In the vocabulary of signal processing, this integral evaluates to $\delta[n]$. Figure 4.2 illustrates this integral.

This one contour integral (4.10) is all that is needed to prove reconstruction of $x[n]$ from the inverse z-transform. Direct substitution of (4.1) into (4.2) yields

$$\begin{aligned}\frac{1}{2\pi j}\oint_C X(z)z^{n-1}dz &= \frac{1}{2\pi j}\oint_C \sum_{k=-\infty}^{\infty} x[k]\, z^{-k+n-1}dz \\ &= \sum_{k=-\infty}^{\infty} x[k]\,\frac{1}{2\pi j}\oint_C z^{-k+n-1}dz \\ &= \sum_{k=-\infty}^{\infty} x[k]\delta[n-k]\end{aligned}$$

Recall from §**??** (2.3) that a time-series $x[n]$ can be constructed using the delta function $\delta[n]$ in superposition:

$$x[n] = \sum_{k=-\infty}^{\infty} \delta[n-k]x[k]$$

This completes the proof that the inverse z-transform faithfully reconstructs the original signal.

4.2 Region of Convergence

In order for the z-transform to exist the infinite sum in (4.1) must converge. Section §3.6 discussed various convergence modes for the Fourier transform, including absolute, mean-square, and generalized convergence. The z-transform admits only absolute convergence, but enlarges the set of signals that converge absolutely as compared to the Fourier transform because of addition of radius r to the series.

The set of admissible convergence modes has changed because z spans the entire complex plane and $X(z)$ represents what in complex analysis is called an analytic function. An analytic function $f(z)$ is a function where $f(z)$ and all of its derivatives are continuous functions of z. Mean-square and generalized convergence modes allow the Fourier transform to be defined for discontinuous functions $X(\omega)$, but there is no analogue in the complex plane.

As carefully stated in [], the convergence-mode discrepancies between the Fourier- and z-transforms mean that, "it is not strictly correct to think of the Fourier transform as being the z-transform evaluated on the unit circle...". It is better to say that for $r = 1$ the z-transform reduces to the DTFT when the latter converges. Nonetheless in a colloquial sense we say that the z-transform reduces to the Fourier transform.

The criterion for absolute convergence of the z-transform may be stated in general:

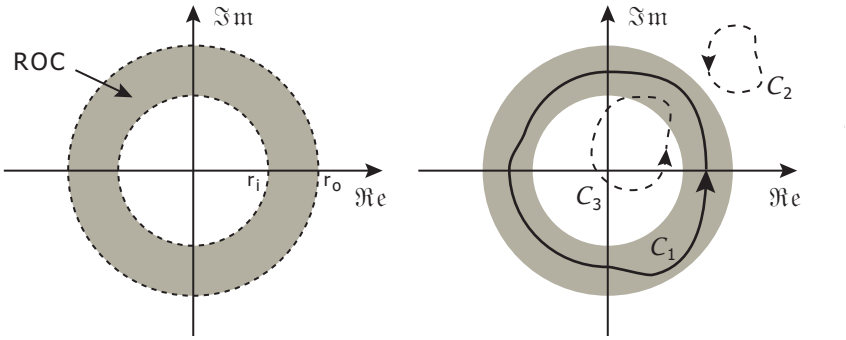

Fig. 4.3 Region of convergence and contour integrals in relation. Left: The most general ROC is an annulus centered at the origin with finite inner and outer radii. The inner radius may go to zero, and the outer radius may go to infinity. Right: Contour paths $\mathcal{C}$ in relation to a specific ROC. Only $\mathcal{C}_1$ lies entirely in the ROC.

$$\begin{aligned} |X(z)| &= \left| \sum_{n=-\infty}^{\infty} x[n] z^{-n} \right| \\ &\leq \sum_{n=-\infty}^{\infty} \left| x[n] z^{-n} \right| \\ &= \sum_{n=-\infty}^{\infty} |x[n]|\, r^{-n} < \infty \end{aligned} \tag{4.11}$$

The "region of convergence" (ROC) refers to all values of z in the complex plane where the z-transform converges. Since the magnitude of z depends only on r, not ϕ, the ROC in the complex plane will be annular with inner and outer circles centered at the origin, see Fig. 4.3(left). In general $r_i \geq 0$ and $r_o \leq \infty$. Which values of r allow convergence depends on the specifics of $x[n]$.

The ROC must always be specified when stating a z-transform expression $X(z)$. Without it there can be ambiguity in the reconstruction of signal $x[n]$.

The ROC defines the area in the complex plane where $X(z)$ is defined. The inverse z-transform is a closed contour integral in the complex plane. Since the inverse transform is the reverse image of $\mathcal{Z}\{x[n]\}$ all points along the contour must lie in the ROC to reconstruct $x[n]$. Figure 4.3(right) illustrates three different closed contours: $\mathcal{C}_1$, $\mathcal{C}_2$ and $\mathcal{C}_3$. Only $\mathcal{C}_1$ lies in the ROC, it is a valid contour to reconstruct $x[n]$. That this contour is deformed loop rather than a circle centered at the origin is only to illustrate that in terms of general complex analysis contours may be deformed as long as they do not cross a singularity. Contour $\mathcal{C}_2$ is completely outside of the ROC and is

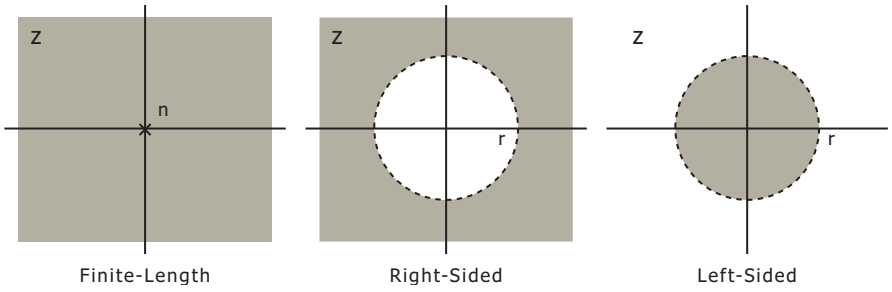

Fig. 4.4 ROC examples. Left: The ROC of a finite delay is the entire complex plane punctured at the origin. Middle: A right-sided sequence has an ROC that excludes a circle with radius r_i; that radius may be zero. Right: A left-sided sequence has an ROC within a circle centered at the origin.

therefore not valid. $\mathcal{C}_3$ crosses into and out of the ROC and is likewise not valid.

4.2.1 Example 1: A Finite-Length Sequence

The simplest case is a finite-impulse response (FIR) sequence $x[n]$ on $[N_-, N_+]$. The absolute value of the z-transform is dominated by

$$\begin{aligned} |X(z)| &= \left| \sum_{N_-}^{N_+} x[n] z^{-n} \right| \\ &\leq \sum_{N_-}^{N_+} |x[n]|\, r^{-n} \end{aligned} \tag{4.12}$$

where $|x[n]| < \infty, \forall n \in [N_-, N_+]$. At $r = 0$ there are n singularities, therefore the origin is not in the ROC. Excluding the origin, the ROC is the rest of the complex plane. The ROC is illustrated in Fig. 4.4.

4.2.2 Example 2: A Right-Sided Sequence

A right-handed signal is zero for all $n < N_{\min}$ and finite otherwise. Generally one sets $N_{\min} = 0$ without loss of generality. This is a single-sided infinite-impulse response (IIR) signal. The absolute value of the z-transform is dominated by

$$
\begin{aligned}
|X(z)| &= \left| \sum_{n=0}^{\infty} x[n] z^{-n} \right| \\
&\leq \sum_{n=0}^{\infty} |x[n]|\, r^{-n}
\end{aligned} \tag{4.13}
$$

There is a minimum r above which the right-handed sequence always converges. Any r below the minimum produces a series that decays too slowly, leaving the sum to go to infinity. All points in the complex plane where $r \geq r_{\min}$ are in the ROC, see Fig. 4.4.

4.2.3 Example 3: A Left-Sided Sequence

Instead of a right-handed signal consider a left-handed one. The absolute value of the z-transform is dominated by

$$
\begin{aligned}
|X(z)| &= \left| \sum_{n=-\infty}^{0} x[n] z^{-n} \right| \\
&\leq \sum_{n=-\infty}^{0} |x[n]|\, r^{-n} \\
&= \sum_{m=0}^{\infty} |x[-m]|\, r^{m}
\end{aligned} \tag{4.14}
$$

Note that the decay term is r^m rather than r^{-n}. Therefore the sense of minimum and maximum reverse, so one can say that for a left-sided sequence there is a maximum r below which the sequence always converges. All points in the complex plane where $r \leq r_{\max}$ are in the ROC, see Fig. 4.4.

Now consider that the left- and right-hand sequences are mirror images of one another about the origin: $x_r[n] = x_l[-n]$. Then

$$
\begin{aligned}
X_r(z) &= \sum_{n=0}^{\infty} x_r[n] z^{-n} \\
&= \sum_{n=0}^{\infty} x_l[-n] z^{-n} \\
&= \sum_{m=-\infty}^{0} x_l[m]\, (1/z)^{-m} \\
&= X_l(1/z)
\end{aligned} \tag{4.15}
$$

And as shown in (4.13-4.14), the ROC between the left- and right-hand sequences are conjugates. Moreover, in cases where $X(z) = X(1/z)$, which do exist, then one must specify the ROC in order to uniquely reconstruct the series $x[n]$.

4.3 Rational Function Representation

This course and much of signal processing in general allows for a specialization of $X(z)$ that reduces the contour integration to a set of rules. While in general $X(z)$ is an arbitrary complex function of the complex variable z, going forward we will only consider the case where $X(z)$ is a rational function of z in the form

$$X(z) = \frac{\mathcal{P}(z)}{\mathcal{Q}(z)} \tag{4.16}$$

where $\mathcal{P}(z)$ and $\mathcal{Q}(z)$ are simple polynomials of z.

Let us review the various polynomial representations. The form we are all familiar with is

$$f(x) = c_N x^N + c_{N-1} x^{N-1} + \cdots + c_1 x + c_0$$

More compactly: $f(x) = \sum_{i=0}^{N} c_i x^i$. A polynomial root is a specific value of x, denote it x_r, where the polynomial is equal to zero: $f(x_r) = 0$. The Fundamental Theorem of Algebra states that there are N roots, real and/or complex, to any N^{th}-order polynomial. Denote the set of roots has $\{x_{r,1}, x_{r,2}, \ldots, x_{r,N}\}$. When two or more roots are equal then the polynomial is said to have degenerate roots.

A polynomial can be factored by its roots to replace the additive expression of (4.17) with a multiplicative one:

$$f(x) = \sum_{i=0}^{N} c_i x^i = c_N \prod_{i=1}^{N} (x - x_{r,i})$$

The latter expression illustrates better that when $x = x_{r,i}$ for any i then $f(x) = 0$.

In the context of z-transforms, where there is a close association with the DTFT, polynomials are written in z^{-1} rather than z. Replace the above using $x = z^{-1}$ and note that the roots are $x_r = z_r^{-1}$ to get

$$f(z) = \sum_{i=0}^{N} c_i z^{-i} = \kappa \prod_{i=1}^{N} \left(1 - z_{r,i} z^{-1}\right) \tag{4.17}$$

where $\kappa = c_N \prod x_{r,i}$.

Let us return to the quotient (4.16). In the context of time-series analysis, the roots of $\mathcal{P}(z)$ are called **zeros**, because $X(z) = 0$ at these values of z. The roots of $\mathcal{Q}(z)$ are called **poles**, which is to say $X(z)$ has singularities at these points. You will have to read the following notation carefully to avoid errant ambiguity. The zeros and poles of $X(z)$ are in the sets $\{z_1, z_2, \ldots, z_{N_\mathcal{P}}\}$ and $\{p_1, p_2, \ldots, p_{N_\mathcal{Q}}\}$, respectively. The complex variable z represents any complex number but z_i represents a specific root of $\mathcal{P}(z)$ which is a zero of $X(z)$. I have done this to minimize the decoration needed on the polynomial roots but the character z is reused. With this notation $X(z)$ is written as

$$X(z) = K \frac{\prod_{i=1}^{N_\mathcal{P}} \left(1 - z_i z^{-1}\right)}{\prod_{i=1}^{N_\mathcal{Q}} \left(1 - p_i z^{-1}\right)} \tag{4.18}$$

This representation in turn can be written as the sum of simpler fractions using the method of partial-fraction expansion.

Partial-fraction expansion is straight forward but there are two points to keep in mind. First, if $N_\mathcal{P} \geq N_\mathcal{Q}$ then a first factoring must be done; second, if there are degenerate poles then derivatives have to be taken to determine some of the coefficients.

Given $N_\mathcal{P}$ zeros and $N_\mathcal{Q}$ poles, $X(z)$ is expressed as

$$X(z) = \mathcal{D}(z) + \frac{\mathcal{R}(z)}{\mathcal{Q}(z)} \tag{4.19}$$

where the order of $\mathcal{D}(z)$ is $(0, N_\mathcal{P} - N_\mathcal{Q} + 1)_+$ and the order of $\mathcal{R}(z)$ is $(N_\mathcal{Q} - 1)_+$. When $N_\mathcal{P} < N_\mathcal{Q}$ then $\mathcal{D}(z) = 0$ and $\mathcal{R}(z) = \mathcal{P}(z)$. In relation to (4.19), **when there are no degenerate poles** the expansion reads

$$X(z) = \sum_{i=0}^{N_\mathcal{P} - N_\mathcal{Q}} D_i z^{-i} + \sum_{i=1}^{N_\mathcal{Q}} \frac{A_i}{1 - p_i z^{-1}} \tag{4.20}$$

The coefficients D_i are found by polynomial long division of $\mathcal{P}(z)/\mathcal{Q}(z)$, where the division is carried out until the order of the remainder $\mathcal{R}(z)$ is $N_\mathcal{Q} - 1$. The coefficients A_i are determined by

$$A_i = \left(1 - z_p z^{-1}\right) X(z)\Big|_{z=p_i} \tag{4.21}$$

That this formula holds is seen immediately by multiplying (4.20) by the simple polynomial with pole p_i, $\left(1 - p_i z^{-1}\right)$, and evaluating at the pole location. All terms drop except for A_i. It is also evident that when there are degenerate poles this formula does not work: the order of $\left(1 - p_i z^{-1}\right)$ is too low to remove the singularity.

When there are degenerate poles the associated coefficients A_i require a different formula. Consider that one pole p_d is s-order degenerate. There are $N_{\mathcal{Q}} - s$ non-degenerate poles. Partial-fraction expansion in this case reads

$$X(z) = \sum_{i=0}^{N_{\mathcal{P}}-N_{\mathcal{Q}}} D_i z^{-i} + \sum_{\substack{i=1 \\ i\neq d}}^{N_{\mathcal{Q}}} \frac{A_i}{1-p_i z^{-1}} + \sum_{m=1}^{s} \frac{C_m}{\left(1-p_d z^{-1}\right)^m} \tag{4.22}$$

where

$$C_m = \frac{1}{(s-m)!\,(-p_d)^{s-m}} \left(\frac{d^{(s-m)}}{d\xi^{(s-m)}} \left((1-p_d\xi)^s X(1/\xi) \right) \right) \Bigg|_{\xi=p_d^{-1}} \tag{4.23}$$

where $\xi = z^{-1}$. The origin of this formula will be addressed below.

The summarize the significance of partial-fraction expansion as applied to $X(z)$, the rational-function representation of (4.16) is in terms of products and quotients of simple polynomials of the form $\left(1-z_r z^{-1}\right)$. The expanded representation of (4.20) and (4.22) is the linear combination of simple polynomials in the forms z^{-1} and $\left(1-z_r z^{-1}\right)^k$. Given the linearity of the z-transform, each term in the partial-fraction expansion can be inverse transformed and summed to arrive at the inverse transform of $X(z)$. Specifically,

$$\begin{aligned} \mathcal{Z}^{-1}\{X(z)\} = & \sum_{i=0}^{N_{\mathcal{P}}-N_{\mathcal{Q}}} D_i \mathcal{Z}^{-1}\left\{z^{-i}\right\} + \\ & \sum_{\substack{i=1 \\ i\neq d}}^{N_{\mathcal{Q}}} A_i \mathcal{Z}^{-1}\left\{\frac{1}{1-p_i z^{-1}}\right\} + \sum_{m=1}^{s} C_m \mathcal{Z}^{-1}\left\{\frac{1}{\left(1-p_d z^{-1}\right)^m}\right\} \end{aligned} \tag{4.24}$$

Consequently we can restrict our focus from the set of all possible functions $X(z)$ whose inverse transform we need to compute to the set of inverse transforms for these three simple polynomials.

4.3.1 A Note About z and z^{-1}

This text and others uses z and z^{-1} interchangeably and while the representations are equal there is a place for both. Historically z-transforms draw from two fields: Fourier analysis in engineering (as apart from Mathematics) and complex analysis. The DTFT from an engineer's perspective uses $e^{-j\omega nT}$ as the basis, which leads to the z^{-n} basis for the z-transform. Complex analysis from a Mathematician's perspective is based on complex functions of z, as is evidenced by Cauchy's Theorems. When we want to draw from one domain

of expertise we cast $X(z)$ into that format, and recast when drawing from the other. To summarize:

z^{-1}	Use for $\mathcal{Z}\{x[n]\}$ calculations, for finite-difference equations, partial-fraction expansion, and look-up tables for transforms
z	Use for pole-zero diagrams, amplitude and phase spectra, complex analysis and contour integrals for $\mathcal{Z}^{-1}\{X(z)\}$.

Knowing when to use one form or the other will save time, but remember that there is nothing fundamentally different.

4.4 Cauchy's Residue Theorem

The preceding section asserted that many system functions of interest are rational functions of polynomials. Partial-fraction expansion was used to recast the rational function as a linear combination of simple polynomials. The result was that the inverse transform is a sum of elementary inverse transforms.

The full theory of the inverse transform of $X(z)$ uses Cauchy's Residue Theorem. The theorem states that

$$\oint_C f(z)dz = 2\pi j \sum_{i=1}^{n} \text{Res}(f; z_{r,i}) \tag{4.25}$$

where the contour $\mathcal{C}$ lies in an analytic, connected region in the complex plane and encloses n singularities of $f(z)$. The residue at s-order singularity z_r is

$$\text{Res}(f; z_r) = \lim_{z \to z_r} \frac{1}{(s-1)!} \frac{d^{s-1}}{dz^{s-1}} \Big((z - z_r)^s f(z) \Big) \tag{4.26}$$

The theorem means that only singularities enclosed by the contour contribute to the integral, and the combined contribution is the sum of the residues at each pole.

For instance, $X(z) = \frac{z}{z-a}$ has a pole at $z = a$. For a contour centered at the origin that encloses the pole, and an ROC such that $|z| \geq a$, the inverse transform is

$$\begin{aligned}\frac{1}{2\pi j}\oint_C \frac{z}{z-a}z^{n-1}dz &= \text{Res}(X(z)z^{n-1}; z=a)\\ &= (z-a)\left(\frac{z}{z-a}z^{n-1}\right)\Big|_{z=a}\\ &= a^n u[n]\end{aligned}$$

Note the resemblance between the second line above and (4.21).

In contrast, $X_i(z) = \frac{z-a}{z}$ is the inverse function of the above and has a pole at $z = 0$. With an ROC such that the signal is right-sided, the inverse transform is

$$\begin{aligned}\frac{1}{2\pi j}\oint_C \frac{z-a}{z}z^{n-1}dz &= \frac{1}{2\pi j}\oint_C \left(\frac{z-a}{z^2}+\frac{z-a}{z}+(z-a)\,z^{(n-2)}\right)dz\\ &= \text{Res}\left(\frac{z-a}{z^2}; z=0\right)+\text{Res}\left(\frac{z-a}{z}; z=0\right)+0\\ &= \delta[n]-a\delta[n-1]\end{aligned}$$

where

$$\text{Res}\left(\frac{z-a}{z^2}; z=0\right) = \frac{d}{dz}\left(z^2\left(\frac{z-a}{z^2}\right)\right)\Big|_{z=0} = 1$$

and

$$\text{Res}\left(\frac{z-a}{z}; z=0\right) = \left(z\left(\frac{z-a}{z}\right)\right)\Big|_{z=0} = -a$$

Observe that the residual over the second-order pole at $z = 0$ for $n = 0$ was calculated using (4.26).

The Cauchy formalism is written in orders of z while the z-transform polynomials are written in orders of z^{-1}. For one thing this is the origin of the difference between the residue formula (4.26) and the coefficient formula for C_m in (4.23). The most straight-forward way to use the residue theorem for z-transforms is to recast $X(z)$ into polynomials of z. Let's do this with (4.18):

$$X(z) = \frac{K}{z^{(N_\mathcal{P}-N_\mathcal{Q})_+}}\frac{\prod_{i=1}^{N_\mathcal{P}}(z-z_i)}{\prod_{i=1}^{N_\mathcal{Q}}(z-p_i)} \tag{4.27}$$

where $(N_\mathcal{P}-N_\mathcal{Q})_+ = \max(0, N_\mathcal{P}-N_\mathcal{Q})$. There are $N_\mathcal{Q}+(N_\mathcal{P}-N_\mathcal{Q})_+$ singularities to evaluate, exactly the same number of terms in the partial-fraction expansion (4.22).

4.5 Causal Systems

At this point in the exposition I can continue in generality or specialize to detail an important case; I chose to specialize. Going forward I consider only causal systems. A causal system is one that does not (can not) anticipate. This seems natural for financial processes. However, before relegating non-causal systems to the ether let us recognize their significance.

A natural example of a non-causal system is our processing of speech. The last time you were listening to someone and were about to ask them to repeat what they said because you did not fully hear or comprehend, think about that your mind was doing. It had the full sentence and was going through combinations of words that would make sense and fulling in the gaps of what you did not hear. There are (very simple by comparison) analogous analytic methods that operate on a blocks of data to alter, in some way, the data based on the entire data set. All of this said, unless you believe in ESP, you can not hear what has not been spoken, and similarly, data blocks are not received before they are sent. At some level we live in a causal world, but there is distinction between streaming causality and block-by-block causality.

In the context of z-transforms causality fixes the ROC to right-sided IIR sequences, detailed in Example 4.2.2. The ROC extends from a inner circle, possibly of zero radius, out to infinity. Sequences derived from inverse transforms will be unique because they will always be to the right. The unit-step series $u[n]$ will now appear regularly to specify that there is no finite signal for $n < 0$. Remember that the "right-sided cutoff" is in general $N_{\min}$, and this is set to zero for simplicity of exposition.

4.6 Poles and the ROC

The ROC for a rational function (4.16) is governed by the location of the poles. Partial-fraction expansion (4.24) showed that there are only three principal complex functions that need to be considered, and these three functions have only two primary pole locations: $z = 0$ and $z = p, p \neq 0$. We need to find the ROC for these two primary functions and their linear combinations given that the series is causal.

Consider first $X(z) = z^{-N}$. The time-series that generates this complex function is $x[n] = \delta[n - N]$, as can be verified by

$$X(z) = \sum_{n=-\infty}^{\infty} \delta[n - N] z^{-n} = z^{-N} \tag{4.28}$$

This series converges for all z except $z = 0$. The ROC is the entire complex plane excluding the multi-order singularity at the origin. This is illustrated in Fig. 4.5. The inverse transform is evaluated along a contour $\mathcal{C}$ that resides

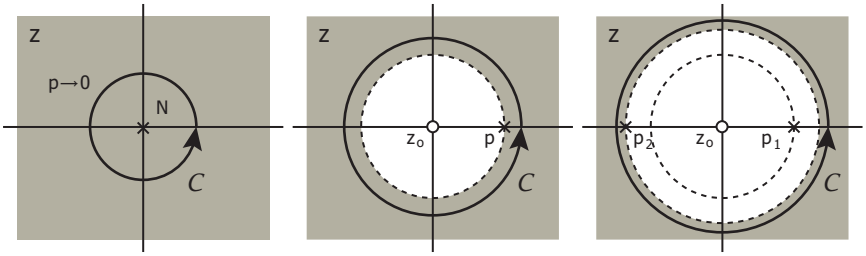

Fig. 4.5 Pole locations, associated (right-sided) ROCs, and contour integrals in relation. Left: A finite delay has a pole at the origin, the ROC is the entire complex plane other than the origin, and the contour is taken with any radius about the origin. Middle: A pole on the real axis, the ROC which starts a radius equal to the pole location, and a contour integral in the ROC. Right: Two distinct poles on the real axis, the ROC which starts at the outer pole.

completely in the ROC. Note also that causality was not invoked: FIR signals have no ambiguity to their sidedness.

Next consider $X(z) = \left(1 - pz^{-1}\right)^{-1}$. The right-sided IIR series that generates this function is $x[n] = p^n u[n]$:

$$\begin{aligned} X(z) &= \sum_{n=0}^{\infty} p^n z^{-n} = \sum_{n=0}^{\infty} \left(pz^{-1}\right)^n \\ &= \frac{1}{1 - pz^{-1}} = \frac{z}{z - p} \qquad |z| > |p| \end{aligned} \tag{4.29}$$

where the last fraction is written in terms of z so that the pole-zero diagram is simple to make, see Fig. 4.5. This series converges for $|z| > |p|$. The ROC is the complex plane except for a circle, including its circumference, centered at the origin with radius $r = p$.

Finally, consider a linear combination of complex functions, or equivalently, time series, with poles $p_{1,2}$. The transform is

$$\begin{aligned} X(z) &= \sum_{n=0}^{\infty} \left(p_1^n + p_2^n\right) z^{-n} \\ &= \sum_{n=0}^{\infty} \left(p_1 z^{-1}\right)^n + \left(p_2 z^{-1}\right)^n \\ &= \frac{z}{z - p_1} + \frac{z}{z - p_2} \qquad |z| > \max\left(|p_1|, |p_2|\right) \end{aligned} \tag{4.30}$$

The pole or multi-order poles that have the maximum radius from the origin determine the ROC of the whole, see Fig. 4.5.

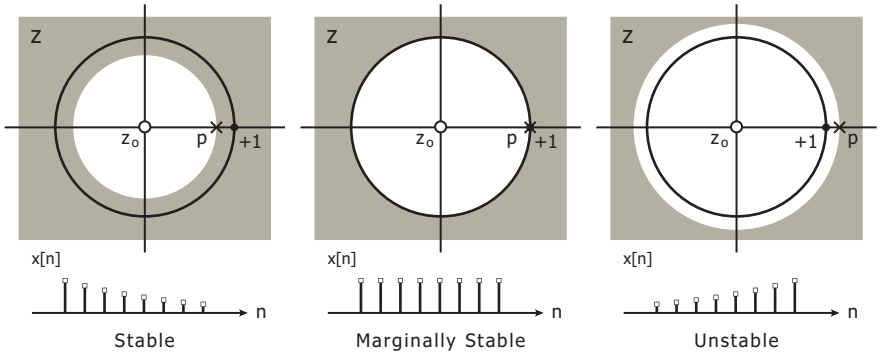

Fig. 4.6 Pole locations, the ROC, the unit circle and stability. Left: The pole lies within the unit circle, the impulse response is stable. Middle: The pole lies on the unit circle, the impulse response is marginally stable. Right: The pole lies outside of the unit circle, the impulse response is unstable.

4.7 Stability and the ROC

The preceding section showed how to find the ROC for FIR and causal IIR signals, where the minimum radius r for convergence of the z-transform is determined by the pole location(s) of the transform. Yet when we construct IIR signals by building a filter we want to ensure that the series itself is *stable*. By stability one means that the IIR signal is bound above, and since the partial-fraction expansion shows that one class of signals is $p^n u[n]$ we really want to guarantee $|p| \leq 1$.

In the complex plane there is a simple rule to determine whether or not a causal IIR signal is stable:

> A causal IIR sequence is stable if and only if the ROC includes the unit circle $|z| = 1$. A causal IIR sequence is marginally stable when the ROC is on the unit circle.

Since the pole locations determine the ROC, the poles alone govern whether or not an IIR signal will be stable once cast to a time series $x[n]$ from a complex function $X(z)$.

Figure 4.6 illustrates these three cases. When the outermost pole lies within the unit circle the system is guaranteed stable. Likewise, when the outermost pole falls outside of the unit circle the system is unstable. In the special case when the outermost pole lies on the unit circle the system is marginally stable[2].

[2] In econometrics this is known as a "unit root", because the pole value is unity, at least in magnitude. Whole books have been written about unit roots, but it is nothing more than a pole on the unit circle. In the following sections it will be shown that this has the effect of an integrator.

To make this more concrete, consider the IIR response to a single pole:

$$x[n] = p^n u[n]$$

Clearly when $|p| < 1$ the series $x[n]$ is bound from above, and when $|p| > 1$ the series explodes. In the marginal case $|p| = 1$ then $x[n] = u[n]$, which is bounded but does not have finite energy. In terms of gain (4.5) the gain is only finite for absolutely stable systems.

4.8 The Role of Zeros: An Overview

The ROC and system stability are governed by the poles of the system. Are zeros not important? In short: they are centrally important. At this point not all of the tools are in place to fully detail this fact, and this course will not even cover some of the ways that zeros govern pole locations.

The statements that can be made at this point in general are these, with no particular order. First, when a system is run backwards, that is $X(z) \to X^{-1}(z)$, the poles and zeros swap roles. This time-reversed system is only stable if the original zeros, which are now poles, lie within the unit circle. Second, the zeros effect the amplitude and phase spectrum of the system, thereby controlling, along with the poles, which frequency bands are and are not attenuated and delayed. This is equivalent to but not so obviously associated with the statement that the zeros control the residue amplitudes A_i and C_m in (4.22).

Zeros will not play much of a role throughout the rest of this chapter but will reappear during the discussion of state-space finite-different methods, in particular ARMA models.

4.9 Principal Functions for Rational Function Representation

Given a rational-function representation of $X(z)$ partial-fraction expansion showed that there are only three inverse z-transforms that need to be considered, c.f. (4.24). They are

$$x_1[n] = \mathcal{Z}^{-1}\left\{z^{-N}\right\} \tag{4.31}$$

$$x_2[n] = \mathcal{Z}^{-1}\left\{\frac{1}{1 - pz^{-1}}\right\} \tag{4.32}$$

$$x_3[n] = \mathcal{Z}^{-1}\left\{\frac{1}{(1 - pz^{-1})^s}\right\} \tag{4.33}$$

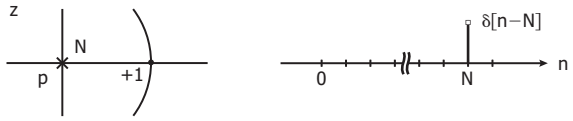

Fig. 4.7 Pole-zero diagram and impulse response pair. An N-order pole at the origin pairs with $\delta[n-N]$.

These components offer three distinct signals which will be detailed below. More complex signals are only linear combinations of these components.

4.9.1 Delay: N-Order Pole At The Origin

Consider (4.31) first. This is an N-order pole at the origin. Equation (4.28) indicates the signal / transform association:

$$\delta[n-N] \quad \overset{\mathcal{Z}}{\longleftrightarrow} \quad z^{-N} \tag{4.34}$$

The ROC is the entire complex plane except $z=0$. Figure 4.5(left) illustrates the case. The inverse transform is

$$\begin{aligned} x_1[n] &= \frac{1}{2\pi j}\oint_C z^{-N} z^{n-1} dz \\ &= \delta\left[n-N\right] \end{aligned} \tag{4.35}$$

That the time series is an impulse is due to Cauchy's Integral Theorem in the form of (4.10) where only z^{-1} contributes to the contour integral, and that is only for $n=N$.

In terms of signals, $\delta[n-N]$ is an N-step delayed version of $\delta[n]$. In the transform space z^{-N} is a delay operator, as illustrated in Fig. 4.7. Note that the sign of N can be positive or negative. Finally, the gain for the delay is unity: $g_1 = 1$.

4.9.2 Geometric Series: A Single Pole

Next consider (4.32). As shown in (4.29) the signal / transform association is

$$p^n u[n] \quad \overset{\mathcal{Z}}{\longleftrightarrow} \quad \frac{1}{1-pz^{-1}} \tag{4.36}$$

Following through to rigorously compute the inverse transform, we have $X_2(z) = \left(1-pz^{-1}\right)^{-1}$ so $f_2(z) = X_2(z)z^{n-1}$. The inverse transform is

$$x_2[n] = \frac{1}{2\pi j} \oint_C \frac{z^n}{z-p}\, dz \tag{4.37}$$

A right-sided sequence is for $n \geq 0$ so the only residue to compute is

$$(z-p)\, f_2(z)\Big|_{z=p} = p^n \tag{4.38}$$

The contour integral required to compute the residue must lie in an analytic region and enclose the pole. The analytic region is the ROC, which lies outside of the pole. Given the identification of the ROC and the residue of (4.38), the time series for $X_2(z)$ is

$$x_2[n] = p^n u[n] \tag{4.39}$$

as expected.

For $|p| < 1$ this is a geometric series with gain

$$g_2 = \frac{1}{1-p} \tag{4.40}$$

The pole-zero diagram is found by writing $X(z)$ in terms of z:

$$X_2(z) = \frac{z}{z-p}$$

As found in §4.7, the magnitude of p determines the stability of $x[n]$. However there is more to say. Figure 4.8 illustrates the significant positions of a (real-valued) pole p with respect to the unit circle and the origin. In case (a) the pole lies outside of the unit circle; the sequence is unstable.

In case (b) the pole on the unit circle at $p = z = 1$. This is significant enough a case identify on its own. The resultant series is the unit step function $u[n]$ and its transform dual is

$$u[n] \quad \overset{z}{\longleftrightarrow} \quad \frac{1}{1-z^{-1}} \tag{4.41}$$

The gain is infinite. It will be shown later than the action of a unit-step function is to integrate[3]. In transform space $\left(1-z^{-1}\right)^{-1}$ is the integration operator.

Cases (c-d) show that the rate of decay of the geometric series depends on how far the pole is from $z = 1$. That is, the pole in (c) is closer to unity than the pole in (d), consequently the (c)-series decays more slowly than (d). In the limit $p \to 0$ the decay is maximum and response is simply $\delta[n]$. All of this behavior has the flavor of frequency, where the (c)-series has a lower frequency than (d). Indeed this is the case, but a rigorous treatment of frequency response will be deferred to later.

[3] Continuous-time integration is replaced in discrete-time by accumulation.

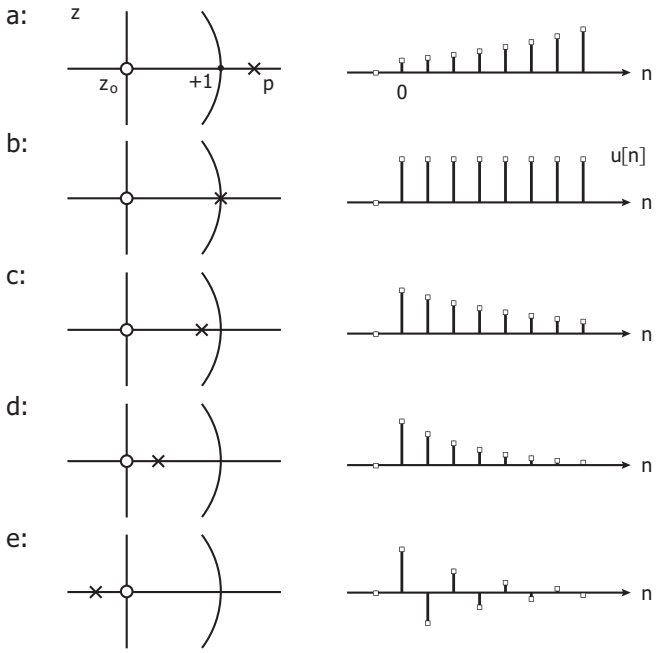

Fig. 4.8 Pole-zero diagram / impulse response pairs for a single real pole (and zero at the origin). The diagrams $(a) \rightarrow (e)$ show the pole being brought in from the right, initially outside of the unit circle and later crossing the origin. The impulse response goes from unstable to stable. The further the pole is away from the unit circle the faster the growth or decay. To the left of the origin the impulse response alternates between positive and negative (but this is not an oscillation).

Finally, case (e) shows that the time series alternates sign when $p < 0$. However the growth / decay envelope is the same as $|p|$.

4.9.3 Oscillating Series: The Complex Pole Pair

The complex-pole pair is not itself a characteristic term in the partial-fraction expansion of rational functions but it plays a sufficiently significant role in system response to have its own section.

There are some general properties of the z-transform to detail first. Given the transform pair $x[n] \overset{\mathcal{Z}}{\longleftrightarrow} X(z)$ is it evident that

$$x^*[n] \quad \overset{\mathcal{Z}}{\longleftrightarrow} \quad X^*(z^*) \tag{4.42}$$

The real and imaginary parts of $x[n]$ in terms of its z-transform are

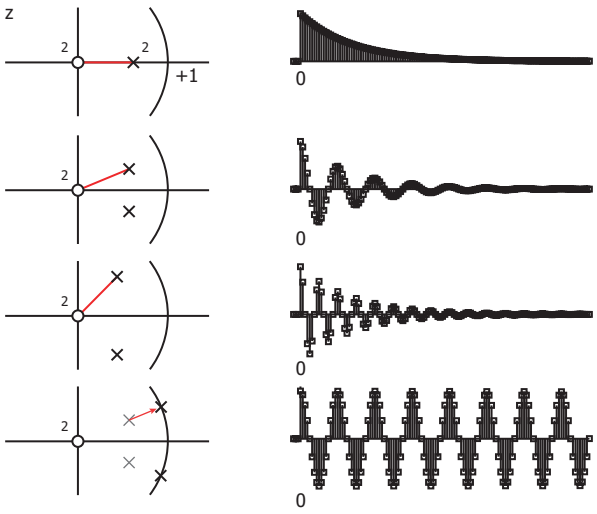

Fig. 4.9 Pole-zero diagram / impulse response pairs for a stable pole pair that comes off the real axis. Note the degenerate zeros at the origin. The diagrams $(a) \rightarrow (c)$ show the poles at a fixed radius and increasing angle away from the real axis. The impulse response which starts critically damped and then begins to oscillate, the oscillation rate increasing with angle. Pair (d) shows the pole pair at the same inclination as (b) but where the poles have been moved to the unit circle. Here, the envelope is marginally stable and the impulse response rings indefinitely.

$$\Re\mathrm{e}\left(x[n]\right) \quad \overset{\mathcal{Z}}{\longleftrightarrow} \quad \frac{1}{2}\Big(X(z) + X^*\left(z^*\right)\Big) \tag{4.43}$$

$$\Im\mathrm{m}\left(x[n]\right) \quad \overset{\mathcal{Z}}{\longleftrightarrow} \quad \frac{1}{2j}\Big(X(z) - X^*\left(z^*\right)\Big) \tag{4.44}$$

Now consider two single poles that have a finite real and imaginary part, and are complex conjugates of each other. In polar form, the location of one pole is $p = p_r e^{j\phi_p}$ where p_r is the radius from the origin of the complex plane and ϕ_r is the angle with respect to the real axis. The location of the other pole is $p^* = p_r e^{-j\phi_p}$. The z-transform has the form

$$X(z) \sim \frac{K}{\left(1 - pz^{-1}\right)\left(1 - p^* z^{-1}\right)} \tag{4.45}$$

We have enough tools now to directly take this inverse transform, but let us instead arrive at this form starting from a specific time series.

Start with the time series

$$x[n] = p_r^n \cos\left(n\phi_p\right) u[n] \tag{4.46}$$

Note that with $\phi_p = 0$ the familiar $x[n] = p^n u[n]$ is recovered. Expanding the cosine into complex exponentials and explicitly taking the z-transform gives

$$\begin{aligned} X(z) &= \frac{1}{2}\sum_{n=0}^{\infty} z^{-n}\left(p^n + p^{*n}\right) \\ &= \frac{1}{2}\sum_{n=0}^{\infty} \left(pz^{-1}\right)^n + \left(p^* z^{-1}\right)^n \\ &= \frac{1}{2}\left[\frac{1}{1-pz^{-1}} + \frac{1}{1-p^*z^{-1}}\right] \\ &= \frac{1-\left(p+p^*\right)z^{-1}/2}{\left(1-pz^{-1}\right)\left(1-p^*z^{-1}\right)} \\ &= \frac{1-p_r\ z^{-1}\cos\phi_p}{\left(1-pz^{-1}\right)\left(1-p^*z^{-1}\right)} \end{aligned} \tag{4.47}$$

which has the form of (4.45).

The series (4.46) has the form of the preceding section but with the added cosine coefficient. The oscillation cycle N_m is $N_m\phi = 2m\pi$. The larger the phase of the complex poles ϕ_p the shorter the cycle. The oscillation is enveloped by the progression of the geometric series p_r^n.

With a pole radius of $p_r = 1$ the series is said to be "critically damped", which is to say that the oscillation rings forever because the exponential envelope is unity.

In real systems time series are always real-valued. Complex poles always come in pairs when representing a real time series. To see this, apply (4.44) to (4.45):

$$\Im\mathrm{m}\left(x[n]\right) \quad \overset{\mathcal{Z}}{\longleftrightarrow} \quad \frac{1}{2j}\frac{K-K^*}{\left(1-pz^{-1}\right)\left(1-p^*z^{-1}\right)} \tag{4.48}$$

When $K = K^*$, which is the case in (4.47), then $x[n]$ is real. As an example to the contrary, based on the preceding it is clear that

$$p_r^n e^{jn\phi_p} u[n] \quad \overset{\mathcal{Z}}{\longleftrightarrow} \quad \frac{1}{2\left(1-pz^{-1}\right)} \tag{4.49}$$

The time series is both real and imaginary.

4.9.4 Polynomial Coefficients: N-Order Poles

Finally, consider (4.33), which is an s-order pole at $z = p$. For all s the ROC is $z > |p|$. In fact the case $s = 1$ has already been calculated. The general expression can be found by evaluating for $s = 2$ and $s = 3$ and extending by

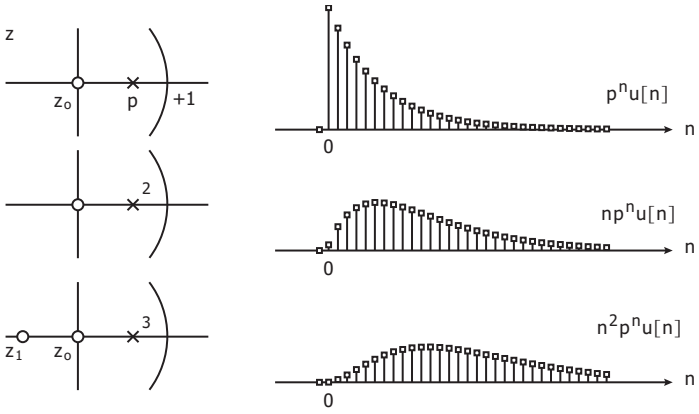

Fig. 4.10 Pole-zero diagram / impulse response pairs for polynomial-coefficient series. Left: A single pole-zero pair corresponds to a geometric decaying series. Middle: Two degenerate poles (and a zero at the origin) impart a linear coefficient to the decaying series. Right: Three degenerate poles (and zeros where shown) impart a quadratic coefficient to the series.

induction. One needs to use Cauchy's Residue Theorem (4.26) to take the higher-order residues. For $s = 2$:

$$X(z) = \frac{1}{\left(1 - pz^{-1}\right)^2} \longrightarrow f(z) = \frac{z^{n-1}}{\left(1 - pz^{-1}\right)^2} = \frac{z^{n+1}}{\left(z - p\right)^2} \tag{4.50}$$

The residue is

$$\begin{aligned} \mathrm{Res}\left(f(z); z = p\right) &= \frac{d}{dz}\Big(\left(z - p\right)^2 f(z)\Big)\Big|_{z=p} \\ &= \frac{d}{dz} z^{n+1}\Big|_{z=p} \\ &= (n+1)\, p^n \end{aligned} \tag{4.51}$$

Therefore the series is

$$x_{3,s=2}[n] = (n+1)\, p^n u[n] \tag{4.52}$$

For $s = 3$, $f(z) = \frac{z^{n+2}}{(z-p)^3}$ and the residue is

$$\begin{aligned}\operatorname{Res}\left(f(z); z=p\right) &= \frac{1}{2!}\frac{d^2}{dz^2}\Big(\left(z-p\right)^3 f(z)\Big)\Big|_{z=p} \\ &= \frac{1}{2!}\frac{d^2}{dz^2} z^{n+2}\Big|_{z=p} \\ &= \frac{1}{2!}\left(n+2\right)\left(n+1\right)p^n \end{aligned} \tag{4.53}$$

The series is

$$x_{3,s=3}[n] = \frac{1}{2!}\left(n+2\right)\left(n+1\right)p^n u[n] \tag{4.54}$$

From these cases its clear than for general s the inverse transform of an s-order pole is

$$x_{3,s}[n] = \frac{1}{(s-1)!}\left(\prod_{k=1}^{s-1}\left(n+s-k\right)\right)p^n u[n] \tag{4.55}$$

The transform pair is then

$$\frac{1}{(s-1)!}\left(\prod_{k=1}^{s-1}\left(n+s-k\right)\right)p^n u[n] \quad \overset{\mathcal{Z}}{\longleftrightarrow} \quad \frac{1}{\left(1-pz^{-1}\right)^s} \tag{4.56}$$

However, this is not canonical form. The form any table of z-transforms will have is simple in series and complicated in transform, the opposite of (4.56) (but no more correct). One can inductively generate the transform function for $n^s p^n u[n]$ in this way. Start with $s=2$,

$$\begin{array}{ccccc} \left(n+1\right)p^n u[n] & = & np^n u[n] & + & p^n u[n] \\ \downarrow & & & & \downarrow \\ \dfrac{1}{\left(1-pz^{-1}\right)^2} & = & ? & & \dfrac{1}{1-pz^{-1}} \end{array}$$

Clearly the missing term is

$$\frac{1}{\left(1-pz^{-1}\right)^2} - \frac{1}{\left(1-pz^{-1}\right)} = \frac{pz^{-1}}{\left(1-pz^{-1}\right)^2}$$

Therefore for $s=2$ the transform pair is

$$np^n u[n] \quad \overset{\mathcal{Z}}{\longleftrightarrow} \quad \frac{pz^{-1}}{\left(1-pz^{-1}\right)^2} \tag{4.57}$$

Similar analysis shows that the n^2 term has the transform pair of

$$n^2 p^n u[n] \quad \overset{\mathcal{Z}}{\longleftrightarrow} \quad \frac{pz^{-1}\left(1+pz^{-1}\right)}{\left(1-pz^{-1}\right)^3} \tag{4.58}$$

Expressions of the form $n^{s-1}p^n u[n]$ are products of an $s-1$-order polynomial in n with a geometric series. If the geometric series is stable (all poles lie inside the unit circle) then the decay of the series dominates the growth of n^s for all s, where s is on the natural positive numbers. Figure 4.10 illustrates the pole-zero diagram and associated impulse response for $s = 1, 2, 3$. The gain of the series $x_3[n]$ in (4.56) is

$$g_3\left(x_3[n]\right) = X_3(z=1) = \frac{1}{(1-p)^s} \tag{4.59}$$

The gains for (4.57-4.58) are similarly calculated.

4.10 Frequency Response

The frequency response for z-transforms that can be expressed as rational functions is particularly simple to evaluate because the contribution from each pole and zero is additive when cast in the appropriate domain. Moreover, unlike stability analysis, the zeros are as important as poles for frequency analysis.

Recall from (4.3) that radius r imparts the generalization of the z-transform with respect to the Fourier transform. But "frequency response" is a Fourier concept, so we must revert to $z = e^{j\omega T}$, or simply $r = 1$. Geometrically the frequency response of $X(z)$ is evaluated along the unit circle.

Rewriting the rational form of $X(z)$ from (4.18) in terms of frequency gives

$$X(\omega) = K\,\frac{\prod_{i=1}^{N_{\mathcal{P}}}\left(1 - z_i e^{-j\omega T}\right)}{\prod_{i=1}^{N_{\mathcal{Q}}}\left(1 - p_i e^{-j\omega T}\right)} \tag{4.60}$$

The reader is reminded that this frequency spectrum is periodic with condition $\omega_n T = 2\pi n$.

The two frequency-dependent functions of interest are the amplitude and group delay of $X(\omega)$. The amplitude response of $X(\omega)$ is just $|X(\omega)|$. The log-amplitude gives an expression that is additive, that is

$$\log|X(\omega)| = \log|K| + \sum_{i=1}^{N_{\mathcal{P}}}\log\left|1 - z_i e^{-j\omega T}\right| - \sum_{i=1}^{N_{\mathcal{Q}}}\log\left|1 - p_i e^{-j\omega T}\right| \tag{4.61}$$

Each pole and zero contributes to the log-amplitude spectrum in superposition to the others. The intensity I, defined as $I \equiv |z|^2$ where z is a complex number, for a generic term $\left(1 - ce^{-j\omega T}\right)$ is

$$\begin{aligned} I(\omega) &= \left|1 - ce^{j\omega T}\right|^2 \\ &= \left(1 - c^* e^{j\omega T}\right)\left(1 - ce^{-j\omega T}\right) \\ &= 1 + c^* c - 2\,|c| \cos\left(\omega T - \phi_c\right) \end{aligned} \tag{4.62}$$

where $c = |c|e^{j\phi_c}$. The modulation depth of such a periodic signal is defined as

$$M \equiv \frac{I_{\max} - I_{\min}}{I_{\max} + I_{\min}} \tag{4.63}$$

which is not a function of frequency. For the single pole or zero expression above, the modulation depth is

$$M = \frac{2|c|}{1 + |c|^2} \tag{4.64}$$

Accordingly, the closer a pole or zero is to the unit circle the larger the modulation depth; and for $|c| = 1$ the modulation depth is 100%.

4.10.1 Principal Value and Unwrapped Phase

Before the group delay spectrum can be calculated we must disambiguate "unwrapped phase" from the principal value of phase. Given a complex number expressed in polar form $z = |z|e^{j\phi_z}$ the angle is

$$\angle z \equiv \phi_z \tag{4.65}$$

This is an analytic definition. If I wrote that $z = |z|e^{j\phi_z + 2\pi n}$ then the angle, by this analytic definition, would be $\angle z = \phi_z + 2\pi n$. However, numerical methods cannot distinguish between orders of n and most, without further specification, will return ϕ_z such that $-\pi \le \phi_z \le \pi$. An angle bounded to one cycle is called the principal value of the phase. "Unwrapped phase" denotes the full phase of the argument, not modulo 2π. Most numerical packages have a function to return the unwrapped phase of a complex number[4]. □

Returning to the group delay spectrum of $X(\omega)$, recall that group delay is defined as

$$\mathrm{grp}X(\omega) \equiv -\frac{d\angle X(\omega)}{d\omega} \tag{4.66}$$

The angle of $X(\omega)$ is simply the contributions of each pole / zero term:

$$\angle X(\omega) = \sum_{i=1}^{N_{\mathcal{P}}} \angle\left(1 - z_i e^{-j\omega T}\right) - \sum_{i=1}^{N_{\mathcal{Q}}} \angle\left(1 - p_i e^{-j\omega T}\right) \tag{4.67}$$

[4] Such unwrap functions can be fooled, however. The results are not rarely perfect.

The delay operator is linear, so accounting for sign the group delay of $X(\omega)$ is

$$\text{grp}X(\omega) = -\sum_{i=1}^{N_{\mathcal{P}}} \text{grp}\left(1 - z_i e^{-j\omega T}\right) + \sum_{i=1}^{N_{\mathcal{Q}}} \text{grp}\left(1 - p_i e^{-j\omega T}\right) \tag{4.68}$$

All other things being equal, zeros reduce the group delay and poles increase it.

The angle of a generic term is

$$\begin{aligned}\angle\left(1 - ce^{-j\omega T}\right) &= \left(1 - |c|e^{-j\omega T + \phi_c}\right) \\ &= 1 - |c|\left(\cos\left(\omega T - \phi_c\right) - j\sin\left(\omega T - \phi_c\right)\right) \\ &= \tan^{-1}\frac{|c|\sin\left(\omega T - \phi_c\right)}{1 - |c|\cos\left(\omega T - \phi_c\right)}\end{aligned}$$

Direct application of the chain rule gives the group delay of this component:

$$\text{grp}\left(1 - ce^{-j\omega T}\right) = \frac{|c|T\left(|c| - \cos\left(\omega T - \phi_c\right)\right)}{1 + |c|^2 - 2|c|\cos\left(\omega T - \phi_c\right)} \tag{4.69}$$

Simplifying this express will give some insight. First, denote $\tau(\omega) = \text{grp}\left(1 - ce^{-j\omega T}\right)$. Also, take c real and compute for the two frequencies $\omega T = 0$ and $\omega T = \pi$. The two group delays are

$$\begin{aligned}\tau\left(\omega T = 0\right) &= -\frac{cT}{1 - c} \\ \tau\left(\omega T = \pi\right) &= \frac{cT}{1 + c}\end{aligned}$$

A negative delay is a lead rather than a lag. Signals may lead in Fourier analysis because of the underlying sine / cosine basis. Interestingly, $\tau(0)$ is unbounded as c approaches unity (from within the unit circle). Moreover, remember that there is another sign to consider: zeros have a negative sign in front of their delay contribution, poles have a positive sign (see (4.67)). If $\tau(\omega)$ refers to a pole, then as the pole approaches the unit circle the delay is arbitrarily large, for one frequency.

4.11 Convolution

As a linear time-invariant system the z-transform has the duality property of convolution in that convolution in one domain (e.g. time) is a product in the dual domain (e.g. z). The z-transform analogue of (3.12) is

$$y[n] = h[n] * x[n] \xleftrightarrow{\mathcal{Z}} Y(z) = H(z)X(z) \qquad \mathrm{ROC}_Y = \mathrm{ROC}_H \cap \mathrm{ROC}_X, \tag{4.70}$$

This property is readily verified by direct substitution:

$$\begin{aligned} Y(z) &= \sum_{n=-\infty}^{\infty} y[n]\, z^{-n} \\ &= \sum_{n=-\infty}^{\infty} z^{-n} \sum_{k=-\infty}^{\infty} h[n-k]x[k] \\ &= \sum_{k=-\infty}^{\infty} x[k] \sum_{n=-\infty}^{\infty} h[n-k]z^{-n} \\ &= \sum_{k=-\infty}^{\infty} x[k] \sum_{m=-\infty}^{\infty} h[m]z^{-(m+k)} \\ &= H(z) \sum_{k=-\infty}^{\infty} x[k]z^{-k} \\ &= H(z)X(z) \end{aligned}$$

As with Fourier transforms, the convolution of two sequences is the product of their respective transforms. The amplitude and delay spectrum of $H(z)$ is imposed onto $X(z)$ to yield an output response $Y(z)$. The additional complexity of the z-transform comes from the region of convergence of the output, which is the intersection of the ROCs of the two inputs.

4.12 Inversion

Given a system response $H(z)$ through which output $Y(z)$ is generated from an input $X(z)$ it is interesting to consider the circumstances under which $X(z)$ can be recovered from $Y(z)$. That is

$$Y(z) = H(z)X(z) \xleftrightarrow{?} X(z) = H^{-1}(z)Y(z)$$

We seek an identity function

$$I(z) = H^{-1}(z)H(z) = H(z)H^{-1}(z) = 1 \tag{4.71}$$

or equivalently in time domain

$$i[n] = h^{-1}[n] * h[n] = h[n] * h^{-1}[n] = \delta[n] \tag{4.72}$$

Let's consider the practical case where $H(z)$ is causal, stable and a rational function. Then

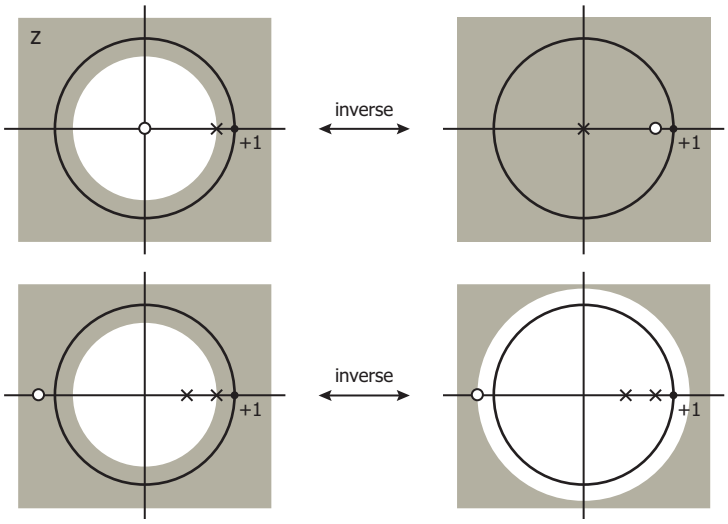

Fig. 4.11 System response inversion. Top: (left) pole-zero diagram of a stable geometric-decay series; (right) the inverse system swaps pole and zero locations, and the ROC changes accordingly. The forward and reverse system are both stable in this case. Bottom: (left) pole-zero diagram of a stable system (due to the poles) and a zero outside of the unit circle; (right) the inverse system is unstable because one pole lies outside the unit circle.

$$H(z) = K\frac{\prod_{i=1}^{N_\mathcal{P}}\left(1 - z_i z^{-1}\right)}{\prod_{i=1}^{N_\mathcal{Q}}\left(1 - p_i z^{-1}\right)} \longrightarrow H^{-1}(z) = K^{-1}\frac{\prod_{i=1}^{N_\mathcal{Q}}\left(1 - p_i z^{-1}\right)}{\prod_{i=1}^{N_\mathcal{P}}\left(1 - z_i z^{-1}\right)}$$

In the inverse system poles become zeros and zeros become poles, but there is no change of location. Causality and stability of $H(z)$ means that the ROC extends outward from a circle of radius $r_{\text{ROC}} \geq \max p_i$ and includes the unit circle. For $H^{-1}(z)$ to also be causal and stable its ROC must extend outward from a circle of minimum radius and include the unit circle. Since the poles of $H^{-1}(z)$ are the zeros of $H(z)$ that minimum radius is $r_{\text{ROC}-\text{inv}-\text{min}} = \max z_i$. In addition, the ROCs of the original and inverse systems must intersect or else $I(z)$ does not exist, see (4.70). Figure 4.11 illustrates two cases of inversion.

Under certain circumstances an IIR response of $H(z)$ becomes and FIR response of $H^{-1}(z)$. The partial-fraction expansion of a rational function (4.19) shows when this is the case. Consider a rational function with $N_\mathcal{P} = 0$ and $N_\mathcal{Q} > 0$; the partial-fraction expansion is

$$H(z) = \mathcal{D}(z) + \frac{\mathcal{R}(z)}{\mathcal{Q}(z)}$$

where the orders are $N_\mathcal{D} = (N_\mathcal{P} - N_\mathcal{Q} + 1)_+ = 0$ and $N_\mathcal{R} = (N_\mathcal{Q} - 1)_+ = N_\mathcal{Q} - 1$. The $\mathcal{D}(z)$ term vanishes. In this case $H(z)$ is purely IIR.

The inverse $H^{-1}(z)$ has $N_{\mathcal{P}} > 0$ and $N_{\mathcal{Q}} = 0$. Its expansion is

$$H^{-1}(z) = \mathcal{D}'(z) + \frac{\mathcal{R}'(z)}{\mathcal{Q}'(z)}$$

where here the orders are $N_{\mathcal{D}'} = N_{\mathcal{Q}} + 1$ and $N_{\mathcal{R}'} = 0$. In case the $\mathcal{R}'(z)/\mathcal{Q}'(z)$ term vanishes leaving only the $\mathcal{D}'(z)$ term, which is purely FIR.

The partial-fraction expansion analysis is complete but a bit long-winded. Simply put, consider $H(z)$ having the form

$$H(z) = K \frac{1}{\prod_{i=1}^{N_{\mathcal{Q}}} (1 - p_i z^{-1})}$$

with a causal ROC. The temporal response is IIR. The inverse system is

$$H^{-1}(z) = K^{-1} \prod_{i=1}^{N_{\mathcal{Q}}} \left(1 - p_i z^{-1}\right)$$

This is just a finite-number of delays each with some weight. This response is FIR.

4.13 Examples

The following examples highlight some of the properties of the z-transform.

4.13.1 Example 4: Delay

Consider a series $x[n]$ is that is subsequently delayed by N steps. The delay operation in time is simply

$$x[n - N] = \delta[n - N] * x[n]$$

Taking the z-transform of both sides yields

$$\mathcal{Z}\left\{x[n - N]\right\} = z^{-N} X(z)$$

where the first term on the right-hand side comes from (4.34). The delay operator in z is thus

$$x[n - N] \quad \overset{\mathcal{Z}}{\longleftrightarrow} \quad z^{-N} X(z) \tag{4.73}$$

Note that the gain of the delay is unity: $H(z = 1) = 1$.

4.13.2 Example 5: Accumulator

Consider the accumulation of a right-sided series $x[n]$:

$$y[n] = \sum_{k=0}^{n} x[k]$$

An equivalent expression is to convolve $x[n]$ with the unit-step function $u[n]$:

$$\begin{aligned} y[n] &= \sum_{k=-\infty}^{\infty} u[n-k]x[k] \\ &= u[n] * x[n] \end{aligned}$$

Taking the z-transform of both sides yields

$$Y(z) = \frac{1}{1-z^{-1}}\ X(z)$$

where (4.41) is used for the unit step. The accumulation operator can be written

$$\sum_{k=0}^{n} x[k] \quad \overset{\mathcal{Z}}{\longleftrightarrow} \quad \frac{1}{1-z^{-1}}\ X(z) \tag{4.74}$$

The gain of the accumulation operator is infinite: $H(z=1) = 1/(1-1)$. Infinite gain of the accumulator is reasonable because a single impulse at the input changes the accumulated value forever. Even after the input returns to zero the new output level persists.

4.13.3 Example 6: Differencer

The first difference of a series is written

$$y[n] = x[n] - x[n-1]$$

The z-transform is found by inspection:

$$Y(z) = (1-z^{-1})X(z)$$

The difference operator can be written

$$x[n] - x[n-1] \quad \overset{\mathcal{Z}}{\longleftrightarrow} \quad \left(1-z^{-1}\right)\ X(z) \tag{4.75}$$

The gain of the differencing operator is zero.

Note that the accumulation and (first) difference operators are inverses of one another. The accumulator is an IIR filter that is marginally stable, and the difference operator is an FIR filter. Since the ROC intersection is finite (in fact an identity) the identity operator exists and the net gain is, in this case, unity.

4.13.4 Example 7: An ARMA(2,1) Model

Consider the recursive difference equation

$$y[n] = \phi_1 y[n-1] + \phi_2 y[n-2] + x[n] + \theta_1 x[n-1]$$

with initial conditions $y[0] = y_0, y[1] = y_1$. Given an input sequence $x[n]$ one generally wants to find the solution $y[n]$ for all n. This equation is hard to solve by long-hand iteration, but simple under the z-transform. Taking the transform of both side by inspection gives

$$\begin{aligned} Y(z) &= \phi_1 z^{-1} Y(Z) + \phi_2 z^{-2} Y(z) + X(z) + \theta_1 z^{-1} X(z) \\ \left(1 - \phi_1 z^{-1} - \phi_2 z^{-2}\right) Y(z) &= \left(1 + \theta_1 z^{-1}\right) X(z) \\ Y(z) &= \frac{1 + \theta_1 z^{-1}}{1 - \phi_1 z^{-1} - \phi_2 z^{-2}} X(z) \\ &= H(z) X(z) \end{aligned}$$

where the system response is

$$H(z) = \frac{1 - z_1 z^{-1}}{\left(1 - p_1 z^{-1}\right)\left(1 - p_2 z^{-1}\right)}$$

This system has zeros at $z = 0$ and $z = z_1$, and poles at $z = p_{1,2}$. Depending on the selection of coefficients $\phi_{1,2}$ and θ_1 the system may or may not be stable, and may or may not have a stable inverse. The gain of the system is

$$g = \frac{1 - z_1}{\left(1 - p_1\right)\left(1 - p_2\right)}$$

Partial-fraction expansion of $H(z)$ yields

$$H(z) = \frac{A_1}{1 - p_1 z^{-1}} + \frac{A_2}{1 - p_2 z^{-1}}$$

where now the inverse transform can be taken by inspection to give the temporal system response

$$h[n] = A_1 \sum_{i=0}^{\infty} p_1^n + A_2 \sum_{i=0}^{\infty} p_2^n$$

The solution $y[n]$ for all n is therefore

$$y[n] = h[n] * x[n]$$

Chapter 5
Linear Finite-Difference Equations

The z-transform is the gateway to fully understand the construction, solution and interpretation behind econometric linear constant-coefficient finite-difference equations. These equations are written in recursive form between input and output so as to capture system dynamics at each increment of time. The solution is an equation that describes the output for all time. All solutions are a combination of delays, exponential moving averages (possibly with polynomial coefficients), differences and accumulations. While solving a system is ultimately mechanical, the construction and interpretation are essential to implementing a meaningful filter. The material covered in preceding chapters allows us to take a critical look at several common examples.

5.1 The ARMA Model

The classical, canonical linear constant-coefficient finite-difference equations used in econometrics is the auto-regressive moving-average (ARMA) model. In my opinion the ARMA model is at best a phenomenological model but because of its prevalent use and some pedagogical import I will start here.

From a signals point of view, the ARMA model transforms a discrete input sequence $x[n]$ to an output sequence $y[n]$ through its intrinsic system response $h[n]$ via convolution

$$y[n] = h[n] * x[n] \tag{5.1}$$

The structure of a particular ARMA model governs the impulse response $h[n]$.

In recursive form a general ARMA(p, q) model is defined as

$$y[n] = \sum_{i=1}^{p} \phi_i y[n-i] + \sum_{j=0}^{q} \theta_j x[n-j] \tag{5.2}$$

There are two parameter vectors: $\boldsymbol{\phi}$ with p entries and $\boldsymbol{\theta}$ with q entries, all of which are constant. The recurrence only uses p lagged output entries and q lagged input entries. As a specific non-trivial example an ARMA$(2,1)$ model is

$$y[n] = \phi_1 y[n-1] + \phi_2 y[n-2] + \theta_0 x[n] + \theta_1 x[n-1]$$

The solution is $y[n]$ for all n and is unique given initial conditions $y[0]$ and $y[1]$. In general p initial conditions are necessary to yield a unique solution to (5.2).

The solution to (5.2) starts with the z-transform. The transform can be taken by inspection: transform linearity means that each term can be transformed individually, and terms of the form $a[n-k]$ are replaced with $z^{-k}A(z)$. The result is a polynomial in z

$$\begin{aligned} Y(z) &= \sum_{i=1}^{p} \phi_i z^{-i} Y(z) + \sum_{j=0}^{q} \theta_j z^{-j} X(z) \\ \left(1 - \sum_{i=1}^{p} \phi_i z^{-i}\right) Y(z) &= \left(\sum_{j=0}^{q} \theta_j z^{-j}\right) X(z) \\ Q(z)Y(z) &= P(z)X(z) \\ Y(z) &= H(z)X(z) \end{aligned} \tag{5.3}$$

where $H(z) = P(z)/Q(z)$. Inverting the transform to recover $y[n]$ gives the convolution expression (5.1).

One can now see the benefit of all the heavy lifting when learning convolution and z-transforms: the solution of an ARMA model is just a rational function of two complex polynomials with p poles and z zeros. The pole and zero locations are governed solely by the parameter vectors $\boldsymbol{\phi}, \boldsymbol{\theta}$ and is completely independent of any specific input $x[n]$. In fact it is clearer to write the solution as

$$Y(z) = H(z; \boldsymbol{\phi}, \boldsymbol{\theta})X(z)$$

Likewise, the system impulse response is $h[n; \boldsymbol{\phi}, \boldsymbol{\theta}]$.

Taking the inverse z-transform depends on the region of convergence (ROC) in the complex plane and stability of the system as governed by the pole locations. In addition, the system is invertible in an input-output sense (although not necessarily stable), so given (5.3) one can write

$$H^{-1}(z)Y(z) = X(z) \tag{5.4}$$

Invertibility in this sense plays an role econometric role.

Let us consider the characteristics of $H(z)$.

Causality: The ARMA(p,q) definition (5.2) includes only lags of x, y. A lead would read

$$y[n] = \phi_{-1} y[n+1] + x[n]$$

but econometrically one cannot know $y[n+1]$ in advance of input $x[n]$; thus leads are excluded. Consequently $H(z)$ is causal, so the ROC extends from a minimum radius outward to infinity in the complex plane and $h[n]$ is right sided.

Gain: The gain g_h of $H(z)$ is $g_h = H(1)$, thus $y[n]$ experiences a gain with respect to $x[n]$. The gain can be zero, such as for the difference recursion $y[n] = x[n] - x[n-1] \longrightarrow Y(z) = \left(1 - z^{-1}\right) X(z)$, or infinite, such as for the accumulator recursion $y[n] - y[n-1] = x[n] \longrightarrow Y(z) = \left(1 - z^{-1}\right)^{-1} X(z)$.

FIR Response: Consider only the moving-average part of the recurrence: ARMA$(0, q)$, or just MA(q). Here $Q(z) = 1$ so $H(z) = P(z)$. There are no poles in $H(z)$, only zeros. The inverse transform of (5.3) is just a series of weighted lags. In detail:

$$Y(z) = \left(\sum_{j=0}^{q} \theta_j z^{-j} \right) X(z)$$

so the system response is

$$H(z) = \sum_{j=0}^{q} \theta_j z^{-j} \quad \xleftrightarrow{\mathcal{Z}} \quad h[n] = \sum_{j=0}^{q} \theta_j \delta[n-j] \tag{5.5}$$

The gain is simply $g_h = \sum \theta_j$ and for finite coefficients the impulse response is stable. As a rule, an MA(q) model has an FIR response.

IIR Response: Converse to the preceding, consider only the auto-regressive part of the recurrence: ARMA$(p, 0)$, or just AR(p). Here $P(z) = 1$ so $H(z) = 1/Q(z)$. The roots of $Q(z)$ are the poles of $H(z)$. In detail:

$$\left(1 - \sum_{i=1}^{p} \phi_i z^{-i} \right) Y(z) = X(z)$$

Factoring the polynomial $Q(z)$ into its roots gives

$$1 - \sum_{i=1}^{p} \phi_i z^{-i} = \prod_{i=1}^{p} \left(1 - p_i z^{-1}\right)$$

The system response is therefore

$$H(z) = \frac{1}{\prod_{i=1}^{p} \left(1 - p_i z^{-1}\right)}$$

Partial-fraction expansion factors the inverse polynomial into single-pole components and since $q = 0$ long polynomial division is not required. In the

case of no degenerate poles $H(z)$ factors as

$$H(z) = \sum_{i=1}^{p} \frac{A_i}{1 - p_i z^{-1}}$$

from which we get the inverse z-transform by inspection since each pole contributes a term $Ap^n u[n]$. The system response dual pair is

$$H(z) = \sum_{i=1}^{p} \frac{A_i}{1 - p_i z^{-1}} \quad \overset{\mathcal{Z}}{\longleftrightarrow} \quad h[n] = \sum_{i=1}^{p} A_i p_i^n u[n] \tag{5.6}$$

While causal the impulse response $h[n]$ is also IIR. Note that both the coefficient vector $\boldsymbol{A}$ and the pole vector $\boldsymbol{p}$ depend only on the vector $\boldsymbol{\phi}$ specified in the AR(p) equation. Stability is governed by the pole locations relative to the unit circle. Specifically all poles of AR(p) must lie within the unit circle.

Inverse FIR Response is IIR: Returning to $Y(z) = Q(z)X(z)$ consider the inverse: $Y(z)/Q(z) = X(z)$. The roots of $Q(z)$ where are the zeros of $H(z)$ are now the poles of $H^{-1}(z)$. The IIR analysis above applies directly. Thus, writing

$$\sum_{j=1}^{q} \theta_i z^{-i} = \kappa \prod_{j=1}^{q} \left(1 - z_i z^{-1}\right)$$

and

$$H^{-1}(z) = \frac{\kappa^{-1}}{\prod_{j=1}^{q} \left(1 - z_i z^{-1}\right)} = \sum_{j=1}^{q} \frac{B_i}{1 - z_i z^{-1}}$$

The FIR response and its inverse are therefore

$$h[n] = \sum_{j=0}^{q} \theta_j \delta[n-j] \quad \overset{\text{inverse}}{\longleftrightarrow} \quad h^{-1}[n] = \sum_{j=1}^{q} B_i z_i^n u[n] \tag{5.7}$$

The inverse of an FIR response is an IIR response.

Let's take a simple example. Define

$$y[n] = x[n] + \theta_1 x[n-1], \qquad |\theta_1| < 1$$

The system response pair is

$$H(z) = 1 + \theta_1 z^{-1} \quad \overset{\mathcal{Z}}{\longleftrightarrow} \quad h[n] = \delta[n] + \theta_1 \delta[n-1]$$

which is FIR with a gain of $1 + \theta_1$. The inverse system is $H^{-1}(z) = \left(1 - z_1 z^{-1}\right)^{-1}$ where the zero location is simply $z_1 = -\theta_1$. The inverse-system response pair is therefore

$$H^{-1}(z) = \frac{1}{1 - z_1 z^{-1}} \quad \overset{z}{\longleftrightarrow} \quad h^{-1}[n] = z_1^n u[n]$$

Consider that $0 < z_1 < 1$, so that $h^{-1}[n]$ monotonically decreases from unity. The coefficient θ is then in the range $-1 < \theta_1 < 0$. The forward impulse response is then simply $h[n] = \delta[n] - z_1\delta[n-1]$. The forward and inverse responses are

$$h[n] = \delta[n] - z_1\delta[n-1] \quad \overset{\text{inverse}}{\longleftrightarrow} \quad h^{-1}[n] = z_1^n u[n] \tag{5.8}$$

This is a very useful pair to remember. The inverse of a weighted first-difference (FIR) is a geometrically decaying IIR sequence. In the limit that $z \to 1$ one has a strict first difference and the unit step-function:

$$h[n] = u^{-1}[n] = \delta[n] - \delta[n-1] \quad \overset{\text{inverse}}{\longleftrightarrow} \quad h^{-1}[n] = u[n] \tag{5.9}$$

Cascading $u[n]$ and $u^{-1}[n]$ gives $u[n]u^{-1}[n] = 1$, the identity operation. The continuous time analogue is integration followed by differentiation, which is again the identity operation.

Inverse IIR Response is not necessarily FIR: In the context of an ARMA(p, q) model, the case of $p = 0$ or $q = 0$ always yields an FIR or IIR response, respectively. For $p > q$ the response is also always IIR because the partial-fraction expansion has no leading-order terms and the poles generate geometrically decaying sequences. But note that there is a subtle difference in meaning: FIR is when $p = 0$ but IIR is when $p > q$, not just $q = 0$. In general the inverse of an IIR response is not FIR, only in the specific case when $q = 0$. When $q = 0$ the system response is called an "all-poles" response. The inverse of a system with $p > q$ has order $p' < q'$ (where $p' = q$ and $q' = p$, so the partial-fraction expansion will create $p' - q' + 1$ leading delay terms and retain q' decay terms.

5.1.1 Econometric Interpretation

The principal use of time-series analysis in this course is to forecast future realizations and measures of their uncertainty. In order to do so we seek to model the processes of the underlying variables, which is turn may have structural and stochastic components. The ARMA model represents the structural component.

To motivate the exposition, consider a single-factor price process in continuous time:

$$dS_t = \mu(t, S_t)dt + \sigma(t, S_t)dW_t$$

where dW_t is a Brownian motion. Coefficients $\mu(t, S_t)$ and $\sigma(t, S_t)$ contain structural information in the relationship between W_t and S_t. Substituting

continuous time t with index n and writing as a finite difference gives

$$S[n+1] = S[n] + \mu(n, S[n]) + \sigma(n, S[n])dW[n]$$

Next, make a model where $\mu(n, S[n])$ and $\sigma(n, S[n])$ are autoregressive in $S[n]$ and $dW[n]$, respectively. The result can be

$$S[n+1] = S[n] + \sum_{i=0}^{p} \phi_i S[n-i] + \sum_{j=0}^{q} \theta_j dW[n-j]$$

We know the solution to this constant-coefficient linear-difference equation:

$$S[n] = h[n] * dW[n]$$

One can read this equation as a representation theorem, in which the observable $S[n]$ is separated into two components. The variable separation is not additive or multiplicative, as is often the case, but is via convolution. Conceptually the equation reads

$$\text{observable} = (\text{structure}) * (\text{random}) \tag{5.10}$$

The signals perspective that we have applied in all the preceding chapters has led us to view $h[n]$ and $dW[n]$ as inputs and $S[n]$ as the output of the equation. The econometric perspective in the reverse. The observables are the inputs and the desired property of the random components is i.i.d. The structural component is used to capture all correlations present in the observations.

The more common way of writing (5.10) in an econometric context is

$$y[n] = h[n] * \epsilon[n] \tag{5.11}$$

where here $y[n]$ are the observations and $\epsilon[n]$ are called innovations. While not directly observable the innovations drive the system to arrive at the observations. The model is calibrated, at least conceptually, by using trial system responses $\hat{h}[n]$ and applying its inverse to $y[n]$, that is

$$\hat{\epsilon}[n] = \hat{h}^{-1}[n] * y[n] \tag{5.12}$$

The ARMA specification that maximally removes structure from $\epsilon[n]$ is the optimal one.

While simple in concept the optimization of (5.12) is a tall order. The ARMA order (p, q) is unknown, parameter vector spaces $(\boldsymbol{\phi}, \boldsymbol{\theta})$ must be searched under the constraint that both $h[n]$ and $h^{-1}[n]$ are stable, all of which leads to a problem of high dimensionality and most probably of a multiplicity of similar solutions. There are statistical measures such as the Bayesian Information Criteria (BIC) and Akaike Information Criteria (AIC)

to help identify the minimum necessary solution dimension but they do not provide intuition into the nature of the solution.

My approach is always to have an interpretable, economic, and even physical model that plausibly captures the structure of the system under study. I would rather have better intuition at the expense of residual structure and/or higher variance in $\epsilon[n]$, knowing as well that a better fit to optimize the random properties of $\epsilon[n]$ at the expense of interpretation is likely an in-sample over fit. Accordingly, I prefer state-space models [2, 7], a few of which are detailed in the following sections. There is a strong relation between state-space and ARMA models, in that the former can always be reduced to the latter, and the latter can be projected, albeit not uniquely, into the former[1].

5.2 Characteristic Time

The geometric series

$$h[n] = (1-d)d^n u[n] \tag{5.13}$$

is so ubiquitous in the solutions of linear finite-difference equations that it deserves further analysis. For a stable system $|d| < 1$; moreover the gain of $h[n]$ above is unity. How does one choose a particular value of d? I certainly have no intuition about what an appropriate value of d should be. The answer is to find the characteristic time implied by d. I call this characteristic time N_{eff}.

The geometric series $h[n]$ is a discrete analogue of the continuous function

$$h(t) = \tau^{-1} e^{-t/\tau} u(t) \tag{5.14}$$

where τ is the characteristic time: at $t = \tau$, $h(t)$ decays by e^{-1}. The discrete analogue of τ is N_{eff}. Figure 5.1 highlights the analogy between continuous and discrete series.

For either continuous or discrete, the characteristic time is the first moment of the series. That is

$$\langle th(t) \rangle = \tau^{-1} \int_0^\infty t e^{-t/\tau} dt, \qquad \langle nh[n] \rangle = (1-d) \sum_{k=0}^{\infty} n d^n \tag{5.15}$$

There are a few ways to calculate the characteristic time for $h(t)$ and $h[n]$, including integration (summation) by parts. I prefer the following method.

Start with the zeroth moment (mean) of $h(t)$

$$\tau^{-1} \int_0^\infty e^{-t/\tau} dt = 1$$

[1] Such a conversion is the discrete equivalent of converting a higher-order ordinary differential equation into a system of first-order differential equations.

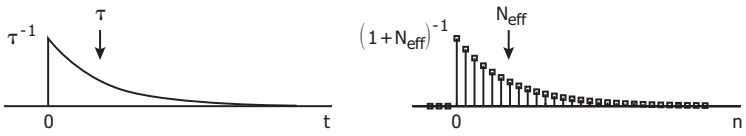

Fig. 5.1 Continuous- and discrete-time comparison of a decaying series. In continuous time the series is an exponential with mean location τ. In discrete time the series is geometric with mean location N_{eff}. Note that while in discrete time the indices are integers N_{eff} is a real number.

and take the derivative on both sides with respect to τ:

$$\begin{aligned}\frac{d}{d\tau}\int_0^\infty e^{-t/\tau}dt &= \frac{d}{d\tau}\,\tau\\ -\tau^{-2}\int_0^\infty te^{-t/\tau}dt &= 1\\ \tau^{-1}\int_0^\infty te^{-t/\tau}dt &= \tau\end{aligned}$$

The characteristic time, or first moment, of $h(t)$ is τ, as advertised. This method works just as well for the discrete version. Thus

$$(1-d)\sum_{n=0}^{\infty} d^n = 1,$$

and take the derivative with respect to d:

$$\begin{aligned}\frac{d}{dd}\sum_{n=0}^{\infty} d^n &= \frac{d}{dd}\,(1-d)^{-1}\\ \sum_{n=0}^{\infty} nd^{n-1} &= (1-d)^{-2}\\ (1-d)\sum_{n=0}^{\infty} nd^n &= \frac{d}{1-d} \equiv N_{\text{eff}}\end{aligned}$$

Decay rate d in terms of the characteristic length N_{eff} is therefore

$$\boxed{d = \frac{N_{\text{eff}}}{1+N_{\text{eff}}}} \tag{5.16}$$

It makes a great deal of sense to talk in terms of characteristic time rather than decay rate d. The properties of this relationship look good: $0 \le d < 1$, and longer N_{eff} brings d closer to unity. The unit step has $d = 1$ which is equivalent to $N_{\text{eff}} \to \infty$. We can take the analogy further by taking a

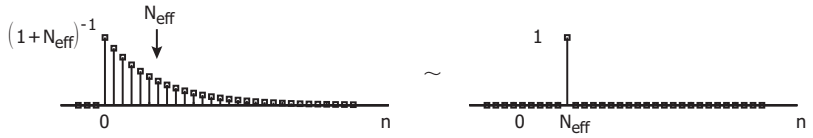

Fig. 5.2 A good heuristic is to consider that a geometric decay (left) has location N_{eff} (right). The difference between the decay on the left and impulse response on the right is shape, but the locations are the same.

large N_{eff} limit. In this case $d = \left(1 + N_{\text{eff}}^{-1}\right)^{-1} \sim 1 - N_{\text{eff}}^{-1}$, so

$$h[n] = (1-d)d^n u[n] = \frac{1}{1+N_{\text{eff}}} e^{n \log d} u[n] \sim N_{\text{eff}}^{-1} e^{-n/N_{\text{eff}}} u[n] \longrightarrow h(t)$$

Conversely, it is hard to think of $N_{\text{eff}} < 1$. Intuitively I take $N_{\text{eff}} = 1$ as a minimum practical value, which leads to $d_{min} = 1/2$. A decay less than one-half has an unappealing characteristic time physically, but it is admissible.

The characteristic time N_{eff} when related to an system response $h[n]$ gives the "speed" of the filter. As an output will be the convolution of $h[n]$ with an input signal, when a system response includes a geometric decay series the output will be delayed order N_{eff} with respect to the input. In fact a heuristic can be used whereby a geometric decay series is replaced with a single impulse whose magnitude is the gain with location N_{eff}, see Fig. 5.2. In a noisy environment, generally one would like to integrate the noise to improve the quality of the output signal; but in doing so N_{eff} must be large which in turn increases the delay of the filter. This is a tradeoff that is fundamental, and any improvement requires a higher-order filter.

5.3 A Single-Factor Local-Level Model

A single-factor local-level model (SF-LLM) is a state-space model that is driven by a single stochastic innovation that has a symmetric distribution [3]. The SF-LLM is directly related to the exponential moving average (EMA), which plays a central role in any time-series model. Whether it is one component of a larger ARMA model or a simpl mthod to find an approximate signal level, the EMA is a standard tool. In fact the EMA has appeared in the preceding sections, just not by name. A critical analysis of the EMA follows, here I start with the general state-space version of the SF-LLM.

The LLM is applicable when the input signal has a level that changes in time, such as the price of an asset. Denote the observation series y_n, where I will use subscripts in the next few paragraphs to simplify notation. We choose to represent this value by the sum of a level and an innovation, for instance

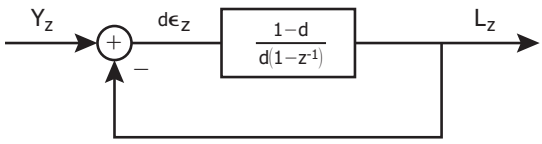

Fig. 5.3 Feedback diagram for the single-factor local-level model, otherwise known as an exponential moving average. An accumulator sits between the error and level, consequently the error can be zero for a finite level. The overall gain is unity but the forward gain is infinite.

$$y_n \equiv \ell_{n|n-1} + \epsilon_n \tag{5.17}$$

where $\ell_{n|n-1}$ is the expectation of the level at n given information up to event $n-1$. So, given any observation, we assert that it is composed of our expectation of the level plus an uncertain part. The LLM defines the level process as

$$\ell_n \equiv \ell_{n-1} + (1-d)\,\epsilon_n \tag{5.18}$$

where the same innovation is used to update ℓ_n as well as y_n; the model is single-factor. The expectation of the level is then $\ell_{n|n-1} = \ell_{n-1}$. Combined, the system of equations is

$$\begin{aligned} y_n &= \ell_{n-1} + \epsilon_n \\ \ell_n &= \ell_{n-1} + (1-d)\,\epsilon_n \end{aligned} \tag{5.19}$$

Note that an equivalent equation pair is

$$\begin{aligned} y_n &= \ell_n + d\epsilon_n \\ \ell_n &= \ell_{n-1} + (1-d)\,\epsilon_n \end{aligned} \tag{5.20}$$

where the second equation was substituted into the first. However now it is confusing, at least to me, what the cause-and-effect relationship is between the variables. While the latter pair is simpler to solve, the former pair better shows the causal relations. The best start in my opinion is to write out the expectations explicitly, as in (5.17), and work from there.

State-space models lend themselves well to block-diagram representations. A block diagram is a terrific tool to understanding the behavior of the system. To draw the block diagram we have to first take the z-transform of the system. The transform of (5.20) is

$$\begin{aligned} Y(z) &= L(z) + d\epsilon(z) \\ L(z) &= z^{-1}L(z) + (1-d)\,\epsilon(z) \end{aligned} \tag{5.21}$$

Evidently, $d\epsilon(z) = Y(z) - L(z)$ and $L(z) = (1-d) \,/\, \left(1 - z^{-1}\right) \epsilon(z)$. The block diagram shows that this system is a feedback loop, see Fig. 5.3. The difference between the observation and level is the scaled error, and the level is the ac-

cumulation of the error. The coefficient d locates the pole of the system, thus governing the system response time. While the reader may not be a controls expert it makes sense, I think, to say that a feedback loop may or may not be stable, depending on how it is constructed. That intuition proves correct with a wide variety of state-space models[2].

Returning to our model, the level and innovation series are extracted from the observations as follows. While the pair of equations in (5.21) is trivial a matrix formalism will be used as a prelude to more complicated systems. The matrix form of (5.21) is

$$\begin{pmatrix} 1 & -1 \\ 0 & 1-z^{-1} \end{pmatrix} \begin{pmatrix} Y(z) \\ L(z) \end{pmatrix} = \begin{pmatrix} d \\ (1-d) \end{pmatrix} \epsilon(z)$$

or

$$\begin{pmatrix} Y(z) \\ L(z) \end{pmatrix} = \begin{pmatrix} 1 & \frac{1}{1-z^{-1}} \\ 0 & \frac{1}{1-z^{-1}} \end{pmatrix} \begin{pmatrix} d \\ (1-d) \end{pmatrix} \epsilon(z)$$

For the level we want to solve $L(z)$ as a function of $Y(z)$ and taken the inverse transform. Following this direction, the system response $H_\ell(z)$ is

$$L(z) = \frac{1-d}{1-dz^{-1}}\, Y(z) \quad \longrightarrow \quad H_\ell(z) = \frac{1-d}{1-dz^{-1}} \tag{5.22}$$

Note that given the choice of coefficients in (5.19) the gain is unity: $H_\ell(1) = 1$. Also, in order for this transform to converge there is a constraint on d, which is $|d| < 1$. The pole-zero diagram of $H_\ell(z)$ has a zero at the origin and a pole on the real axis at d. Since all poles and zeros lie within the unit circle $H_\ell^{-1}(z)$ is stable as well.

The impulse response $h_\ell[n]$ is simply

$$h_\ell[n] = (1-d)d^n u[n] \tag{5.23}$$

and the level as a function of the observed is $\ell[n] = h_\ell[n] * y[n]$.

The transform solution (5.22) also indicates how to write the recursive relation between level and observed. Rewriting gives

[2] For the reader familiar with feedback systems, the transfer function T between input and output given the forward- and feedback-path system responses H and G, respectively (following conventional controls notation) is

$$T = \frac{H}{1+GH}$$

In the present case $H = \frac{1-d}{d(1-z^{-1})}$ and $G = 1$, giving

$$T = \frac{1-d}{1-dz^{-1}}$$

which corresponds to (5.22).

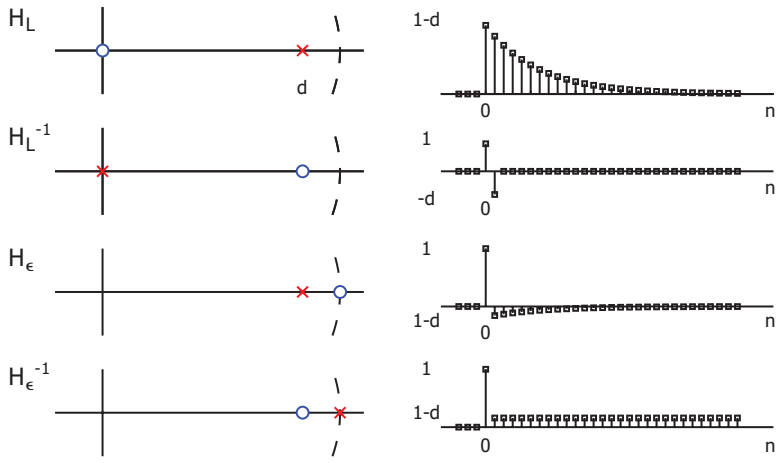

Fig. 5.4 Pole-zero diagram / impulse response pairs for the forward and inverse level and error system responses, all for the single-factor local-level model. Top: Forward level response has a single pole-zero pair, here indicated as stable. The temporal response is a geometric decay. Next: The inverse level response swaps poles and zeros and is a differencer in time. Note that this differencer is a first difference and the impulse weights are 1 and $-d$, so this not strictly a derivative. Next: Forward error response places a zero on the unit circle at $+1$ and has a stable pole. Bottom: Inverse error response is marginally stable.

$$\left(1 - dz^{-1}\right) L(z) = (1 - d)\, Y(z)$$

and some rearrangement after taking the inverse transform gives

$$\ell[n] = d\, \ell[n-1] + (1-d) y[n] \tag{5.24}$$

To initialize the recursion one takes $l[0] = y[0]$.

The innovations are solved similarly. The system response $H_\epsilon(z)$ relating $\epsilon(z)$ to $Y(z)$ is

$$\epsilon(z) = \frac{1 - z^{-1}}{1 - dz^{-1}}\, Y(z) \quad \longrightarrow \quad H_\epsilon(z) = \frac{1 - z^{-1}}{1 - dz^{-1}} \tag{5.25}$$

Note that the $\left(1 - z^{-1}\right)$ in the numerator indicates that a first difference is taken on $y[n]$; indeed the gain is $H_\epsilon(z = 1) = 0$. Since the order of z^{-1} is the same in the numerator and denominator the inverse transform first requires long division to reduce the polynomial order. The result is

$$H_\epsilon(z) = \frac{1}{d} - \frac{(1-d)/d}{1 - dz^{-1}} \tag{5.26}$$

The inverse transform now can be written by inspection

$$h_\epsilon[n] = (1/d)\,\delta[0] - (1-d)/d\,d^n\,u[n] \tag{5.27}$$

The innovation time series is thus $\epsilon[n] = h_\epsilon[n] * y[n]$. The recursive expression is found by inspection from (5.25)

$$\left(1 - z^{-1}\right)\epsilon(z) = \left(1 - dz^{-1}\right)Y(z)$$

or

$$\epsilon[n] = d\epsilon[n-1] + y[n] - y[n-1] \tag{5.28}$$

In a noisy environment the first difference of $y[n]$ will amplify the noise. Only the AR(1) component to $\epsilon[n]$ is available to integrate out the amplified noise.

5.3.1 The Exponential Moving Average

The exponential moving average (EMA) is a workhorse in time series analysis. This often touted filter is a consequence of the SF-LLM in the relation between level and observation, see (5.24), and is equivalent to a simple AR(1) process. Rewriting using a general input $x[n]$ and output $y[n]$ the EMA is defined by the recursion

$$y[n] = dy[n-1] + (1-d)x[n], \quad y[0] = x[0] \tag{5.29}$$

The impulse response is given in (5.23). The recursion starts with the first instance of the input, $x[0]$. Thereafter the output is a blend of the preceding output and the next input value. Since typically $d \sim 1$ the injection of the input to the recursion is small. The input-output delay is on the order of the filter characteristic time N_{eff}. For $|d| < 1$ the filter is stable and invertible; the forward filter having a pole on the real axis located at d.

5.4 A Single-Factor Local-Trend Model

A single-factor local trend model (SF-LTM) is an augmentation of the SF-LLM where an estimate of the slope is added alongside the estimate of the level [3][3]. The purpose is to improve the forecasting ability of the LLM by accounting for the current (estimate of) drift. I will start with a simplified model that is intuitive and at the end add a component that speeds up the filter, albeit at the expense of noise. The tradeoff can be superior with respect to the LLM model, thus it is worth our while.

As with the LLM we only have an observation series $y[n]$, and likewise we choose a representation that this observation is the expectation of the level

[3] The gain in the Hyndman *et. al.* system is not unity.

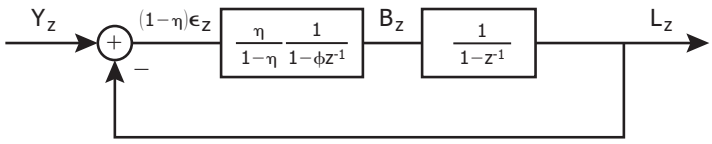

Fig. 5.5 Feedback diagram for a simple single-factor local-trend model. An EMA sits between the error and slope, so the slope is a smoothed version of the level errors. The slope is integrated by the accumulator to generate the level.

plus an innovation, (5.17). Denote by $b[n]$ the slope and define the relation between level and slope as follows

$$\begin{aligned} \ell_n &\equiv \ell_{n-1} + b_n \\ b_n &\equiv \phi b_{n-1} + \beta\,(1-\phi)\,\epsilon_n \end{aligned} \tag{5.30}$$

The level expectation is then

$$\ell_{n|n-1} = \ell_{n-1} + \phi b_{n-1}$$

The canonical system of equations is then

$$\begin{aligned} y_n &= \ell_{n-1} + \phi b_{n-1} + \epsilon_n \\ \ell_n &= \ell_{n-1} + b_n \\ b_n &= \phi b_{n-1} + \beta\,(1-\phi)\,\epsilon_n \end{aligned} \tag{5.31}$$

We see that the level is the accumulation (integration) of the slope, and the slope is an AR(1) process driven by a scaled version of the innovations. While this system very well represents the causal relationship of the hidden variables $\{\ell_n, b_n, \epsilon_n\}$, it can be simplified for analysis. A bit of algebra shows that the right-hand side of the y_n equation can be rewritten to give

$$\begin{aligned} y_n &= \ell_n + (1 - \beta\,(1-\phi))\,\epsilon_n \\ \ell_n &= \ell_{n-1} + b_n \\ b_n &= \phi b_{n-1} + \beta\,(1-\phi)\,\epsilon_n \end{aligned} \tag{5.32}$$

The block diagram of this system is illustrated in Fig. 5.5. In comparison with the SF-LLM an EMA is inserted between the error and the level; the intermediate variable is the slope. The slope is an EMA of the scaled error, and the level is the accumulation of the slope. One consequence of the additional EMA is the addition of delay between the

The solution to (5.32) is found via the z-transform. Define the temporary variable $\eta = \beta\,(1-\phi)$. In matrix notation, after taking the transform and bringing all terms but for the innovations to the left-hand side gives

$$\begin{pmatrix} 1 & -1 & \\ & 1-z^{-1} & -1 \\ & & 1-\phi z^{-1} \end{pmatrix} \begin{pmatrix} Y(z) \\ L(z) \\ B(z) \end{pmatrix} = \begin{pmatrix} 1-\eta \\ 0 \\ \eta \end{pmatrix} \epsilon(z)$$

and after inversion

$$\begin{pmatrix} Y(z) \\ L(z) \\ B(z) \end{pmatrix} = \begin{pmatrix} 1 & \frac{1}{1-z^{-1}} & \frac{1}{(1-z^{-1})(1-\phi z^{-1})} \\ & \frac{1}{1-z^{-1}} & \frac{1}{(1-z^{-1})(1-\phi z^{-1})} \\ & & \frac{1}{(1-\phi z^{-1})} \end{pmatrix} \begin{pmatrix} 1-\eta \\ 0 \\ \eta \end{pmatrix} \epsilon(z) \tag{5.33}$$

References

1. A. Brace, *Engineering BGM*. New York, New York: Chapman & Hall, 2008.
2. J. Durbin and S. Koopman, *Time Series Analysis by State Space Methods*. Oxford, United Kingdom: Oxford University Press, 2001.
3. R. Hyndman, A. Koehler, J. Ord, and R. Snyder, *Forecasting with Exponential Smoothing*. Berlin, Germany: Springer-Verlag, 2008.
4. A. V. Oppenheim and R. W. Schafer, *Digital-Time Signal Processing*, 3rd ed. Upper Saddle River, New Jersey: Pearson Higher Education, 2010.
5. E. B. Saff and A. D. Snider, *Fundamentals of Complex Analysis*. Englewood Cliffs, New Jersey: Prentice–Hall, 1976.
6. W. M. Siebert, *Circuits, Signals, and Systems*. Cambridge, Massachussets: The MIT Press, McGraw-Hill Book Company, 1986.
7. R. S. Tsay, *Analysis of Financial Time Series*, 2nd ed. Hoboken, New Jersey: Wiley-Interscience, 2005.